Supernova Monitoring in the SNO Detector

by

Michael H. Schwendener

Department of Physics and Astronomy

Submitted in partial fulfillment
of the requirements for the degree of
Master of Science in Physics

Faculty of Graduate Studies
Laurentian University
Sudbury, Ontario
September 2002

LAURENTIAN UNIVERSITY/UNIVERSITE LAURENTIENNE

FACULTY OF GRADUATE STUDIES

CERTIFICATE OF EXAMINATION

Thesis Examiners/Examinateurs de Thèse

Dr. Clarence J. Virtue (supervisor/superviseur)

Dr. E. D. Hallman

External Examiner/Examinateur externe

Dr. R. Haq

The thesis by

Michael H. Schwendener

entitled

Supernova Monitoring in the SNO Detector

is accepted in partial fulfillment of the

requirements for the degree of

Master of Science in Physics

Date

Dean of Graduate Studies and Research

ACKNOWLEDGEMENTS

I have absolultely no idea where to draw the line when it comes to how and how not to acknowledge all that assisted me in the completion of this work. I know that the list of people who influenced me is too long to write, and I am sure there are many whose assistance I was not even aware of. If I could write the names of everyone who will eventually open this book to this this page, it would be a good start. There are a few people who I know would liked to have done so but will not be able to, to them I would give a personal acknowledgement. Not only all these people, but many places, things, and events deserve a word of acknowledgement here as well, but again the list is too long.

ABSTRACT

The Sudbury Neutrino Observatory (SNO) is an underground heavy water Čerenkov Detector capable of detecting bursts of neutrinos released by nearby core collapse supernovae. The burst of neutrinos precedes the optical display of the supernova by as much as several hours, which provides a unique opportunity for astronomers to be forewarned of the impending supernova and to prepare for detailed observation. To help realize this opportunity, a program of real-time burst monitoring has been developed at SNO.

The burst monitoring system consists of successive levels of detection, analysis, and notification. Burst detection is accomplished by monitoring a datastream received from the SNO data acquisition system. Bursts are analyzed automatically and the results are made available online. Notification of the analysis is provided to the detector operator and a group of 'supernova experts' by audio-visual alerts, emails, and/or automated phone calls, depending on the analysis results.

After being in operation for over a year, the performance of the system has been evaluated. To date no supernovae have been detected, and no known galactic supernovae have gone undetected. Response time to supernova candidate bursts was found to be well within the desired 20 minute window identified by the international supernova watch community. Identification of bursts caused by known pathologies was studied and some improvements are suggested.

This is written for everyone who wanted to actually read it.

TABLE OF CONTENTS

LIST OF FIGURES

LIST OF TABLES

Chapter 1

Introduction

> Now it is the characteristic of thought in physics, as of thought in natural science generally, that it endeavors in principle to make do with "space-like" concepts *alone*, and strives to express with their aid all relations having the form of laws. The physicist seeks to reduce colours and tones to vibrations, the physiologist thought and pain to nerve processes, in such a way that the psychical element as such is eliminated from the causal nexus of existence, and thus nowhere occurs as an independent link in the causal associations.
>
> I wished to show that space-time is not necessarily something to which one can ascribe a separate existence, independently of the actual objects of physical reality. Physical objects are not *in space*, but these objects are *spatially extended*. In this way the concept of "empty space" loses its meaning.
>
> - A. Einstein 1952

It is easy to lose perspective when focusing on a small part of something large, missing the forest for the trees, so to speak. This work concerns many forests and many trees, and perspective can easily be lost. This introduction attempts to describe the current understanding of very small things and very large things, through particle

physics, and neutrino astronomy.

1.1 Particle Physics and Neutrinos

Over 2400 years ago, Democritus suggested that an understanding of the laws of nature could be found by investigating the laws governing the building blocks of the natural world. This school of thought was termed atomism, and assumed that there was a fundamental limit to which matter could be subdivided and classified. In this tradition of looking ever closer at the building blocks of our world, we have developed the fields of solid state physics, atomic physics, nuclear physics, and now particle physics, which is the state of the art in atomism. This section is meant to be a broad overview of the field of particle physics, and the reader is directed to one of many university level texts for a more detailed treatment of the subject. [1], [2]

In particle physics, all of physical reality is composed of a set of elementary particles. The game is to discover what all the particles are, and how they interact. The rules governing the particle interactions are written as renormalizable quantum field theories, such as the Electroweak Theory of interaction, and Quantum Chromo Dynamics. In the Standard Model of particle physics there are fermions which have half integral spin $(\frac{1}{2}, \frac{3}{2}, \frac{5}{2}, \ldots)$, and bosons which have integral spin $(0, 1, 2, \ldots)$. The universe is manifest through the exchange of various types of bosons between various types of fermions.

1.1.1 Constituents of Matter

The elementary fermions are the basic constituents of matter, and consist of 6 leptons and 6 quarks, arranged in three generations of quark and lepton doublets as shown in Figure 1.1. Leptons and quarks of the first generation are stable, and represent matter fields which constitute objects in the physical world. The way in which they

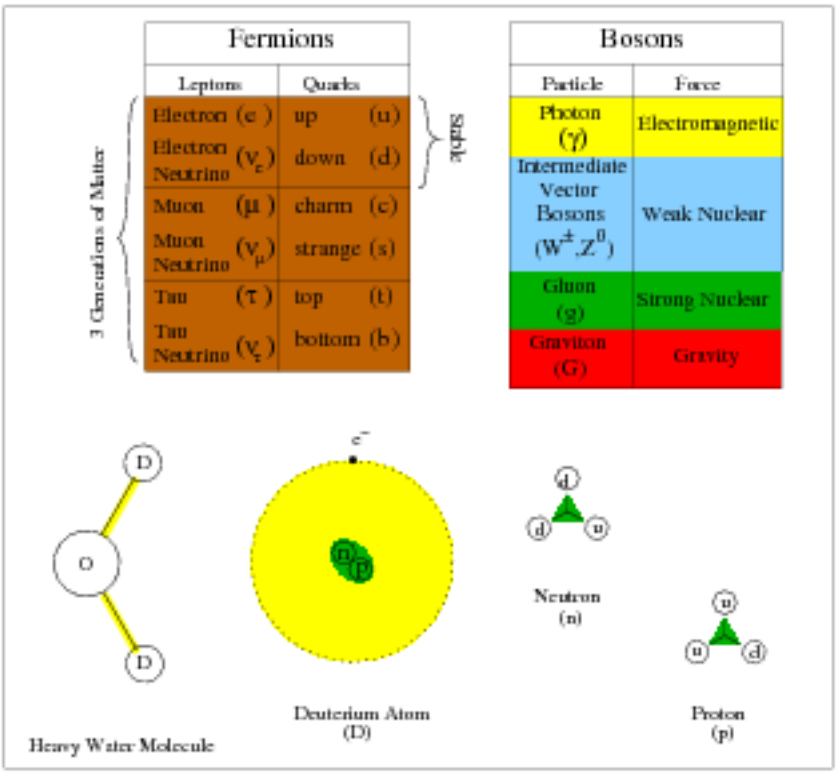

Figure 1.1: The universe is manifest through the interaction of matter and forces.

combine with each other is governed by their interactions via the forces. For example, the quarks can combine in threes forming protons and neutrons, which bind together to form nuclei. Electrons can combine with nuclei forming atoms, which bind together to form amorphous and crystaline structures which make up the macroscopic objects of the visible world.

The role of neutrinos in the construction of the physical world is a subtle one as they are not subject to either the strong or the electromagnetic force, and they have an exceedingly small mass. They are not bound into confined systems like the atom in which they can be studied closely. The only way that neutrinos can interact with other matter and be perceived[1], is through the weak force. Though they are not easily detected, they constitute a large fraction of the physical world, accounting for

[1]depends on what one means by perception

0.1% to 18% of the critical density of the universe.[3]

1.1.2 Elementary Forces

The elementary bosons are the vehicles of interaction between matter, and are each associated with a force of nature. Properties of the fermions such as charge or mass determine which bosons can be exchanged, and thus which forces the particles are subject to. The gluon (g) is associated with the strong nuclear force and affects particles which have a colour charge; this is the force which binds the quarks to form nucleons. The photon (γ) is associated with the electromagnetic force and affects particles with an electric charge; this is the force which binds electrons to the nucleus to form atoms. The graviton (G) (which has not yet been directly observed) is associated with the gravitational force and affects particles which have mass; this is the force which binds matter to form the objects of the solar system. The intermediate vector bosons ($W^{\pm}$ and Z^{0}) are associated with the weak force, and affect all particles. The effects of this force are difficult to perceive, but are seen for example, in radioactive decay.

1.1.3 Fundamental Interactions

The concept of fundamental particle interaction is often hard to grasp, as our perception is dominated by electromagnetism and gravitation. Although these forces act through the discrete exchange of bosons, these exchanges take place very frequently and only involve the transfer of small quantities of momentum. The interaction is not perceived as discrete events, but rather as a continuous force. These continuous interactions take the form of orbits, closed and elliptical for attractive forces or open and hyperbolic for repulsive forces. Discrete interactions are described by an initial and final state, and can be very different depending on the nature of the interaction. In particle physics, Feynman diagrams are used to depict fundamental interactions,

and represent formal rules for calculating the probable result of an interaction.

Further confusing one's intuition is the weak force, which through the exchange of a charged $W^{\pm}$ boson can transfer not only momentum but charge as well. By exchanging charge, the fundamental identities of the initial particles can be changed. It is difficult to envision the discrete interaction of two indivisible objects in which their fundamental properties are changed.

The ranges of forces are also very different owing to the mass of the exchanged boson. In the transmission of a force, an exchange boson is spontaneously emitted from one fermion and absorbed by another. The spontaneous emission of a particle violates energy conservation, and is only allowable within the limits of the time-energy uncertainty relationship. In this limit, a massless particle such as a photon can exist for an indefinite time and travel an infinite distance before being absorbed by the second particle, while a massive Z^0 or $W^{\pm}$ particle can only travel a very short distance. For this reason the electromagnetic force has an infinite range, while the weak force has an exceedingly short range.

1.1.4 Neutrino Interactions

The neutrino, being a charge-less and almost[2] mass-less lepton, is effectively subject to only the weak force. That is to say that neutrinos can interact with all particles, but only through the exchange of the intermediate vector bosons ($W^{\pm}$ and Z^0). Interactions involving the exchange of a charged $W^{\pm}$ particle are called charged current interactions, and those involving the exchange of a Z^0 particle are called neutral current interactions. Figure 1.2 shows some examples of Feynman diagrams for neutrino interactions with quarks and leptons through charged current (CC) and neutral current (NC) interactions.

An atom, consisting of neutrons, protons, and electrons, possesses an electric field

[2] the subject of neutrino mass is currently an active topic of investigation

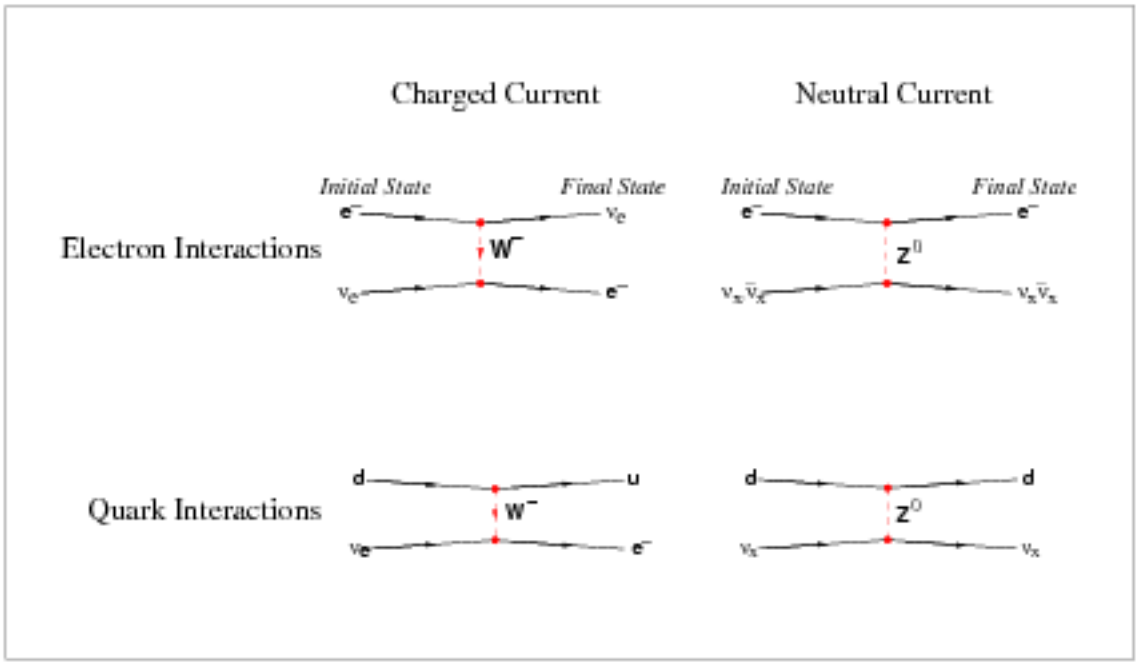

Figure 1.2: A few of the fundamental electroweak interactions through which neutrinos can interact with matter.

and a much smaller weak field. Seeing only the weak and not the electromagnetic fields, a neutrino is far less likely to interact with the atom. This difference is so large that a neutrino may pass through on the order of one light year (10^{16} meters) of solid lead before striking (interacting with) any of the lead nuclei or electrons. This makes the presence of neutrinos very difficult to detect. The topic of neutrino interactions is revisited in chapter 2, specifically in section 2.1.3 where the specific neutrino interactions used by the SNO detector are discussed.

1.2 Astrophysics and Supernovae

The sun-centered model of the solar system is an early example of an astrophysical theory. This resolved astronomical observations of the sun, moon, and planets' motions with terrestrial observations of gravitation and mechanics through the math-

ematics of calculus.

Much of astrophysics today is concerned with the study of stars, attempting to understand how they radiate energy and evolve with time. Detailed study of the sun, combined with knowledge of nuclear and particle physics, has led to an understanding of how energy is produced in the sun's core through thermonuclear fusion, mainly of hydrogen to form helium. Studying stars of different ages and compositions has led to models of stellar evolution, describing how a star progresses through various stages of nuclear burning. Although these models do not completely describe the initial condensation from the interstellar medium and the final fate of some stars, they describe much of a star's evolution very well.[3]

1.2.1 Stellar Evolution

As a star ages and its internal composition and processes change, its outward temperature and luminosity change as well. The Hertzsprung-Russell (HR) diagram shown in Figure 1.3 is useful when describing stellar evolution. By observing many "model stars" (those not in rapid rotation, subject to strong magnetic fields, or in a tight binary system), snapshots of various stages of stellar evolution are captured. When plotted on the HR diagram, more than 90% of stars observable from the earth are found around the line running from upper left to lower right labeled Main Sequence, with many other stars found in the regions labeled Giant and Dwarf. These regions represent prolonged periods of stability in the evolution of stars.

After condensing from the interstellar medium and initiating nuclear burning, a star quickly attains hydrostatic equilibrium with temperature and luminosity that place it on the main sequence. This phase occupies most of the star's thermonuclear evolution, during which energy is produced through the fusion of hydrogen to form helium. For low mass stars with less than twice the mass of the sun ($< 2\ M_{\odot}$), this

[3]For a full development of stellar evolution consult an astrophysics textbook.[4], [5]

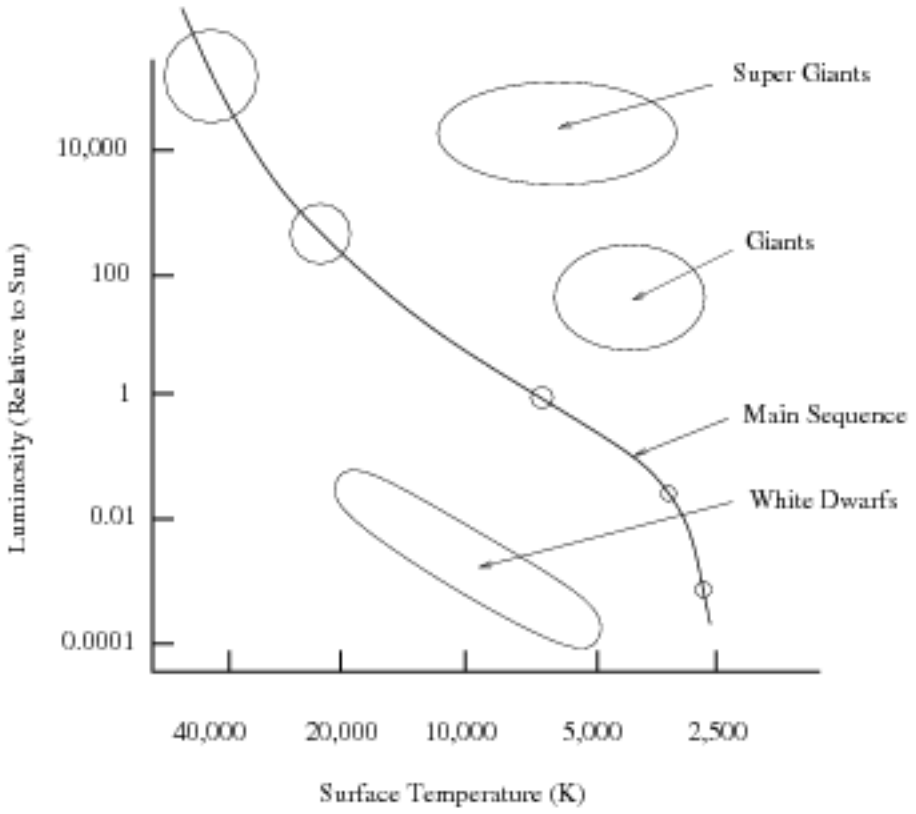

Figure 1.3: The observable properties of a distant star include temperature and luminosity which vary as it evolves. Stars begin on the main sequence burning hydrogen to helium, and can end up as large cool giants, or small hot dwarfs.

occurs mainly through the proton proton ($p-p$) cycle, while in higher mass stars the hotter core temperature allows hydrogen burning through the carbon-nitrogen-oxygen (CNO) cycle as well. The temperature dependence of the CNO cycle compared to the $p-p$ cycle causes higher mass stars to develop a convective core in which the burning hydrogen fuel and the helium ash become well mixed, while low mass stars develop an isothermal radiative core of inert helium surrounded by a convective hydrogen burning shell.[4] This difference in core configuration has an important effect on the future evolution of the star.

An inert isothermal core can only support a mass fraction (q) which depends on the relative molecular weights of the core (μ_i) and envelope (μ_o). Above this limit, called the *Chandrasekhar-Schönberg* (C-S) limit, the core must contract to maintain equilibrium.[5]

$$q_{C-S} \equiv \frac{M_c}{M} \leq 0.37\,(\frac{\mu_o}{\mu_i})^2 \tag{1.1}$$

A low mass star develops an inert helium core quickly, and is partially supported by electron degeneracy pressure before reaching the C-S limit. Electron degeneracy pressure arises when electrons cannot be packed any closer due to the Pauli exclusion principal. When the temperature of the degenerate core reaches approximately 10^8 K, runaway helium burning takes place until the degeneracy is removed in what is called the helium flash. After this short violent period, the star enters a stable period of core helium burning occupying the giant region of the HR diagram. During this phase, the hydrogen burning shell is supported by radiation pressure from the helium burning core. Eventually the helium fuel is depleted and the fusion rate decreases. No longer supported by radiation pressure, the hydrogen burning shell becomes unstable and is extinguished. A white dwarf star is left to slowly cool. This marks the end of the evolutionary path of a low mass star.

Higher mass stars ($> 5M_\odot$) develop a mixed helium-hydrogen core, and approach

the C-S limit without becoming degenerate. The predominantly helium core contracts and ignites helium fusion in a more orderly fashion. As core helium burning sets in, hydrogen burning continues in a convective shell around the helium burning region. This is similar to the giant phase of the low mass star, although in this case, the hydrogen burning shell is convectively coupled to the helium burning core.

Very massive stars ($> 7M_{\odot}$) continue this process of contraction and ignition of other nuclear reactions, forming concentric burning regions of increasingly dense nuclei. Each successive phase of burning occurs more rapidly than the former, with the initial hydrogen burning lasting several million years, and the final ones lasting only days. If the star is massive enough ($> 8M_{\odot}$) fusion reactions producing iron are permitted, and an iron core begins to form. Iron is the most tightly bound nucleus, and no further fusion reactions in the core will release additional energy. The inert core continues to grow, supported by electron degeneracy pressure.

These stars reach their end when gravitational pressure overcomes the electron degeneracy pressure, and the core undergoes a rapid and violent gravitational collapse. This collapse may result in a massive release of energy which completely destroys the star in a supernova explosion, or in the continued collapse of the core into a black hole.

1.2.2 Supernovae

Supernovae are among the most brilliant events in the universe, marking the sudden end of a star with an enormous release of energy in the form of light and neutrinos. From the earth a supernova appears as the sudden brightening and eventual disappearance of a star in our galaxy, or the brief appearance and disappearance of a star in a distant galaxy as one previously unnoticeable star briefly out shines its entire home galaxy. The light reaches its maximum brightness in a period of just hours or days, then gradually fades and expands in size over the course of months and years.

Although other events have been suggested, the first clearly recorded observation of a supernova was circa 1054 AD by Chinese astronomers, who described it as a brilliant celestial display called the guest star, stating that it was visible for many months. This event was only confirmed by western astronomers (science) in the mid 20th century after examining the Crab Nebula, which was eventually concluded to be the remnant of a supernova from around AD 1054. Other brilliant nearby supernovae have been observed by Schuler, Hainzel, Lindauer, Brahe (1572), Kepler (1604), and most recently Ian Shelton (1987). Supernovae in distant galaxies are now routinely observed by modern deep space observatories at a rate of several per night.

Estimates of supernova rates can be made by several different methods. First by extrapolating from the observation rate since recorded history, second by studying the number and age of nearby supernova remnants, and finally by studying the supernova rate in many distant galaxies. Depending on what method is used, the estimate of the rate of supernovae within our galaxy ranges from one every 30 to 50 years.[6]

The apparent brightness of a supernova depends on the distance from the earth, and the amount of intervening dust or gas. The guest star of 1054, located 2.0 kpc from earth, would likely have been as bright as Venus (very bright), and clearly visible to the naked eye. Betelgeuse is a star in the constellation Orion, located about 0.13 kpc from earth. Were Betelgeuse to go supernova (being a red super-giant it is susceptible to gravitational collapse), it would likely be far brighter than the full moon, visible in broad daylight, and remain visible for years as it slowly dimmed from a bright point into a large glowing disc.

Two broad classifications of supernovae based on optical observation are type I and type II, respectively referring to the absence or presence of hydrogen absorption lines in the optical spectrum. The absorption of light by hydrogen however is mainly determined by the outer composition of the star, and does not provide much insight into the underlying nature of the event.

Conditions for gravitational collapse may come about in a number of ways, such as the evolution of a massive ($> 8M_{\odot}$) star as described in the preceding section, or as a result of rapid mass accretion by a white dwarf from its companion in a binary system. It is believed that the former mechanism is associated with type II supernovae, while the latter is associated with type Ia supernovae. This work is mainly concerned with supernovae resulting from the collapse of the predominantly iron core of a massive star, as this mechanism is known to produces neutrinos.

The condition for gravitational collapse of an iron core star is determined by the C-S limit (equation 1.1). The mean molecular weight of the core is that of iron (μ_i=55). That of the outer envelope depends on the structure and thus the detailed history of the star, and is certainly less than that of iron ($\mu_o < 55$). The value of 1.4 $M_{\odot}$ for the mass of the core (M_c) is often referred to as the Chandrasekhar mass limit or simply the Chandrasekhar mass. This limit is supported by astronomical observation, as no white dwarf stars above this mass have been observed. For a star of mass (M) equal to 10 $M_{\odot}$, the mean molecular weight of the envelope is calculated to be around 34, which is consistent with reasonable assumptions of the structure of the envelope.

Contraction of the core forces electrons and protons to combine through inverse β decay forming neutrons and neutrinos, reducing the electron degeneracy pressure and yielding almost no energy for support of the core. With no electromagnetic support, nuclear matter collapses unhindered through several orders of magnitude. In a fraction of a second the core collapses from a density on the order of $10^7 \frac{g}{cm^3}$ to $10^{14} \frac{g}{cm^3}$, contracting from about the size of the earth to just a few kilometers.

Infalling matter reaches velocities of one quarter the speed of light and attains tremendous kinetic energy as it falls. Eventually the fall is abruptly halted by neutron degeneracy pressure, and a fraction of the infalling matter bounces back ("core bounce") with comparable energy. This shock-wave ripples through the outer man-

tle, destroying the star in a supernova explosion. A neutron degenerate mass is left behind to cool through neutrino emission and to form a neutron star.

In the formation of the physical world, supernovae play a major role in the creation and distribution of the elements. All elements heavier than iron were formed in the neutron rich environment of a supernova. These elements, along with those formed over millions of years of nuclear burning (including such important things as carbon and oxygen) are released from the gravitational binding of the star and cast out into the interstellar medium by supernova explosions. These elements may eventually condense forming the satellites of a solar system (planets and moons), and other objects (asteroids and comets).

1.3 Observing Supernovae With Neutrinos

Recently the fields of neutrino astronomy and neutrino astrophysics have emerged, allowing great new potential for astronomical observation. The path of a neutrino produced in an astrophysical process is rarely obstructed by intervening matter and is not altered by strong magnetic fields, as can occur with other particles. This allows for observation of processes occurring deep in the core of stars or behind distant clouds of dust, which would be impossible with optical astronomy.

Only the brightest (in neutrino luminosity) phenomena can be observed by neutrino astronomy, due to the difficulty of detecting the tiny particles. This leaves fusion reactions in the core of our nearby sun, and gravitational collapse supernovae in our galaxy among the few phenomena observable by current neutrino telescopes. The gravitational collapse of a nearby massive star produces a copious amount of neutrinos which is easily detectable above the solar neutrino background.

Several neutrino detectors were in operation on February 23 1987 when a blue supergiant in the Large Magellanic Cloud, known as Sanduleak -69° 202 went supernova (designation SN1987A).[7] Although quite sparse, these measurements consititute an

unambiguous signal above background, and mark the first neutrino observations of phenomena outside of the solar system.

1.3.1 Supernova Neutrino Emission

Detailed predictions of the time and energy spectra of neutrinos emitted from a supernova are based on unconfirmed models of supernovae, and must be viewed with caution. Supernova models generally agree on the mechanism of gravitational collapse, but differ on the detailed mechanism of supernova explosion. For the purpose of detecting (as opposed to analyzing) a supernova signal it should suffice to overlook the model specific predictions of the explosion period and focus on generic predictions of the overall signal.

The total energy emitted in the form of neutrinos during a gravitational collapse is approximately equal to the gravitational binding energy of the core, which is roughly 3×10^{53} ergs.[8] Neglecting the details of the explosion period, there are effectively two distinct periods of neutrino emission, namely neutronization and cooling. Figures 1.4 and 1.5 are plots generated using the supernova model of Burrows et. al[9], and display the expected features of the neutrino signal. These features include 1) rapid turn on of neutrino luminosity followed by decay over several tens of seconds, 2) an enhancement of electron neutrino luminosity at the onset of the signal, and 3) a hierarchy of neutrino energies according to flavour.

During the neutronization phase, matter in the collapsing core of the star is converted to neutrons through electron capture on protons producing a large amount of electron neutrinos. This occurs very quickly, lasting less than 50 ms.

$$e^- + p \rightarrow n + \nu_e \tag{1.2}$$

At the onset of collapse these neutrinos are readily emitted from the core, and the electron neutrino luminosity rises quickly. As the temperature and pressure in the

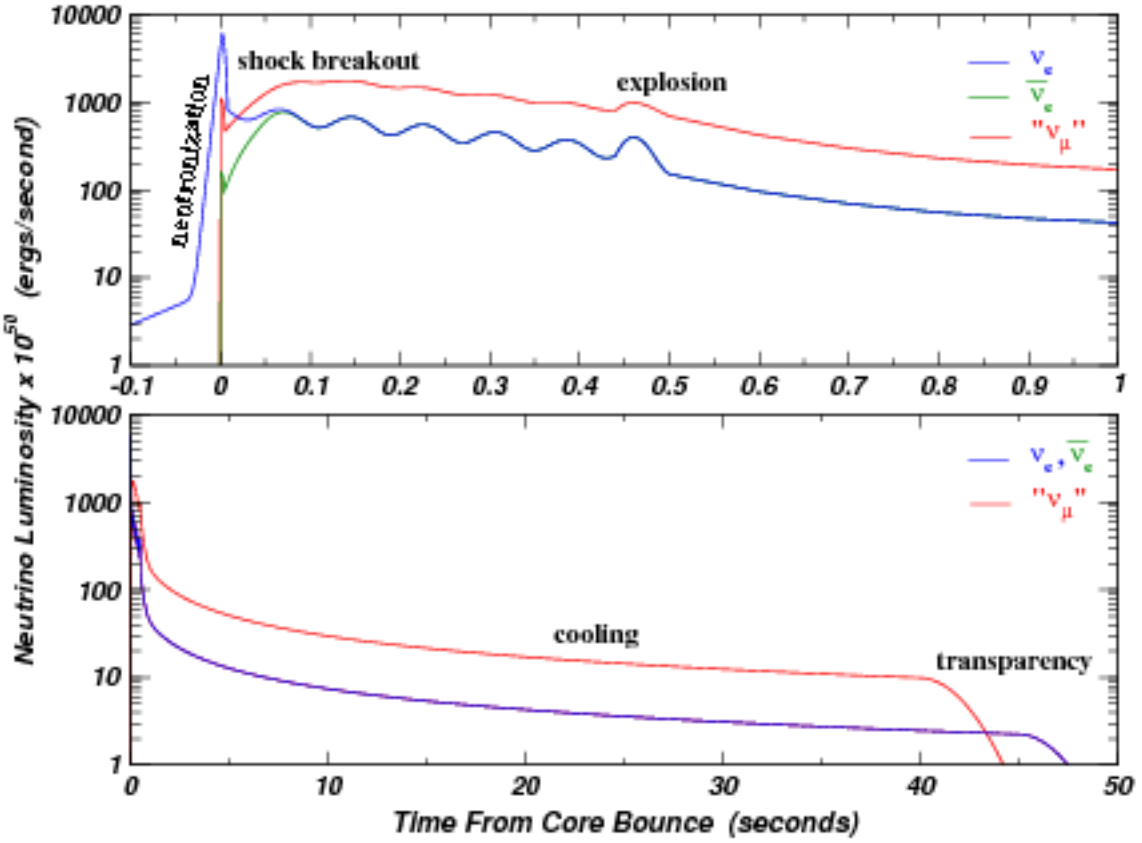

Figure 1.4: The neutronization peak and the time scale of the cooling period are generic predictions for luminosity, while the details of the explosion period are model dependent. "ν_μ" refers to the combined luminosity of muon and tau neutrinos and their antiparticles.

core rise however, the mean free path length for neutrinos becomes shorter than the diameter of the core, and neutrinos inside a diameter of about 30 km are trapped. The boundary of this trapping region becomes a radiating surface for neutrinos called the neutrinosphere, much like the photosphere is for photons in an ordinary star.

After this core bounce (t=0 in Figures 1.5 and 1.4), the temperature and pressure in the wake of the expanding shock-wave allow several pair production processes (Table 1.1) to turn on. When the shock-wave passes the neutrinosphere these neutrinos are able to escape, and the luminosity of all neutrino species rises suddenly ("shock

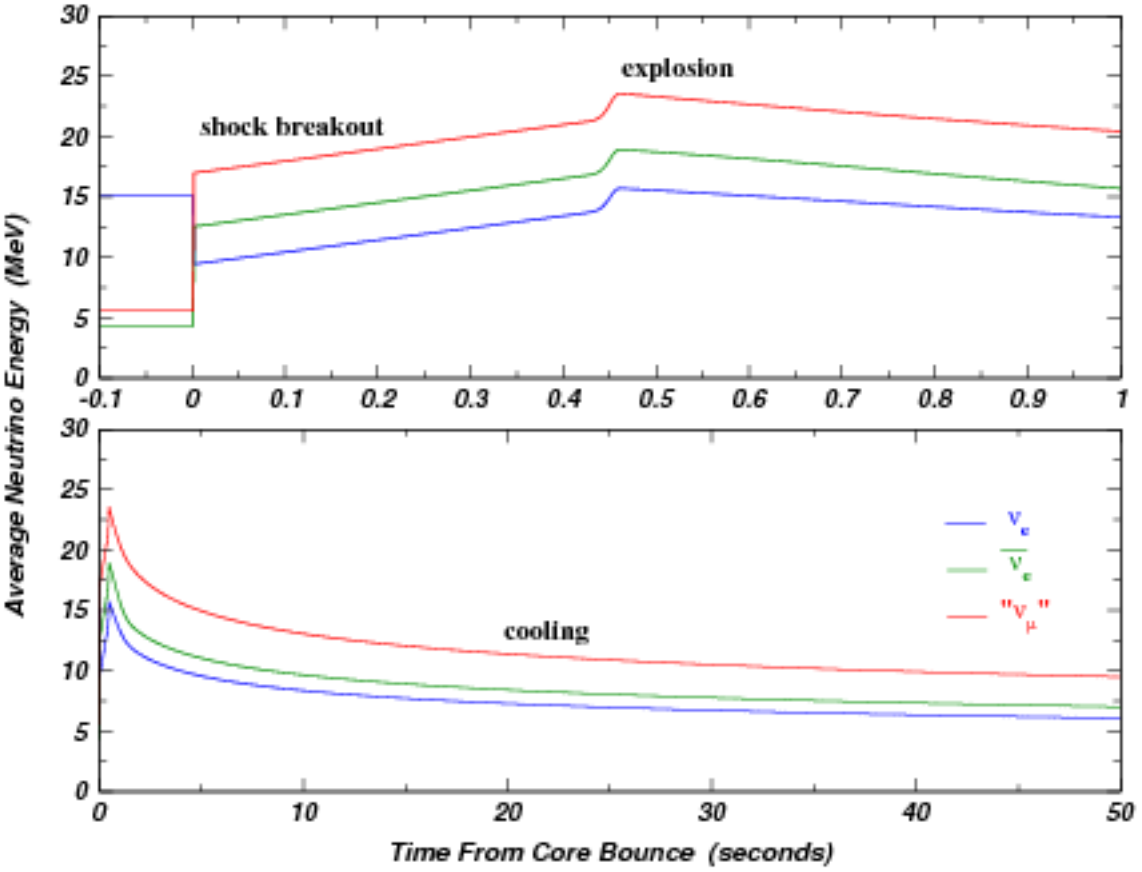

Figure 1.5: The hierarchy of neutrino energies $E_{\nu_e} < E_{\bar{\nu}_e} < E_{\text{“}\nu_\mu\text{”}}$ is a robust feature present in many supernova models. “ν_μ” refers to the average energy of muon and tau neutrinos and their antiparticles.

breakout" in Figure 1.5). After a brief period of instability during which the actual explosion takes place, the hot protoneutron star settles into a cooling phase, during which most of the gravitational binding energy is shed through neutrino emission.

Neutrinos of different types have different mean free path lengths dependent on the number of interaction channels available, and hence are emitted from neutrinospheres of different radii with energies given by the radial temperature profile. Muon and tau neutrinos and antineutrinos, interacting only through the neutral current have the longest mean free path length, and are emitted from a neutrinosphere deepest in

Pair Annihilation:	$\gamma + \gamma \rightleftharpoons e^+ + e^-$	$\rightarrow$	$\nu_x + \overline{\nu}_x$
Plasmon Decay:	*plasma excitation* $\rightarrow e^+ + e^-$	$\rightarrow$	$\nu_x + \overline{\nu}_x$
Photoneutrino:	$\gamma + e^-$	$\rightarrow$	$e^- + \nu_x + \overline{\nu}_x$
Bremßtrahlung:	$e^- + (A, Z)$	$\rightarrow$	$(A, Z) + e^- + \nu_x + \overline{\nu}_x$

Table 1.1: Several pair production processes create neutrino/antineutrino pairs. Energy is carried away by the neutrinos, cooling the hot protoneutron star.

the core, and hence with the highest energies. Electron neutrinos and antineutrinos are emitted with lower energy due to the charged current channel of interaction. Of these two, the electron antineutrino has a slightly higher energy, owing to the high neutron to proton ratio in the core. The relative order of this hierarchy of energies ($E_{\nu_e} < E_{\overline{\nu}_e} < E_{\nu_\mu}, E_{\nu_\tau}$) is a generic prediction, while the magnitudes are model dependent.

1.3.2 Detectors

Most neutrino detectors capable of detecting a supernova are designed with a different physics objective (proton decay searches, solar neutrino flux measurements), with the possibility of supernova detection as a secondary motivation. The widely varying detector designs provide different but complementary sensitivity to a supernova neutrino signal.

A neutrino detector generally consists of a massive target with which neutrinos interact, and an experimental apparatus for detecting when such an interaction has occurred. The response of the detector to neutrinos of various flavours and energies is a function of the target medium and the detection mechanism. As with any particle physics detector, the objective is to identify particles and to measure their energy

and momentum. A detector's ability to detect and record supernova neutrino bursts can be summarized by its: 1) ability to measure time and energy spectra of the neutrino burst, 2) ability to measure the direction of the neutrino burst, 3) sensitivity to multiple neutrino flavours. Table 1.2 [10] lists the capabilities of detector types currently running worldwide.

Detector Type	Target Material	Energy	Time	Pointing	Flavour
Scintillation	C, H	yes	yes	no	$\overline{\nu}_e$
Water Čerenkov	H_2O	yes	yes	yes	$\overline{\nu}_e$
Heavy Water	D_2O	NC: no	yes	no	all
		CC: yes	yes	yes	ν_e, $\overline{\nu}_e$
Long String Water Čerenkov	H_2O	no	yes	no	$\overline{\nu}_e$
High Z/Neutron	NaCl, Pb, Fe	no	yes	no	all
Radiochemical	^{37}Cl, ^{127}I, ^{71}Ga	no	no	no	ν_e

Table 1.2: A list of the existing types of neutrino detectors and their ability to detect and record the neutrino signal from a galactic supernova.

Radiochemical experiments rely on inverse β decay interactions that produce radio-isotopes in the target medium. On an infrequent basis the target is assayed for the product isotope using radiochemical methods. This type of detector is well suited for measuring average fluxes over days or weeks, but can provide no information about the time, energy, or angular distribution of the signal.

Čerenkov type detectors rely on radiation emitted by the fast moving charged particles produced in many neutrino interactions. Čerenkov light is radiated in a conical shape along the path of a relativistic charged particle as it traverses a medium above the speed of light for that medium. The target medium must be optically transparent in the range of wavelengths spanned by the Čerenkov light to transmit it from the tar-

get volume to a detection region where it can be measured by photomultiplier tubes. For some types of neutrino interactions, the charged particle direction is correlated with the neutrino direction, giving some angular sensitivity to the signal.

Scintillation type detectors convert the energy deposited by a neutrino interaction into isotropic light which is then detected by photomultiplier tubes or other light detectors. By using a scintillator any angular information about the signal is lost, but the higher photon yield generally gives improved energy response with respect to Čerenkov detectors.

Neutron type detectors rely mainly on neutral current interactions to produce neutrons. These detectors use a high density target medium to maximize the cross section for neutral current interactions. Although sensitive to all flavours of neutrinos, these detectors provide poor sensitivity to energy and none to direction.

The only supernova neutrino data to date were recorded in 1987 from SN1987A. Two water Čerenkov detectors, one in Japan (Kamiokande II) and one in the United States (Irvine Michigan Brookhaven-IMB) detected simultaneous bursts of neutrinos. Two scintillation type detectors, one in the USSR (Baksan) and one in Italy (LSD), also detected bursts of neutrinos. Issues mainly concerning the synchronicity of the events, called into question the validity of some of the observations. The twelve events detected at Kamiokande II and the eight events detected at IMB are considered to be the commonly accepted neutrino signal associated with SN1987A, with the Baksan events sometimes included with an overall shift in arrival time. The energy and time measurements of the neutrino events from Kamiokande II, IMB, and Baksan (corrected for offset in time) are shown in Figure 1.6.

1.3.3 Physics Potential

Detecting and analyzing the neutrino signal from a nearby supernova will provide a wealth of physical knowledge. The full potential of this observation cannot be

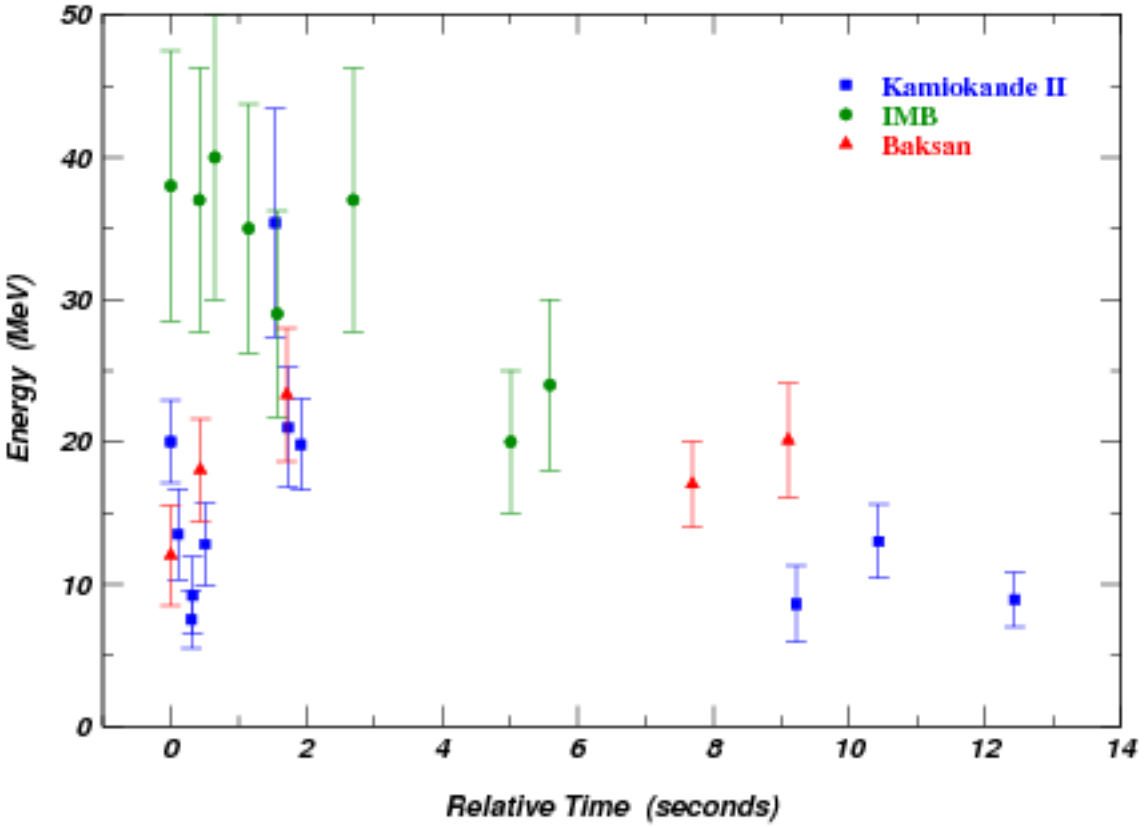

Figure 1.6: The neutrino events recorded from SN1987A; Energies are of the recoil electron/positron, and the event times are relative to their first event for each detector.

fully appreciated until after it is analyzed, yet alone be fully discussed in this short section. Potential gains will certainly include advances in the fields of astronomy, neutrino physics, and astrophysics.

Simply detecting the neutrino signal will provide an opportunity for a unique astronomical observation. Models indicate that neutrinos produced in the collapsing star escape up to several hours before the optical display. In order to capitalize on this opportunity to observe the early moments of a supernova explosion, neutrino experiments must be capable of prompt detection and confirmation of a supernova neutrino signal. Notification of the signal must also be passed on to the astronomical

community in short order. This is the primary motivation for a real time supernova neutrino monitoring program.

The most obvious pieces of neutrino physics data to be extracted from a supernova signal are limits on the neutrino masses. Several methods of mass measurements exploit the spread in neutrino arrival time as a function of energy and flavor. These methods are all limited by the uncertainty of the time and energy distributions of supernova neutrino emission.

First, since a neutrino of finite mass travels at less than the speed of light, a correlation between time of flight and neutrino energy should be evident. Using only one neutrino species ($\overline{\nu}_e$), the spread in arrival time Δt (s) is related to energy E (MeV) through the particles mass m_ν (MeV) and supernova distance D (kpc):

$$\Delta t = 0.0515(\frac{m_\nu}{E})^2 D \tag{1.3}$$

This however assumes an instantaneous turn on of neutrinos of all energies at the source. The typical mass limit $m_{\overline{\nu}_e} < 20$ eV inferred from the SN1987A neutrino signal by this method is not particularly impressive compared to laboratory measurements. Even with today's detectors, this method is not expected to improve on laboratory measurements of $m_{\overline{\nu}_e}$.[10]

A second method of estimating the mass of the most massive neutrino species involves the abrupt signal cutoff expected from the formation of a black hole.[11] Assuming that the neutrino signal cutoff is uniform in time and energy at the source, an energy dependent cutoff in arrival time is due to mass dependent time of flight, as described above. This method may offer a more precise measure of neutrino mass if the formation of the black hole is rapid.

A third method allows an estimate of $m_{\nu_{\mu,\tau}}$, by including the data from detectors capable of measuring both neutral current and charged current signals, or by combining data from several experiments. In this method, the delay in time of the $\overline{\nu}_e$ signal compared to that of the $m_{\nu_{\mu,\tau}}$ signal is used to estimate the difference in mass of the

species. The current limits on the mass of these flavours are 190 keV and 15.5 MeV respectively.[12] It may be possible to improve greatly on these limits, as this method may offer sensitivity to $m_{\nu_{\mu,\tau}}$ on the order of tens of eV to keV.[13].

In addition to the neutrino physics potential, significant improvements in the astrophysical theories that describe the terminal phase of high mass stellar evolution should also be possible. Several gravitational collapse supernova models have been developed since the observation of SN1987A, all of which are consistent with that single experimental observation.[9] The sparse nature of the data set allows for a large amount of variability between the models, and a rich signal from the next galactic supernova should clarify the situation by confirming and rejecting different aspects of the various models.

The remainder of this thesis is structured as follows: Chapter 2 contains a description of the Sudbury Neutrino Observatory, with emphasis on the ability to detect supernova neutrinos. Chapter 3 describes the implementation of the supernova monitoring system, including a detailed description of the SNO data stream. In Chapter 4, the performance of the supernova monitoring system is studied, and finally in Chapter 5 the thesis is concluded with a summary of accomplishments, and a look to the future.

Chapter 2

Supernova Neutrino Detection in SNO

All is atoms and void – Democritus

All is flux – Heraclitus

The Sudbury Neutrino Observatory (SNO) is a heavy water Čerenkov detector, built primarily to address the solar neutrino problem by independently measuring the ^{8}B solar neutrino flux. Whereas the solar neutrino detection rate is of the order of events per day, the neutrino burst accompanying a nearby supernova will produce of the order of hundreds to hundreds of thousands of detectable neutrino interactions within seconds. A Monte Carlo simulation has been developed[14] to study the response of the detector to the expected signal. Background and instrumental sources give rise to bursts in the detector signal rate, and the character of the burst is the main identifier of a supernova signal.

2.1 Neutrino Detection

2.1.1 Overview

The overall structure of the Sudbury Neutrino Observatory[15] is shown in Figure 2.1. The detector is located in INCO's Creighton mine near Sudbury, Ontario, under 6800 ft of mostly norite rock, providing 6000 meters water equivalent depth. The center

of the detector consists of a 1,000 tonne heavy water (D_2O) target contained in a clear acrylic vessel of 12m diameter. The vessel is suspended within a barrel shaped cavern which is coated with a water and gas tight liner, and filled with ultra pure H_2O. Suspended in the H_2O and surrounding the acrylic vessel, is a stainless steel geodesic PMT support structure (PSUP) on which photomultiplier tubes (PMTs) are mounted to observe the D_2O volume and a portion of the H_2O volume.

The PMT array consists of 9438 PMTs fitted with light concentrating reflectors housed in hexagonal cells. Together the PMTs and concentrators effectively provide approximately 59% coverage of the geodesic sphere. Each PMT is capable of detecting single photons of light in the visible and near ultra-violet range. Light generated in the detector is registered by some number of PMTs and recorded as an 'event'. The number of tubes hit is called the "NHIT" of the event, and for physics events is related (through geometry, optics, and physics) to the energy of the interaction. The primary hardware detection threshold requires 16 tubes to be hit within 100 ns, which corresponds to an energy of approximately 2 MeV.

2.1.2 Particle Detection

Particles that can be detected by SNO include energetic charged particles (e^+/e^-), gamma rays, and free neutrons (through neutron capture).

Charged particles are detected by the Čerenkov radiation they emit. When a charged particle traverses a medium at a velocity greater than the speed of light in that medium, the electromagnetic equivalent of a "shock wave" is produced. This generates photons which are emitted at a characteristic angle α relative to the particle direction. For the relativistic velocity β of the particle, and refractive index n of the medium:

$$\cos\alpha = \frac{1}{\beta n} \tag{2.1}$$

For electrons of a few MeV in D_2O, this results in a cone of light in the near UV

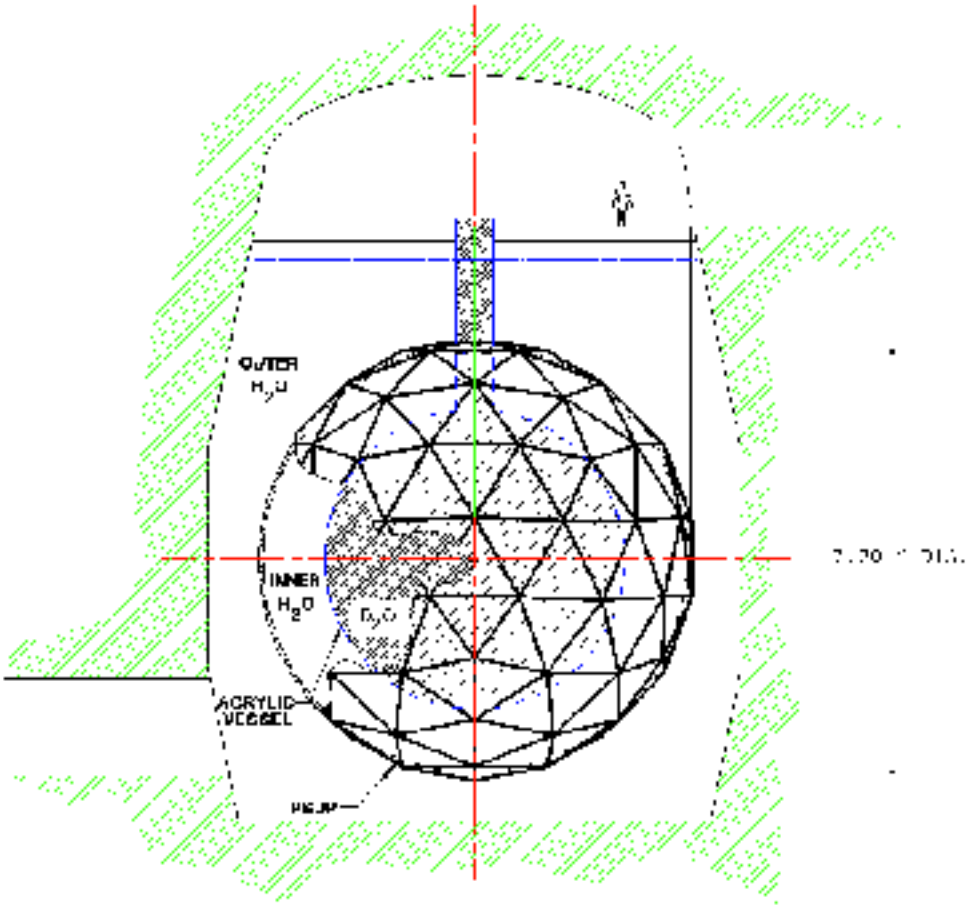

Figure 2.1: The SNO detector is a heavy water Čerenkov detector, located 6800 ft. underground in Sudbury.

range, with an opening angle of approximately 42°. This cone of light shines on the PMT array striking a number of tubes in a circular pattern. The detection threshold for electrons is about 2 MeV of kinetic energy.

Gamma rays travel a short distance before interacting through the photo-electric effect, Compton scattering, or pair production, depending on their energy. Through Compton scattering or pair production, an energetic electron, or e^+/e^- pair may be created. Electrons or positrons with sufficient energy to produce Čerenkov light are detected as described above. The detection threshold for gamma rays is slightly higher

than that of an electron, as the Compton scattered electrons (which is the dominant process at the relevant energies) have somewhat less energy than the incoming gamma ray.

Neutron detection is critical to SNO's solar neutrino measurement, and three methods of neutron detection are planned over three 1 year phases of running. In the pure D_2O phase, neutrons are detected by the single 6.25 MeV gamma ray produced when neutrons capture on deuterium. The neutron capture efficiency on pure D_2O is quite low (24%), and the mean capture time is quite long (40 ms). In the salt phase, NaCl is added to the D_2O to increase the neutron sensitivity. Neutrons are readily captured on ^{35}Cl, and detected by the multiple gamma rays produced (total 8.6 MeV). The capture efficiency for this process is much higher (83%), and the mean capture time is much shorter (4ms). In the NCD (Neutral Current Detector) phase, dedicated ^3He neutron counters are deployed in the D_2O to measure the neutron flux independent of the PMT array. The neutron capture efficiency of the NCD array is approximately 37%, with an average capture time of 16ms[15].

2.1.3 Neutrino Interactions

Neutrinos can interact with electrons, deuterons, and oxygen nuclei in the D_2O, and electrons, protons, and oxygen nuclei in the H_2O to produce detectable particles. The majority of the detectable interactions occur with electrons, deuterons, and protons due to the high energy threshold for the oxygen interactions. Table 2.1 shows a list of neutrino interactions detectable by SNO, including the interaction energy threshold and the detectable secondary particles. The neutrino interactions are often grouped into three classes, charged current (CC), neutral current (NC), and elastic scattering (ES).

Charged current interactions involve the exchange of a charged $W^{\pm}$ particle. Only electron neutrinos and electron antineutrinos take part in the charged current inter-

Reaction	Region	Energy Threshold (MeV)	Detected Particles
Charged Current:			
$\overline{\nu}_e + p \rightarrow n + e^+$	H_2O	1.806	e^+
$\nu_e + d \rightarrow p + p + e^-$	D_2O	1.442	e^-
Neutral Current:			
$\nu_x + d \rightarrow \nu_x + p + n$	D_2O	2.225	n
$\overline{\nu}_x + d \rightarrow \overline{\nu}_x + p + n$	D_2O	2.225	n
Elastic Scattering:			
$\nu_x + e^- \rightarrow \nu_x + e^-$	D_2O	0.0	e^-
$\overline{\nu}_x + e^- \rightarrow \overline{\nu}_x + e^-$	D_2O	0.0	e^-
$\nu_x + e^- \rightarrow \nu_x + e^-$	H_2O	0.0	e^-
$\overline{\nu}_x + e^- \rightarrow \overline{\nu}_x + e^-$	H_2O	0.0	e^-

Table 2.1: Detectable neutrino interactions in the H_2O and D_2O are classified as Charged Current (CC), Neutral Current (NC), or Elastic Scattering (ES).

actions. Neutral current interactions involve the exchange of a neutral Z^0 particle. Neutrinos of all flavours (ν_x: electron, muon, tau) can take part equally in the neutral current interactions. Elastic scattering interactions are neutrino electron scattering interactions, and occur through both the charged current and neutral current processes. All flavours of neutrinos take part in elastic scattering equally through the neutral current process, but electron neutrinos can also take part through the charged current interaction. The net result is that the combined elastic scattering cross section for ν_μ and ν_τ is approximately 15% that of ν_e.

2.2 Supernova Neutrino Signal

2.2.1 Supernova Monte Carlo

In order to understand the response of the SNO detector to the expected supernova neutrino signal, a Monte Carlo simulation program has been developed by Jaret Heise[14]. The simulation consists of a supernova generator which creates a list of neutrino interactions and detected particles for a model supernova, and a SNOMAN analysis (SNOMAN is the SNO detector Monte Carlo software[16]) which describes the detector response to the list of particles.

In the generator, neutrinos are emitted from a supernova with time and energy spectra given by one of several different models, including those of Burrows[9], Beacom and Vogel[13], Bruenn[17], and Liebendorfer[18]. The distance from the source to the detector is specified, and the luminosity is scaled appropriately. The number of interactions occurring in the detector through a given detection reaction (those listed in Table 2.1) then depends on the interaction cross section and the number of target particles for that interaction.

For an interaction with cross section $\sigma(E_\nu)$ and N_t targets, the number of interactions in the detector (N_{det}) for a supernova with neutrino time and energy flux $\frac{d^2N_{src}}{dE_\nu dt}$, occurring at a distance D, is given by:

$$N_{det} = N_t \frac{1}{4\pi D^2} \int_0^\infty \int_0^\infty \sigma(E_\nu) \frac{d^2N_{src}}{dE_\nu dt} dE_\nu dt \tag{2.2}$$

For each detection reaction, N_{det} neutrino interactions are generated, choosing time and energy randomly sampled from the supernova model flux distributions. The final state particles from each neutrino interaction are then sampled from the differential cross sections of the interaction, with the energy, time, and direction governed by the kinematics of the interaction.

The interaction positions are distributed randomly within the appropriate detector

volume, and the response of the detector is simulated by the SNOMAN program.

2.2.2 Distance Sensitivity

Using Burrows 10 $M_\odot$ model as a nominal supernova, Figure 2.2 illustrates SNO's sensitivity to supernovae as a function of distance in terms of number of events detected. Also highlighted are some points of reference for the stars in our galactic neighborhood.

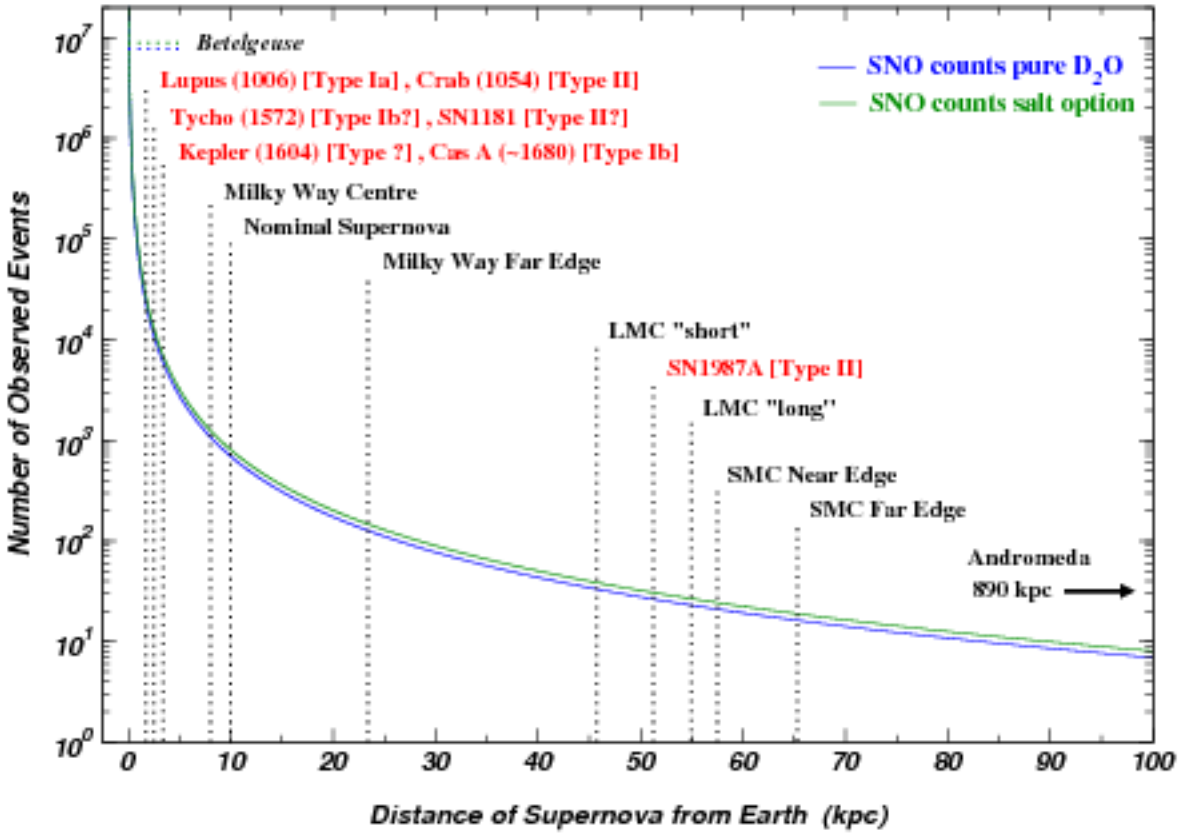

Figure 2.2: Number of events detected for a nominal supernova during salt and D_2O neutron detection phases, and some highlights of the Milky Way galaxy.

The Milky Way galaxy is approximately 30 kpc in diameter, with our star (and earth, the planet) located towards the edge, approximately 8 kpc from the center.

The nearest supernova candidate star is Betelgeuse (Alpha Orionis), a scant 130 pc away. A supernova at this distance would produce several million events in SNO. At about 24 kpc, the most distant stars in the galaxy are on the far edge of the galactic disc. A supernova at this distance would produce on the order of 100 events in SNO.

Outside of the Milky Way galaxy there is a large expanse of relatively empty space (star wise) before encountering the first of two small satellite galaxies called the Large and Small Magellanic Clouds (LMC and SMC). A supernova in one of these clusters of stars (the LMC was the location of SN1987A) would produce a few tens of events in SNO.

Beyond the Magellanic Clouds there are effectively no stars until reaching Andromeda, the next neighboring galaxy at a distant 890 kpc. A supernova at that distance would produce less than 1 event in SNO.

2.2.3 Signal From a Nominal Supernova

Using Burrows 10 $M_{\odot}$ model at a distance of 10 kpc as a nominal supernova, the supernova generator indicates total event counts of 620, 795, and 683 depending on the neutron detection scheme being used; D_2O, Salt, and NCD respectively. Table 2.2 shows the contributions to the counts from neutrino type, interaction type, and interaction region. Some of the generic features expected of a supernova signal are illustrated in Figure 2.3, including the vertex position, angle, time, and energy distributions of the events.

Interaction Vertex Distribution

The neutrino signal arrives as a plane wave, exposing all parts of the detector to the same neutrino flux. Differences in the cross sections as well as the overall volumes of the H_2O and D_2O regions lead to differences in the number of events occurring in the two volumes. Aside from this difference between the D_2O and H_2O volumes, event

Reaction	**Total Detected Counts**		
	D_2O	**Salt**	**NCDs**
Charged Current:	492	543	510
Neutral Current:	96	220	140
Elastic Scattering:	31	31	31
Total SNO ν_e Events	111	128	118
Total SNO $\overline{\nu}_e$ Events	430	498	454
Total SNO $\nu_{\mu,\tau}$ Events	78	168	110
Total SNO D_2O Events	280	455	343
Total SNO H_2O Events	339	339	339
Total SNO $e^{\pm}$ Events	484	484	484
Total SNO n Events	136	311	198
Total SNO Events	**620**	**795**	**683**
Total SNO Events (with O)	**632**	**807**	**695**

Table 2.2: Number of events detected for the three neutron detection phases. The events are roughly evenly distributed between the heavy and light water, with slightly less than half in the heavy water during the pure D_2O phase, and slightly more than half during the salt phase.

positions are distributed more or less evenly and randomly throughout the detector.

Angular Distribution

Elastic scattering interactions exhibit an energy dependent correlation between incident neutrino direction and scattered electron direction, favouring electron scatter in the forward direction. The contribution to the signal from elastic scattering gives rise to a spike in the angular distribution in the opposite direction to the supernova. The charged current interactions also exhibit a weak correlation with neutrino direction, and give rise to a slight overall gradient in the angular distribution. As well as helping to recognize a supernova burst, the angular distribution of events can be used to determine the location of the supernova.

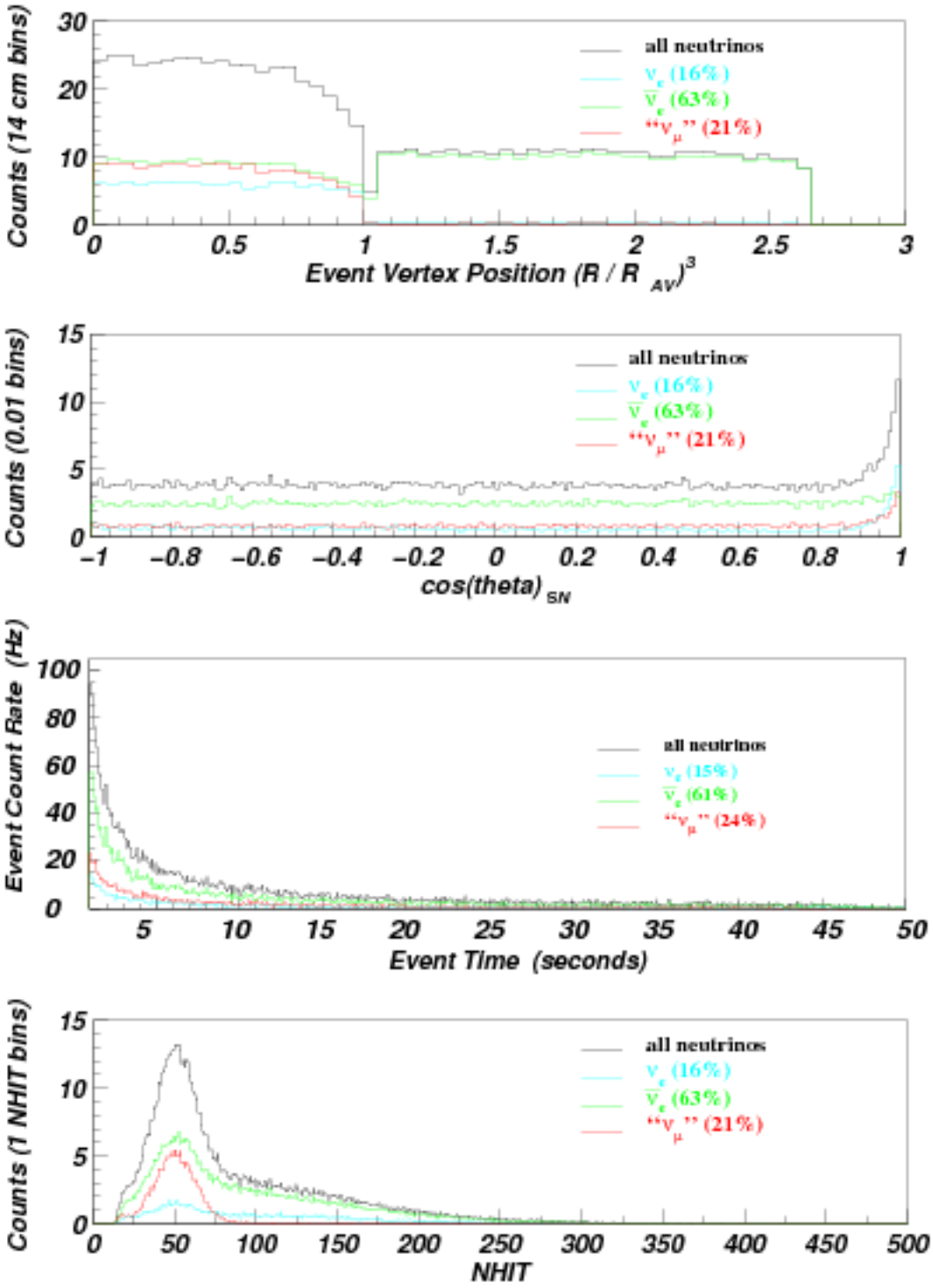

Figure 2.3: Many of the features of a generic supernova are noticable in the Monte Carlo data generated for a supernova at 10 kpc using the Burrows model. Figure courtesy J. Heise.

Time Distribution

Overall, the event rate rises quickly and decays over most of a minute, with roughly 50% of the events occurring in the first 1-2 seconds. Some features of the time distribution are model dependent, and the fine details of the first second during the explosion are not shown in Figure 2.3. The enhancement of ν_e flux due to neutronization is however noticeable in an expanded plot of time.

Energy (NHIT) Distribution

The energy distribution exhibits a large peak at around the neutron capture energy (8.6 MeV or about 48 NHIT) during the salt phase of running. A broad distribution extending up to several tens of MeV underlying the neutron peak is also evident. This high energy tail extends well above the solar neutrino spectrum, and distinguishes the events from the solar neutrino background.

2.3 Supernova Backgrounds

Sources of background in SNO are usually discussed with reference to the solar neutrino signal, which is on the order of events per day. Backgrounds of this magnitude are negligible to the supernova signal which is on the order of Hz to kHz. Although there are few natural backgrounds of this magnitude, there are several induced by instrumental effects.

The only sources of background known to give rise to multiple synchronous physics events in the detector are high energy cosmic ray muons. A high energy muon may penetrate the overburden of rock, and arrive in the detector volume with a considerable amount of energy. The energy of such a muon is sufficient to dissociate an oxygen nucleus in either the H_2O or D_2O. This can give rise to multiple spallation products which are detected as a burst of events with neutron capture energies, and

a rate falling off in accordance with the neutron capture time.

A muon may also undergo deep inelastic lepto-quark scattering in which a high energy muon interacts directly with a proton, completely dissociating it and creating multiple pions. Pions quickly decay to muons, which quickly decay to electrons and neutrinos. This causes a large number of events to be detected, many with neutron capture energies, and some with higher energies due to muon decays, with the rate falling off as a combination of the neutron capture time and the muon decay time. Both types of muon induced bursts can be identified by the high NHIT muon event immediately preceding the burst, as well as by the characteristic NHIT and time distributions.

Since continuous supernova monitoring is carried out in SNO, sources of instrumental background attributed to calibration activities must be considered. Several calibration sources are periodically deployed into the detector using the source manipulator system. This system consists of a source mounting head connected to an umbilical for deployment in the D_2O and in the H_2O. The umbilical contains lines for instrumentation, gas transport, and light transmission.

Calibration sources give rise to an increased rate of real physics events, and two methods of coping with this increase are used in the supernova monitoring system. Some sources provide an independent tag of calibration events through the detector trigger system, allowing these events to be discarded at a low level. Sources which do not tag calibration events require the supernova monitoring system to discard all events below an appropriate NHIT during the source deployment.

In addition to events from the calibration source itself, movement of the manipulator system induces large bursts of events, likely from static discharge as the umbilical cable is moved. The events caused by this background can be high in NHIT, and must be identified as non-physical and removed by higher level cuts.

The detector is in general a very sensitive piece of equipment, and is subject to

bursts of events from several other sources including electrical pickup, PMT failure, electronics failure, abnormal water circulation, and seismic activity. Several of these instrumental burst sources are discussed further in Chapters 3 and 4.

Chapter 3

Supernova Monitor Implementation

> Even if they have the millions of dollars needed for a space station vacation, delinquents, liars, drunks and the infamous need not apply.
> - NASA (AP)

3.1 Overview

The supernova monitoring system works in concert with components of the SNO datastream to detect and evaluate spikes in the signal rate and provide the appropriate level of notification to the detector operator, the SNO supernova experts, and the international supernova watch community. The monitoring system consists of three levels. Figure 3.1 illustrates how these levels are integrated with the electronics system, the data acquisition system (DAQ), and the data analysis software.

Event triggering and measurement of PMT pulses are performed by the electronics system. The time and integrated charge of PMT pulses, along with the event trigger information, are read out by the DAQ system and built into an event record. This event record is a brief snapshot of the overall signal, and forms the basic unit of signal measurement. Events are recorded to tape archive for later analysis, and 'dispatched' over ethernet for data monitoring in near-to-realtime. The event data can be monitored without interfering with the archive data by accessing this dispatched

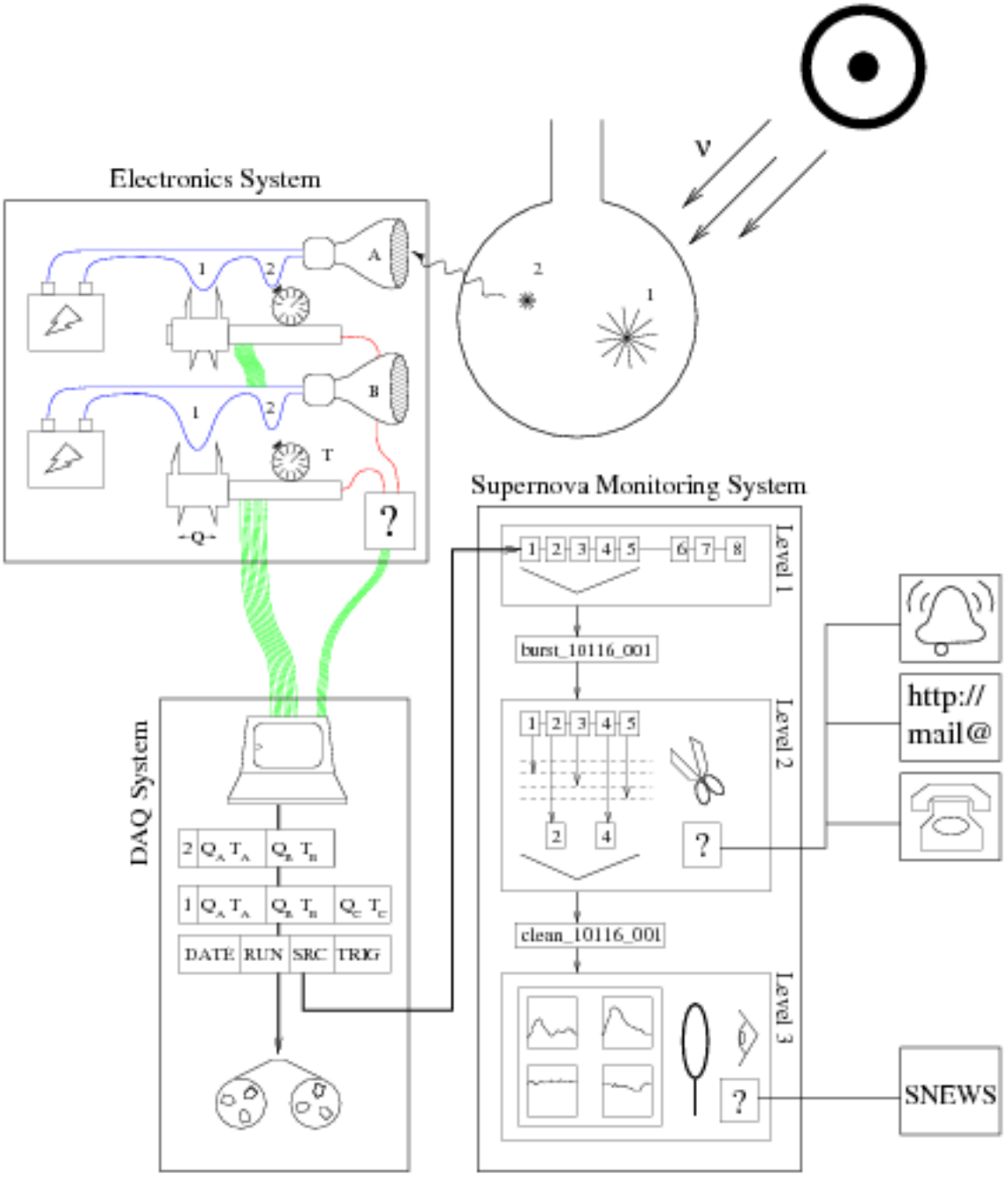

Figure 3.1: The Supernova Monitoring System makes use of the dispatched datastream to monitor for bursts of events, determine the source of the burst, and provide prompt notification.

datastream.

The level 1 system monitors event data through the dispatched datastream, defines a burst criteria, and writes bursts of events to burst files. The level 2 system analyzes the burst files, and identifies significant bursts based on the fraction of events passing a set of data cleaning cuts. Notification and summary of the level 2 analysis is provided to the detector operator and a group of supernova experts by phone, email, and audiovisual alerts. The level 3 system performs event reconstruction on the surviving events of significant bursts. A summary of the level 3 analysis, including several plots of event distributions, is presented to the supernova experts who perform the final evaluation of the burst source. If it is concluded that supernova neutrinos are a possible source of the burst, the astronomical community is notified through the Supernova Early Warning System (SNEWS)[19]. SNEWS requires a coincident alert from multiple supernova-capable detectors to alert the astronomical community.

The supernova monitoring system was developed by the supernova working group of the SNO collaboration. This group includes C. Virtue (Laurentian), R. Tafirout (Laurentian), Jaret Heise (UBC), and the author. The contributions of the author are mainly in the level 1 monitoring system, the dialout computer system, and the audio-visual operator alerts. The evaluation of performance described in chapter 4 is also the work of the author.

3.2 SNO Data

In order to discuss the implementation of the supernova monitoring system in detail, a fairly deep understanding of the SNO data and the tools used to study it is required. This discussion proceeds by describing the format of the SNO data, starting with the datastream shown in Figure 3.2.

3.2.1 Datastream

Although the datastream is actually a continuous flow of data, it is logically divided into runs for ease of analysis. Each run indicates a period of static detector configuration which is controlled by a user interface program called SHaRC (SNO Hardware and Run Control). Detector configuration information is incorporated into the datastream in the form of the Run Record and the Trig Record.

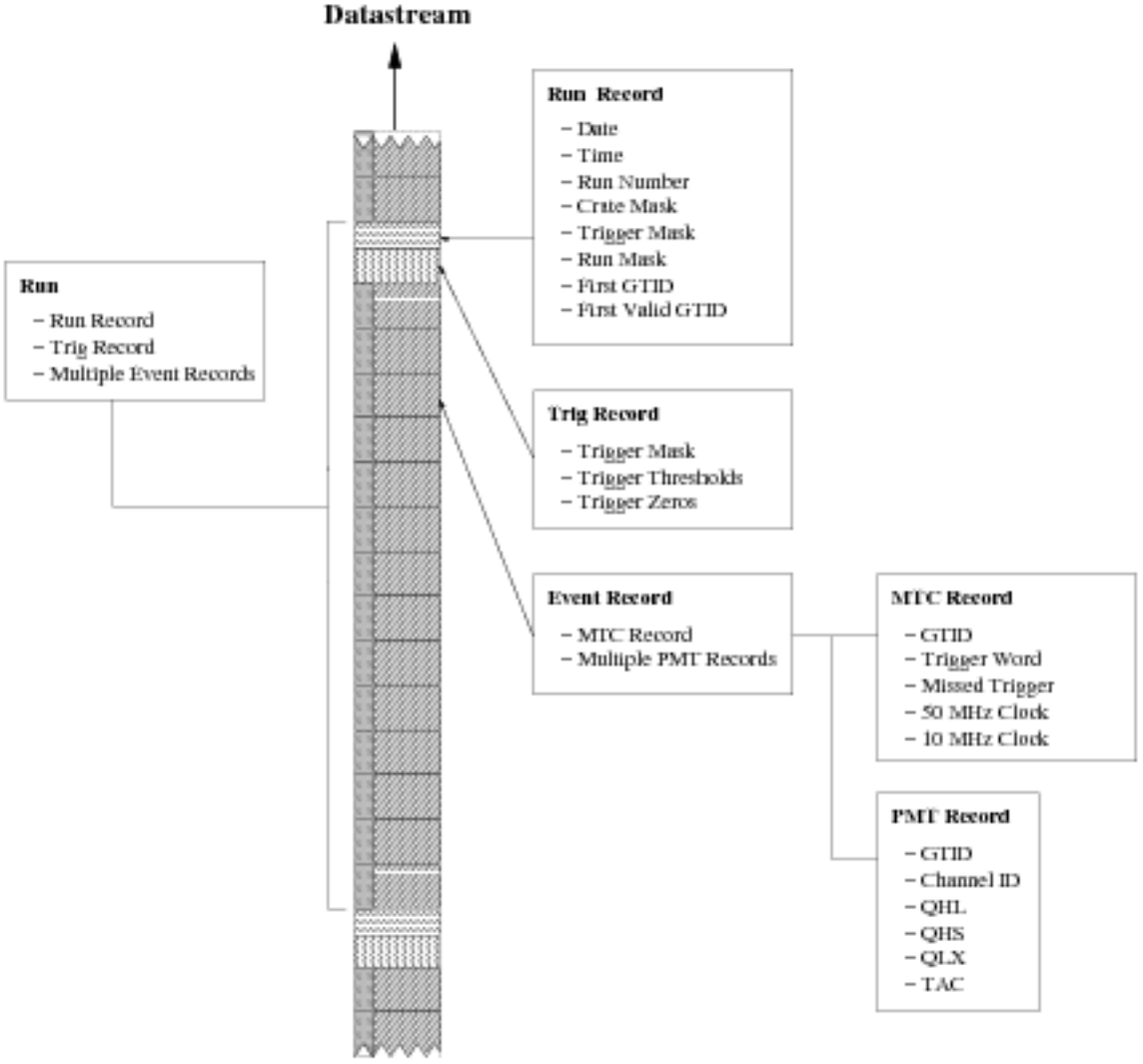

Figure 3.2: The SNO datastream, which is written to tape archive and dispatched pseudo-realtime over the network.

Run and Trig Records

In addition to the date, time, and run number, the Run Record contains three bit-masks. The crate mask indicates which of the 19 crates of signal processing electronics are enabled, the source mask indicates what source (if any) is deployed in the detector, and the run mask indicates which of a set of predefined run conditions are in effect. Two GTID numbers (see Trigger System) which identify the first events of the run are also included in the Run Record. Specifically, these GTIDs identify the first overall event of the run, and the first event after which all hardware changes have taken effect.

The Trig Record contains data which describes the status of the trigger system for the run. The trigger system is complex, and crucial to understanding the data. A description of the trigger system, including the contents of the Trig Record is given below.

Trigger System

The trigger system is part of the electronics system, as shown in Figure 3.3. Signals from the PMT array itself (physics triggers), as well as those from other sources are used to trigger the detector.

The primary physics trigger is called NHIT100, and constitutes a measure of the number of tubes which have detected light within a sliding 100 nanosecond time window. The signal for this trigger is constructed from up to 9438 uniform height 100 ns wide square pulses. These pulses are generated by the PMT channels when their discriminators fire, and are combined in a fast detector-wide analog summation. A similar signal called NHIT20 is constructed from 20 ns wide pulses. The ESUM signal (Energy Summation) is a detector wide summation of the shaped PMT pulses, and forms another physics trigger. Two final physics triggers called OWLN and OWLE are formed from the NHIT and energy summations of a small set of tubes mounted

on the outside of the PSUP (OutWard Looking tubes).

Several calibration sources are capable of producing suitable trigger signals, and occupy the external triggers (EXT_3-8). A hydrophone installed in the H_2O volume is permanently connected to the EXT_2 trigger, which is now called the HYDRO trigger. Two triggers called PONG and SYNC are used by the timing system (see Event Timing). The PGT trigger (Pulsed Global Trigger) is used mainly for detector diagnostics, and is triggered at a constant rate by a pulsed signal. The period of this signal is programmed by the DAQ system and is recorded in the Trig Record.

The Master Trigger Card (MTC) monitors for pulses in the trigger signals, and consists of an analog and a digital component. The analog component of the MTC contains many discriminators, providing up to three detector triggers per trigger signal (e.g. NHIT100 hi/med/lo). When a trigger discriminator fires, a signal is sent to the digital component of the MTC. There a trigger mask is consulted, to determine if the trigger is enabled. The trigger mask, the discriminator thresholds, and the trigger zeros, are programmed by SHaRC and are recorded in the Trig Record. When a discriminator fires on an enabled trigger, the MTC issues a Global Trigger (GT) pulse.

Whenever a GT pulse is issued, a 24 bit counter on the MTC is incremented. This number is called the GTID (Global Trigger ID) and is the primary way of identifying data within a run. Upon receiving a GT signal, the front end electronics updates a local copy of the GTID counter. Any PMT measurements made within the past few hundred nanoseconds are then stored along with the GTID.

Event Record

Events must be assembled from the asynchronously acquired PMT and MTC data, based on their GTIDs. This is performed by the Builder, a program running on a SUN workstation as shown in Figure 3.4. The Builder acquires MTC and PMT data from

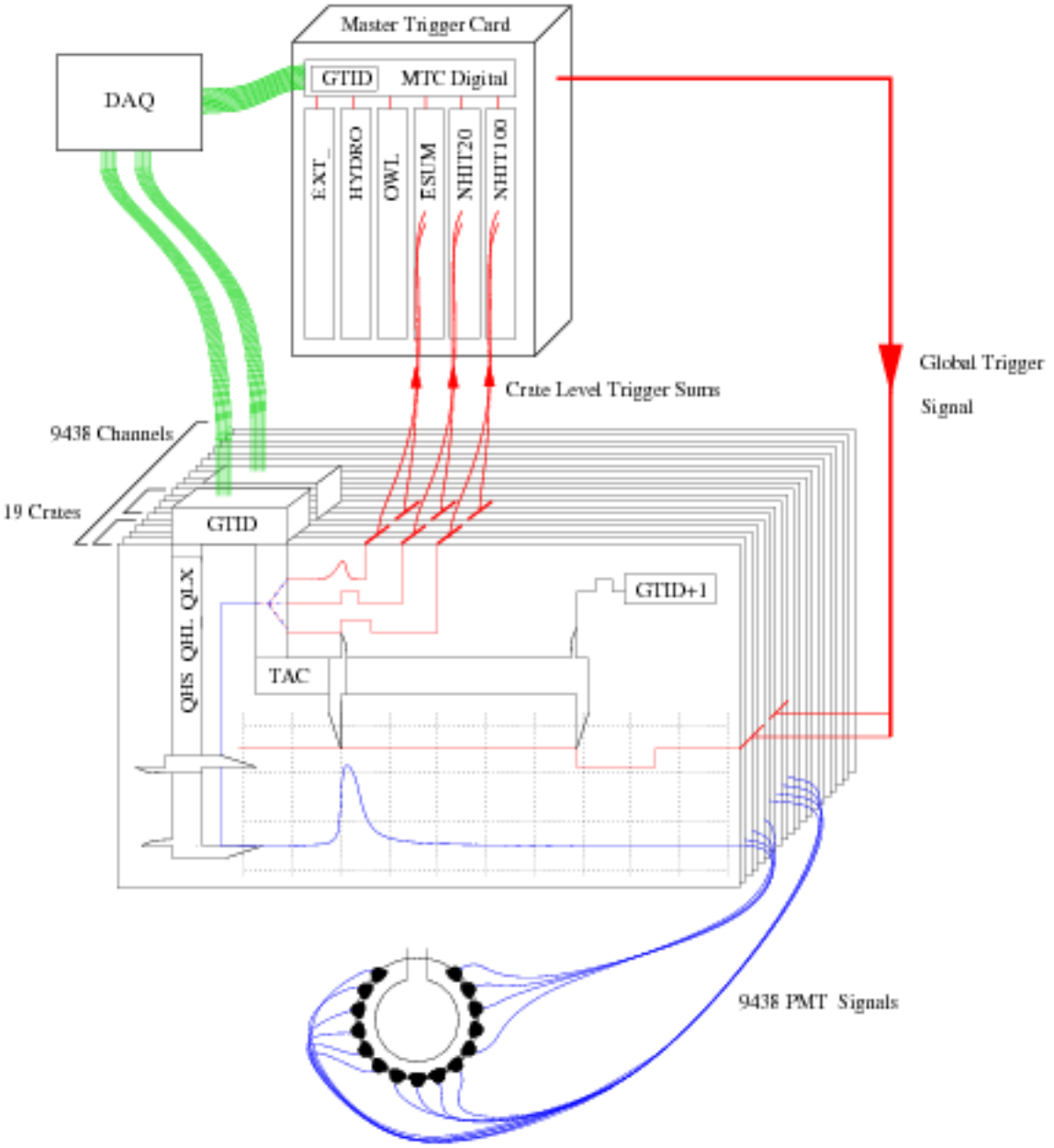

Figure 3.3: The SNO electronics provides sub-nanosecond charge and time measurement of 9500 PMT pulses and prepares them for readout by the data acquisition system.

two circular buffers, and holds it for as long as possible, waiting for late data packets. Data which cannot be built into an event becomes orphan data, and often ends up as an event with a GTID number of zero. This happens in high rate situations (kHz for supernova neutrino energies) as a result of buffer overflows. A properly built Event Record is identified by a valid GTID number, and consists of one MTC Record and the appropriate number of PMT Records.

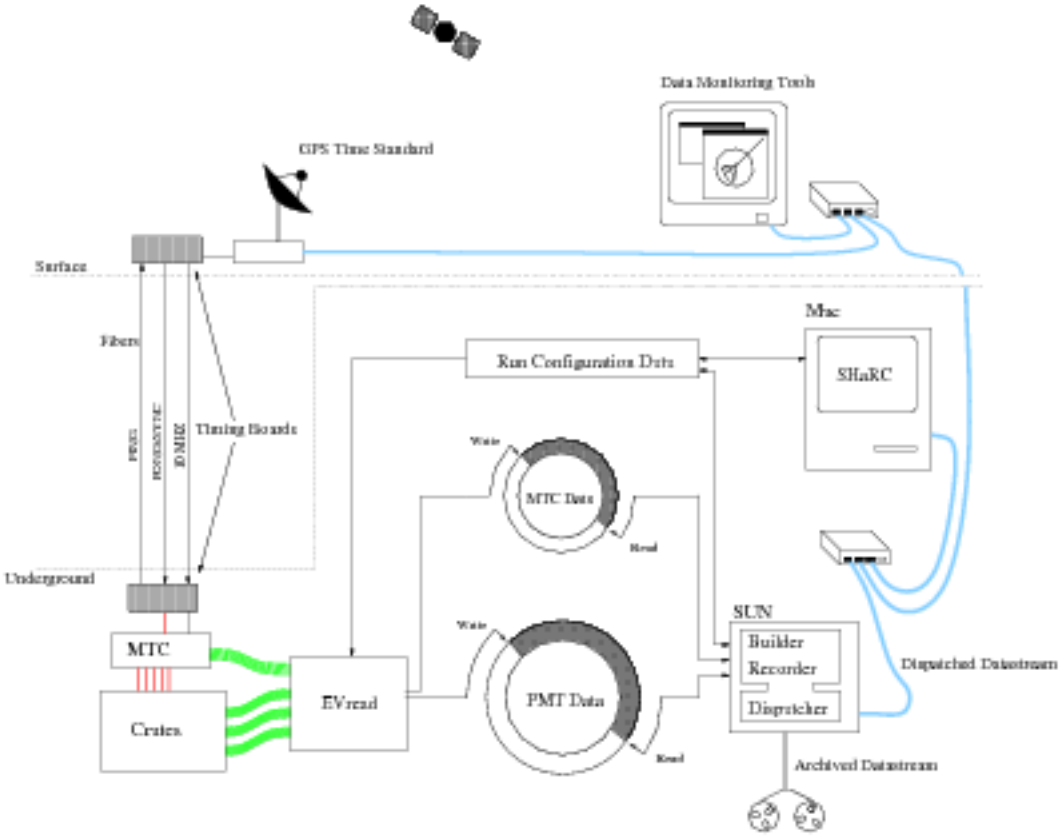

Figure 3.4: The DAQ system controls the configuration and the read-out of the front end electronics. The configuration information and the read out data are assembled into the SNO datastream.

Along with the GTID of the event, the MTC Record contains trigger information, and event timing information. The triggers which fired to form the event are indicated by the Trigger Word. Triggers which fire after the formation of the event, but before

the lockout time for the next event are indicated by the Missed Trigger bit. The 10 and 50 MHz clocks contain the event timing information. Event timing is important for supernova data, and is discussed in some detail below.

Event Timing

Two counters on the MTC keep track of the passage of time. One counter is incremented at 50 MHz and contains 43 bits, meaning that it will roll over approximately every two days. This counter is driven by a 100 MHz free running quartz oscillator, and is not tied to any absolute time standard. The purpose of this counter is to provide accurate inter-event time interval measurements, with approximately 20 ns precision.

The other counter is incremented at 10 MHz, contains 53 bits, and will not roll over for approximately 28 years. When set properly, the value of this counter is equal to the number of 10 MHz cycles which have occurred since Midnight January 1 1996. To stay in synchronization with an external time standard, the 10 MHz clock is driven by a GPS disciplined oscillator. A commercial GPS unit located at the surface lab building generates a 10 MHz pulse train, the frequency of which is steered to stay synchronized with the frequency of atomic clocks on the GPS satellites. The pulse train is transmitted from surface to underground through a fiber optic cable where it is used to increment the counter.

A total of three fiber optic cables, and two small boards are used by the 10 MHz clock system. The two boards, one on surface and one underground, interface the GPS unit and the MTC to the fiber optic links. One fiber is dedicated to the transmission of the 10 MHz pulse train, while the other two are used for synchronizing the counter and measuring the fiber delay time. In order to set the 10 MHz clock, SHaRC requests the MTC to load an appropriate time into a register, and for the GPS unit to provide a SYNC pulse for that same time. Upon receiving the SYNC pulse, the new time is

loaded from the register into the counter between 10 MHz pulses.

Each SYNC pulse generates a Global Trigger signal, forming an event stamped with the newly loaded time. Upon receiving a SYNC pulse underground, the timing boards exchange PING and PONG signals to measure the fiber delay. Upon receiving a PONG signal underground, another event is formed. By comparing the times of the SYNC and PONG signals, the round trip fiber delay can be measured to within 20 ns[20].

PMT Record

PMT Records form the remainder of the event record, and also the majority of the datastream. Each PMT Record contains a GTID number, a channel identification number, and PMT pulse measurement data. The channel identifier indicates which tube the data is from, and the GTID indicates which event.

PMT pulse measurement data consists of a time measurement and three charge measurements. These measurements are performed by a custom built chipset consisting of dynamic range integrator, a fast discriminator, and a time sequencer.

Charge data is acquired by integration of the PMT signal after the discriminator fires. Two high gain measures, performed over a long and a short integration time, form the QHL and QHS charge data. The third charge measurement is performed at a lower gain and forms the QLX charge data. The low gain measure is performed over either a long or short time, programmable by the DAQ. The low gain measure allows pulses to be measured when the high gain measurements are saturated.

The PMT pulse time measurement is started when the channel discriminator fires. If a Global Trigger signal is received within approximately 200 ns of the discriminator firing, the measurement is stopped, otherwise the timer is reset. This measurement specifies the PMT pulse time relative to other PMTs in the event with sub-nanosecond resolution. This measurement forms the PMT time data called the TAC.

3.2.2 SNO Database

A database called SNOdb contains slowly varying detector parameters not included in the datastream. This includes 'static' variables such as physical constants. SNOdb contains such things as; the geometry and composition of the detector, such as where all the PMTs are located and where the D_2O volume is; electronic calibrations such as what the pedestal value of channel #4327 is; hardware information such as which channels have been removed or physically disabled; 'invariable' physical properties such as the speed of light in pure D_2O; astronomical information such as where to find the sun on June 24 2023; and lots of other information of import when accurately reconstructing the source of the signal.

Every database entry has a validity range, indicating the period of time that value is to be considered valid. Calibration constants for example are valid only until the next calibration is performed.

3.2.3 Offline Data Analysis

The datastream is written to disk and to tape by the Recorder as shown in Figure 3.4. It is converted to the CERN zebra [21] format before being written to "zdab" files, which are named according to run and sub-run numbers (e.g. SNO_0000023960_001.zdab). The subrun numbers serve to limit the individual file size to under 176 Mb.

SNOMAN is the program used to analyze SNO zdab files. SNOMAN combines the physical state of the detector as recorded in SNOdb, with the observed signal recorded in the zdab files. Loading the entire database, with years of calibration data, is costly in CPU cycles and memory. SNOMAN can be run without the database, instead loading the detector parameters from text files called 'titles' files. This can be faster and easier for some analyses.

Data Cleaning Cuts

Significant effort by the collaboration was put into developing a set of cuts aimed at removing instrumental background events. Cuts are either designed to identify a known source of background, or to identify events with characteristics unphysical for a Čerenkov event. These data cleaning cuts are used for off-line data reduction in the unified solar neutrino analysis and are very well documented.[22][23][24][25][26][27] The supernova monitoring system uses a subset of the data cleaning cuts when evaluating bursts.

Not all of the data cleaning cuts are appropriate for evaluating bursts, as they may cut valid supernova events (e.g. the 'burst' cut would be a bad idea). The data cleaning cuts that are used by the supernova monitoring system system are:

AMB Cut The Analog Measurement Board (AMB) measures the peak, integral, and derivative of the analog trigger sum at threshold crossing. The AMB cut removes events for which the peak measurement of the ESUMHI signal is more than 3.7σ away from the average value for the appropriate NHIT. This removes many types of non-physics events, including e.g. events due to a noisy PMT.

Neck Cut Four PMTs are installed in the neck of the acrylic vessel to identify a type of event in which light is apparently generated around the neck of the detector. The Neck cut removes events in which at least two neck tubes are hit, or only one is hit with slightly high charge and early time. Neck events tend to light up tubes at the bottom of the detector.

QvT Cut The Charge vs. Time cut removes events in which the maximum PMT charge is more than a set amount away from the average value, and the TAC is more than a set time earlier than the median channel time.

FTS Cut The Fitter-less Time Spread cut removes events in which the median tube-to-tube pairwise time-spread exceeds a set value, for tubes occurring early in

the event, and within close proximity.

QvN The Charge vs. NHIT removes events for which most of the charge is deposited in only a few channels.

Iso The Isotropy cut removes events where more than 70% of the hits occur on one crate, and more than 80% of those hits occur on two adjacent cards. This makes use of the fact that a large discharge signal on one channel is picked up by adjacent channels in the crate.

ROF Cut The Ring Of Fire cut removes events in which most of the hits occur in the two outer slots of a crate (0 and 15). This is effectively the isotropy cut with a wrap around from slot 0 to slot 15.

QCl Cut The Charge Cluster cut removes events in which four or more channels within a five channel window are hit, and at least one has high charge.

ITC Cut The In-Time Cut removes events in which the ratio of number of early hits in a short time window to the total number of hits is small.

FGC Cut "Flasher" events are caused by microdischarges in the dynode chain of the PMT. Light escapes from the face of the PMT and is detected by tubes on the opposite side of the detector. The Flasher Geometry Cut removes events in which a tight cluster of hits is accompanied by several hits slightly later on the other side of the PSUP.

MUON Cut The Muon Cut is not used as a cut, but as a tag. The muon cut identifies events with high NHIT, and OWL tubes.

Event Reconstruction

Using various fitting routines, SNOMAN can attempt to reconstruct the energy, position, and direction of detected particles from event records. Two basic fitters are

the Elastic Fitter and the Time Fitter.

Time Fitter The Time Fitter assumes that photons move from a point within the detector to the PMTs without any refraction, reflection, or scattering. PMT hits which are obviously out of time are excluded, and the times and locations of the remaining PMT's are used in the fit. The fit parameters are the X,Y,Z, and time coordinates of the event. A routine calculates the expected hit time, and the derivative of the hit time, for each PMT given the current values of the fit parameters. A nonlinear least squares algorithm (Levenberg-Marquart) is then used to find the best fit values of position and time. The fitter then uses the vectors from the hit PMTs to the fitted vertex to find the event direction. The direction which gives the least squared deviation from these vectors is the event direction.

Elastic Fitter The Elastic Fitter is basically a fancy time fitter with a minimisation that uses a simulated annealing technique. In addition, a different method for ignoring out of time or noise hits as the fit proceeds is used. This fitter also performs a fit for direction.

3.2.4 Online Data Monitoring

As well as being recorded to disk for offline analysis, the datastream is also made available for near-to realtime monitoring. Through shared memory on the SUN workstation, the Dispatcher has access to the entire datastream from the Builder/Recorder. Data in the form of built events, or as raw packets, can be received through the network by dispatcher client applications. A client registers with the Dispatcher, subscribing for a subset of the data under specific flags such as PMT data, MTC data, TRIG data, etc.

The two primary data monitoring tools which connect to the Dispatcher are Xsnoed for examining individual events, and Snostream for examining data trends. Xs-

noed is a highly visual tool. A histogram of PMT data (QHL, QHS, QLX, or TAC) sets the colour scheme for several projections of PMT hits, including a 3D geodescic view, electronics crate map, and several flat maps. Several text windows are also available, displaying event and hit information. Snostream displays mainly histograms, and has hundreds to choose from. Histograms of rate, or cumulative counts, for every crate, card, and channel can be displayed on a single screen of histograms. A stacked strip chart of event trigger rates is usually displayed, along with an NHIT distribution, and perhaps a 2D histogram of crate and card counts. Figure 3.5 is a cluttered screenshot, showing windows from both Xsnoed and Snostream.

3.3 Supernova Monitoring: Level 1

3.3.1 Introduction

The purpose of the level 1 supernova system is to monitor the dispatched datastream and record bursts of events for further analysis. A burst is defined as the occurrence of more than N_{event} events within T_{win} milliseconds each with NHIT > $NHIT_{min}$. These three parameters define the level 1 threshold, and are assigned dynamically depending on detector configuration.

The level 1 system is written as an extension to the monitoring tool Snostream. Snostream runs on one of two dedicated supernova monitoring/analysis computers named Betelgeuse and Sanduleak which are dual processor x86 PCs running the Solaris 8 operating system. Incorporating the level 1 system into an actively used monitoring tool provides access to the datastream with no additional load on the Dispatcher, and also assures continuous human monitoring.

Before discussing the operation of the system, here is a list of the files used for input and output by the level 1 system.

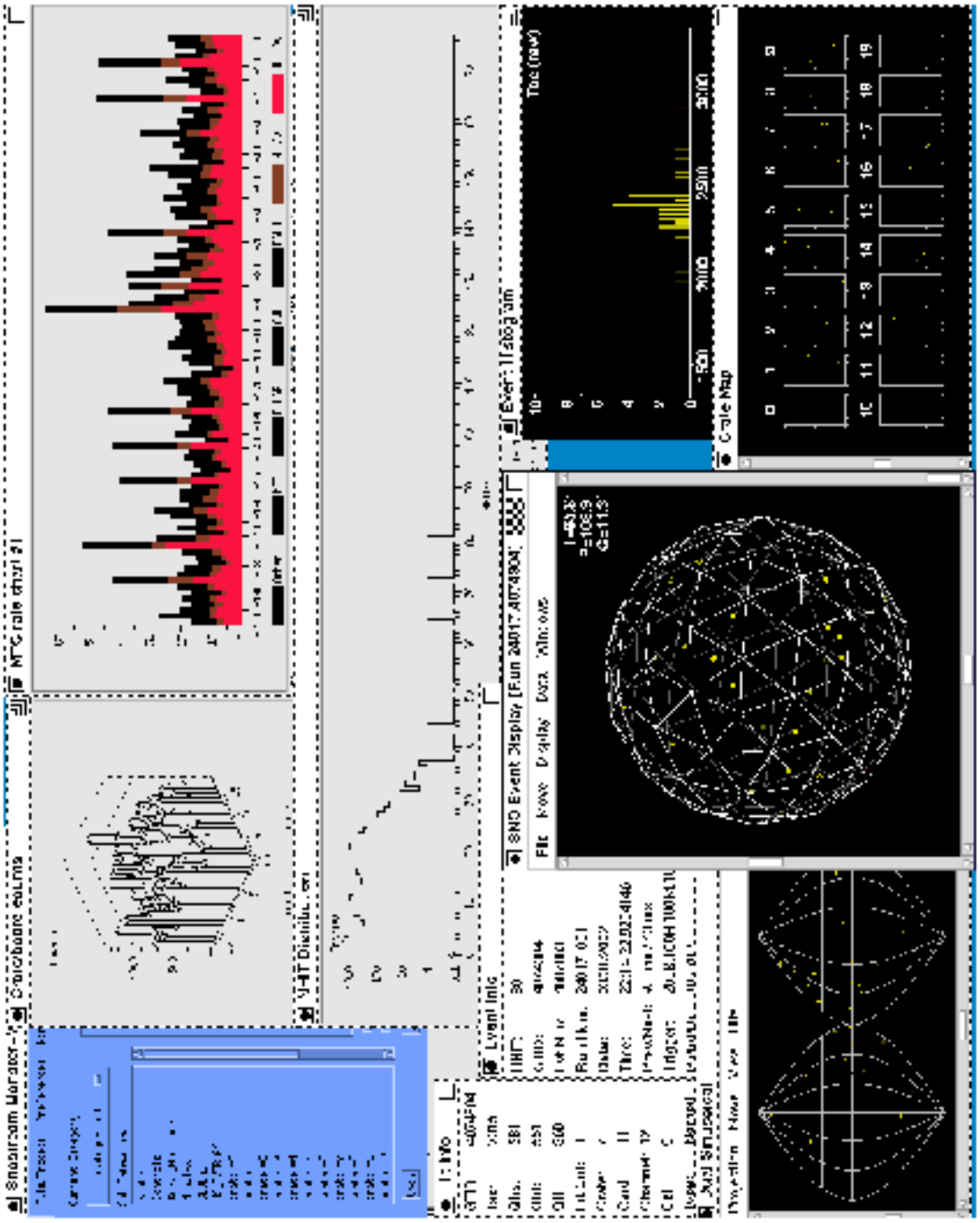

Figure 3.5: Xsnoed and Snostream are used by the detector operator to monitor the event data and data rates. Windows from Snostream are shown in the upper portion of the screen, and Xsnoed in the lower.

3.3.2 Files

Most files reside in a directory called snwatch, which is located in /scratch/lt/sstream/snwatch on each of the supernova computers Betelgeuse and Sanduleak.

Threshold Initialization File (trig.ini) This file contains the burst parameters for various run conditions. It is read on startup by Snostream, and located in the directory from which Snostream is executed (/users/sstream/snostream/).

Snostream Lock File (sstream.lock) This file prevents multiple instances of Snostream from trying to write files at the same time. On startup, Snostream runs in read only mode if the file is found to be locked.

This file is also used to preserve information across Snostream restarts, including the run number, burst number, and burst parameters.

Burst zdab Files (e.g. burst_20343_001.zdab) These files contain the burst data in standard SNO data format. Each file contains a Run Record, a Trig Record, and a burst of Event Records. The files are named according to the run number and burst number.

Log File (burst_log.ss) This file records the activity of the level 1 system. Entries include trigger started, run header caught, and burst detected. An example is shown in Figure 3.6.

Level 2 Initialization Script (supernova.sh) This is a Unix shell script which initiates the level 2 supernova system whenever a burst file is written.

3.3.3 Dynamic Thresholds

The run and source masks contained in the Run Record are used to set the level 1 threshold. A set of unique burst parameters for each run type and source type can be

defined in the threshold initialization file. Currently dynamic burst parameters are defined for the following conditions:

Default ($\mathrm{NHIT}_{min} = 35$, $\mathrm{N}_{event} = 30$, $\mathrm{T}_{win} = 2000$)

The default threshold provides supernova distance sensitivity beyond the far edge of the galaxy, while maintaining a manageable rate of level 1 bursts during standard neutrino running.

Source = ^{16}N ($\mathrm{NHIT}_{min} = 70$)

The ^{16}N source produces 6.13 MeV gamma rays when ^{16}N decays through an excited state of oxygen. This is accompanied by a β-decay which is observed by a PMT in the source. The signal from the PMT is connected to an external event trigger to tag events. The ^{16}N gas is delivered to the source decay chamber through the umbilical by a gas transport system. Decays occurring in the ^{16}N

```
##########################
Supernova Trigger Started:
----------------------
Date:   Tue Jul 31 16:09:22 2001
Time Win(nsec): 2000.00
N_event:        50
N_hit_min:      35
N_hit_max:      10000
##########################

##########################
Run Header Caught:
----------------------
Run Num/ndab:   20534
Trig Set:       default
Time Win(nsec): 2000.00
N_event:        50
N_hit_min:      35
N_hit_max:      10000
##########################

*****************
Run Number:     20534
Start Day:      07/08/2001
Burst Number:   1
Start GTID:     539912
End GTID:       539153
Start Time:     01:54:34.0997085
End Time:       01:54:35.7123423
Burst Dur(sec): 1.612333800
Burst Size:     72
Burst Nhit:     8596
Total nqhl:     0
Average Nhit:   119
Missed GTIDs:   0
epoch time:     994398874.099709
*****************
```

Figure 3.6: The three types of entries in the level 1 burst log file.

gas delivery system, and decays occurring through channels without a β-decay are not tagged.

Source = ^{8}Li ($\mathrm{NHIT}_{min} = 70$)

The ^{8}Li source produces energetic electrons with an energy spectrum endpoint of around 13 MeV. The signal from a PMT in the source is used to tag these events. Although all decays occurring in the source are tagged, decays occurring in the gas delivery system are not.

Source = pT ($\mathrm{NHIT}_{min} = 200$)

The pT source[28] produces 19.82 MeV gamma rays through the proton-Tritium reaction. The efficiency of event tagging is not 100%, and neutrons produced by the source are not tagged.

Source = ^{252}Cf (hi/lo) ($\mathrm{NHIT}_{min} = 70$)

The ^{252}Cf source produces neutrons through the fission of ^{252}Cf. No events from this source are tagged.

Source = ^{238}U ($\mathrm{NHIT}_{min} = 45$)

The ^{238}U source produces gamma rays through the decay chains of ^{238}U. Some gamma rays are energetic enough to produce neutrons by photo-disintegration of deuterium. No events from this source are tagged.

Source = ^{232}Th ($\mathrm{NHIT}_{min} = 45$)

The ^{232}Th source is similar to the ^{238}U source, producing gamma rays through the decay chains of ^{232}Th.

Source = Laserball ($\mathrm{NHIT}_{min} = 75$)

The Laserball source produces isotropic light from a pulsed N_2/dye laser. Light is transmitted from the laser to a diffusion ball on the source, through fiber optic cables in the umbilical. Although events occurring promptly after laser

firing are tagged, those resulting from reflected light are not. When operated at higher intensities, the amount of reflected light increases.

Run = Source Moving ($\mathrm{NHIT}_{min} = 125$)

When the source manipulator system is in motion, a large amount of light is often produced in the detector (likely from static on the umbilical). Although bursts above 125 NHIT still occurr, the rate is manageable by level 2.

Run = Bubblers ($\mathrm{NHIT}_{min} = 70$)

The bubbler system allows water level measurements, by bubbling gas out of a tube inserted into the water volume. Light is produced when this system is used, likely from static charge built up on the acrylic tube. Use of this system has been largely abandoned, and replaced by an ultrasonic level sensor.

As shown in Figure 3.7, when a Run Record is received by Snostream, it is copied to a buffer which holds the most recent Run Record. The run type word and source type word are examined, and the appropriate values for the burst parameters are assigned. Some confusion can arise for runs in which multiple sets of parameters apply. In any case, the most restrictive value of each parameter is used (i.e. the highest NHIT_{min}, the lowest T_{win}, and the highest N_{event}).

As Run Records are only dispatched at the beginning of a run, a chance of losing track of the appropriate burst parameters exists. This may occur due to a communication failure, or if Snostream is restarted after the beginning of a run. The burst parameters, the run number, and the burst number, are written to the Snostream lock file whenever a new Run Record is received to avoid the second scenario. The file is then used to assign the initial parameters when Snostream is restarted.

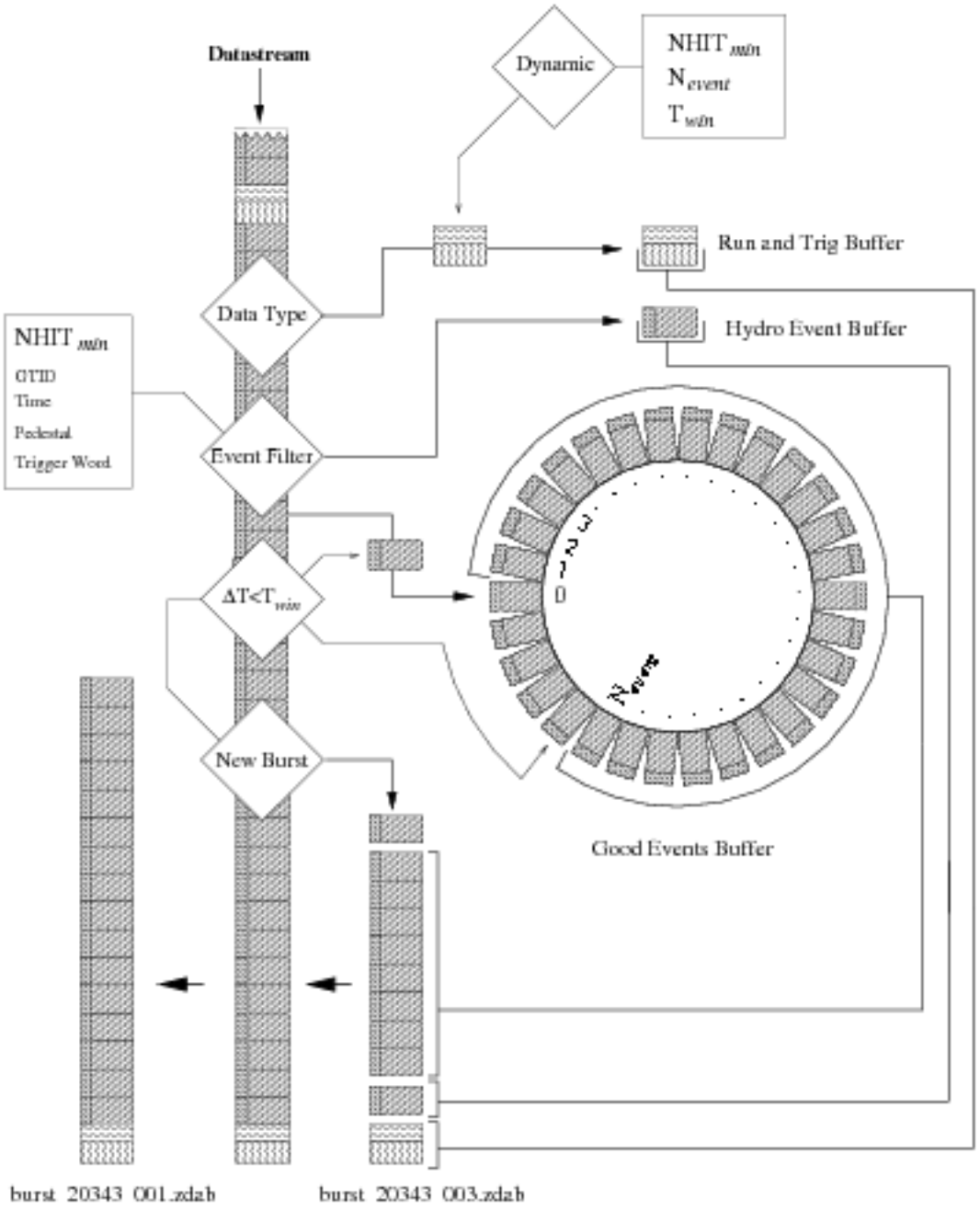

Figure 3.7: Dynamic burst parameters are loaded when a Run Record is received. The burst detection algorithm works on an event by event basis. Events passing an event filter are written to a circular buffer. The burst criteria is evaluated by loooking back N_{event} positions in the buffer and comparing the event times. Bursts of events along with Run and Trig Records are written to burst zdab files.

3.3.4 Burst Detection Algorithm

As seen in Figure 3.7, the level 1 algorithm operates on an event by event basis. Events are first filtered based on the information in the MTC header. At this point the $NHIT_{min}$ burst parameter is applied, along with several other event requirements:

GTID Events with GTID=0 (orphans), and events with out of sequence GTID are rejected.

Event Time Events received out of sequence in time are also rejected.

Pedestal Events with the pedestal bit set are rejected. These events are part of the electronics calibration process.

External Triggers Events with external trigger bits set are rejected. Most of these are calibration events, the exception being external trigger 2, which is now connected to the hydro-phone.

Hydrophone Events The hydrophone events are not entirely rejected, as they indicate seismic activity in the detector which is sometimes correlated with bursts of events. The hydrophone events and the burst may be separated by a substantial amount of time (a few seconds), and so the most recent hydrophone event is held in a separate buffer.

To evaluate the burst criteria, a comparison is made between the time of the current event, and that of the event N_{event} prior. In order to accomplish this, all events that pass the event filter are written onto a circular buffer of length greater than N_{event}. If the difference between the time of the current event and that of the event stored N_{event} positions back in the buffer is less than T_{win}, then the burst criteria is satisfied.

If the burst criteria was satisfied on the previous evaluation, then the current event is part of an ongoing burst, and is appended to an already existing file. When

the burst criteria is satisfied for the first time however, a new burst zdab file must be created. Buffered data is written to the new file first, starting with the Run and Trig records. This may be followed by the hydrophone event if it preceded the burst by less than sixty seconds. Following this, the past N_{event} events from the circular buffer are written. Once the buffered data is written, the current event is appended to the file.

A burst file is closed either when the burst criteria is no longer met, or when the burst has been in progress for a prolonged period. A burst may be prolonged because the events themselves are spread over a large time, or because their acquisition is spread over a large time. The latter can occur in the situation of a short but very high rate burst. A one million event supernova would fill the 1 Gbyte of memory on the front-end electronics in a few seconds, but the DAQ would take close to an hour to read out the data.

Determining how long the burst has been in progress for can be difficult, as the burst algorithm is not running in a realtime environment. Two methods of determining if an ongoing burst should be truncated are implemented. First, if the time stamp of the first event of the burst (excluding hydrophone events) and the current event differ by greater than 60 seconds, and second if Snostream has undergone three display update cycles with the same burst in progress. The time between Snostream display update cycles depends on the CPU load, but is at least 3 seconds.

It is important for those examining bursts to know that the files can be truncated in this manner, as there is no mechanism in place for identifying them. This situation is remedied (and confused) by burst concatenation in the level 2 system.

The level 2 system is initiated by the the shell script *supernova.sh* every time a burst file is closed.

3.4 Supernova Monitoring: Level 2

3.4.1 Introduction

The purpose of the level 2 supernova system is to perform a quick analysis of the level 1 burst zdab files, to notify the detector operator and supernova experts, and to launch the level 3 analysis if needed. The analysis consists of applying the data cleaning cuts mentioned in section 3.2.3 to the events in the burst zdab file. The burst is classified based on the fraction of events surviving the data cleaning cuts. The classification of the burst determines the amount of notification required, and the necessity to perform the level 3 analysis.

The level 2 supernova system is a collection of scripts and processes which run on Sanduleak or Betelgeuse. The level 1 script *supernova.sh* calls the level 2 queuing script *process_zdab.sh*. This queuing system groups bursts detected in rapid succession for batch analysis, thus avoiding the overhead of starting several analyses. The script *snlevel2.sh* then performs the level 2 analysis on the burst or group of bursts.

3.4.2 Burst Classification

The most important bursts are those identified as 'significant'. A burst is said to be significant if more than 35% of the events pass all of the data cleaning cuts. This indicates that the burst possesses substantial physics content, and warrants further examination.

In addition to the classification of significant, a burst may be identified as Unknown, or as being caused by a known pathological burst source. This identification is performed automatically using the fraction of events passing each of the data cleaning cuts, information from the Run Record, and the presence of hydrophone events in the burst. Currently there are eleven sources of bursts that can be identified (with varying efficiency) by the level 2 system:

Flasher (QCl≥0.50, FGC≥0.45)

Flashers are caused by micro-discharges in the PMT. This emits light which is seen by PMTs on the other side of the detector. Bursts of flashers are correlated with seismic activity.

Neck (Neck≥0.90, AMB≥0.65, FTS≥0.50, QvN≥0.33)

Neck events originate in the neck of the detector, and sometimes occur in small bursts.

Flat TAC (MAX[Cuts]=ITC)

Flat TAC events have a broad (flat) distribution in PMT times. Bursts of these events are produced as components in the PMT base begin to glow due to resistive heating. These bursts often indicates the immanent death of a PMT channel.

Manipulight (Run=Source_Moving, AMB≥0.75, ITC≥0.65, Neck≥0.20)

Manipulight is the name given to the events generated when operating the source manipulation system. The events are likely caused by static discharges from the umbilical and almost always come in large bursts.

Electrical Pickup (QvN≥0.33)

The electronics is very sensitive to interference from electrical noise in the local environment. Bumping a crate of electronics, turning on a lamp, or dropping a wrench can induce a burst of these events.

D_2O Circulation (Run=D_2O_Circ, (MAX[Cuts]=FTS, or Neck≥0.75, FTS≥0.50))

Light appears to be generated whenever water (heavy or otherwise) is passed over acrylic surfaces. When the D_2O circulation system is run, bursts of these events are often produced.

Wet End Breakdown (AMB≥0.75, QCl≥0.35, QvT≥0.35, ITC≥0.35,

QvN≤0.20, Neck≤0.35, FTS≤0.35, FGC<0.45)

This is high voltage breakdown at the PMT end of the HV chain. This was a problem earlier in the experiment and is not common anymore

Dry End Breakdown (Iso≥0.80)

This is high voltage breakdown at the crate end of the High voltage chain. Breakdown in or near the crate leads to large bursts of events due to electrical pickup.

PCA Re-trigger (Source=PCA, QvN≥0.33)

During PCA (PMT CAlibration) the laser system is used to generate events. Most of the events are triggered externally and are rejected by the level 1 system. Reflected light however can give rise to NHIT triggered events between laser firings. At high laser rates and intensities this can give rise to bursts of events.

Broken 10 MHz Clock (Duration=0 (10 MHz), Duration≥1 second (50 MHz))

On occasion, the 10 MHz clock has experienced problems, causing all events to have the same time stamp. This gives rise to huge bursts from level 1.

Spallation (1 Muon Tag, 0.35≤Physics_Content≤0.90)

High energy muon events can create numerous secondary particles which are detected as a burst of events.

UNKNOWN Bursts which do not match any of the pathological burst identities are labeled as unknown, and some additional notification is provided to the operator

3.4.3 Notification

Several methods of notification are used by the level 2 system, including a web based logbook, emails, audio-visual alerts, and telephone alerts. These methods are used to

notify the detector operator and the supernova experts. The detector operator is the first person to be aware of a burst, as she is constantly monitoring the detector. She has the best understanding the state of the detector, which is important when determining the source of a burst. The supernova experts are a group of SNO collaborators who are familiar with studying bursts, and understand the expected supernova signal. The supernova experts have also made a commitment to carry a cell phone and to respond quickly to supernova alerts. There are effectively three different notification schemes as shown in Table 3.1, based on the classification of the burst.

	Significant	**Unknown Source**	**Known Pathology**
Web Posting	operator/expert	operator/expert	operator/expert
Email	operator/expert	operator/expert	operator/expert
Audio Visual	operator	operator†	none
Phone	experts	none	none

Table 3.1: Significant bursts require the fast coordinated response of the detector operator and the supernova experts, while bursts from known pathologies can simply be logged.
† The operator is notified, and may pursue further investigation.

Supernova Online Log-book

The supernova log-book is an area on the SNO internal document server (running Lotus Domino) where all supernova related information is archived. This includes all of the level 2 and level 3 analysis summaries, Monte Carlo versions of the analysis summaries, supernova monitoring procedures, phone numbers for supernova experts, and documentation for the supernova monitoring system. All bursts regardless of classification have a summary of their analysis, including a text summary (Figure 3.9) and two pages of histograms (Figure 3.10), posted to the supernova online log-book.

Email Notification

Bursts which are either significant or unknown have their analysis summaries (text and histograms) sent by email to the detector operator and to the supernova experts. In the case of non significant but unknown bursts this is the only direct notification sent to the supernova experts.

Audio Visual Alerts

These alerts consist of a pop-up window and an audio file played through the sound cards of Sanduleak and Betelgeuse. There are two versions of the pop-up window, corresponding to significant bursts and unknown bursts. The message displayed for significant bursts is shown in Figure 3.8. A button on the pop-up window allows the operator to quickly open the burst file in Xsnoed for examination.

Dial-out Computer

The dialout computer places a call to the supernova experts who are 'on call', and plays an audio summary derived from the level 2 analysis summary text file. When a supernova expert acknowledges an alert, email is sent to the operator indicating that the supernova expert has been contacted. The dialout mechanism is only used in the event of a significant burst.

3.4.4 Output Files

Level 2 Summary Text File This file is a comprehensive summary of the level 2 analysis. The file contains information about the run conditions, the burst parameters (time, number of events, duration, etc.), the data cleaning results, and the burst classification. A sample burst summary file is shown in Figure 3.9.

```
Alert Posted on Jul 5 2001 12:42 Sudbury local time

============================ Burst 206322_001 Detected ============================

            A burst of events has passed the Level 3 threshold.
        The cause of this SIGNIFICANT burst requires investigation.

 As the detector operator, you are expected to initiate a conference call
 using the conference centre phone number and passcode listed on the
 Supernova Numbers sheet in the control room:

        Telephone: (416) 820-2500
        Chairperson: 3622309 (press *2 to start the call)

 The available on-call supernova support personnel will join the conference
 call as participants (please allow up to 10-15 minutes).

 Proceed according to the \"SNO Supernova Monitoring and Response\"
 checklist and procedure, and investigate this burst using:

   1) The results of the Level 2 analysis (summary, histograms)
   2) Examination of the burst/clean ZDAB files with \"zscope\"
   3) Your knowledge of the detector's status.

 Watch for the results of the Level 3 analysis to appear shortly
 in the snodaq\@surf email account and on 'manhattan'. Post your findings on
 'manhattan' by using the 'Edit' button at the top of the Level 2 posted
 comment response form page.

----------------------------< Burst Data Locations >----------------------------

 The raw data for these events are available in two locations:

 * Events passing the Level 1 burst monitor are written to:

  --> SANDBLEAK in /scratch/lt/satream/snwatch/zdabs/burst_206322.zdab

 * Events passing the Level 2 data cleaning cuts are written to:

  --> SANDBLEAK in /scratch/lt/satream/snwatch/clean_zdabs/clean_206322_001.zdab

----------------------------< 'Manhattan' Locations >---------------------------

 RESPONSE CHECKLIST & PROCEDURE:
   --> Supernova Logbook:/ Procedures

 ANALYSIS RESULTS:
   --> Supernova Logbook:/ Burst Analysis / Level 2 / Analysis
   --> Supernova Logbook:/ Burst Analysis / Level 3 / Analysis

 EXAMPLE BURSTS:
   --> Supernova Logbook:/ Burst Analysis / Level 2 / Examples
   --> Supernova Logbook:/ Burst Analysis / Level 3 / Examples
------------------------------------------------------------------------------
```

Figure 3.8: The Message displayed to the operator in the event of a significant burst.

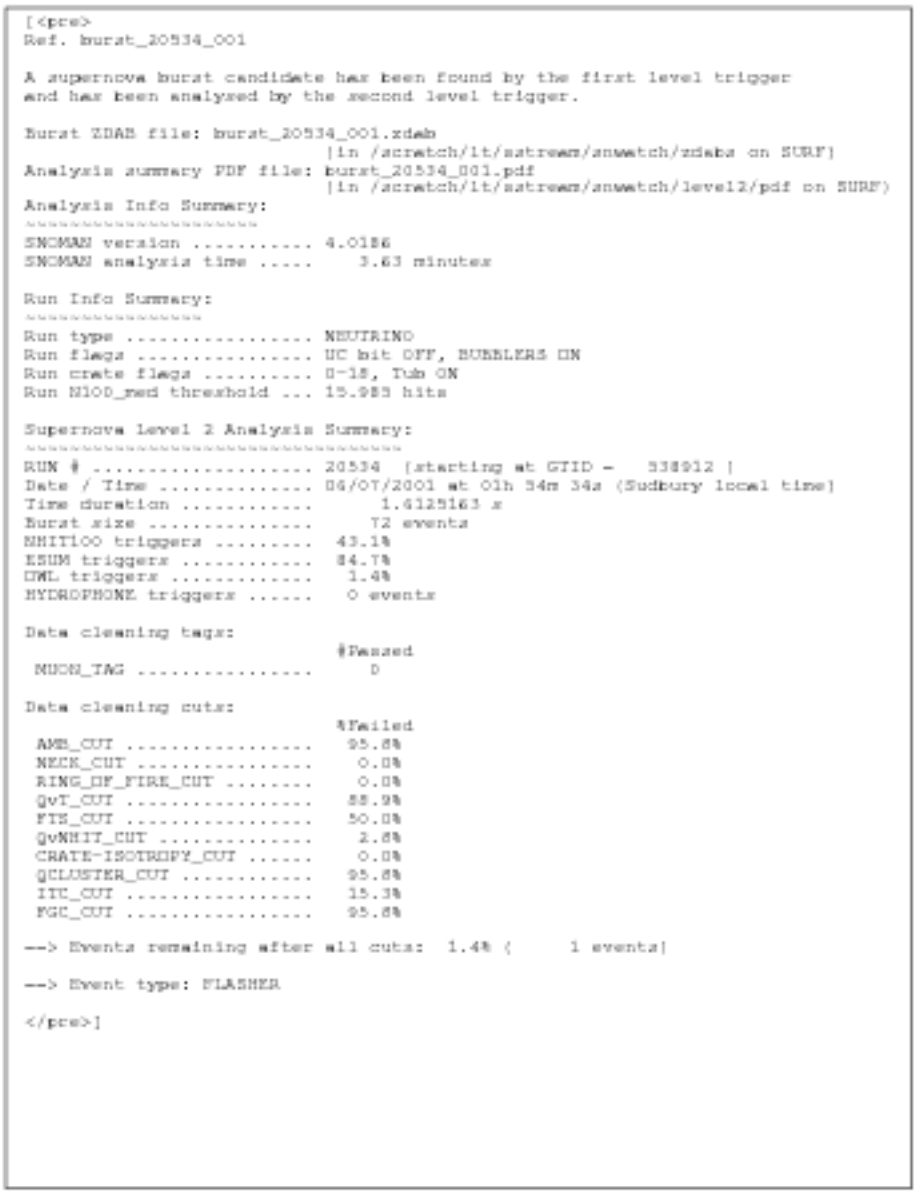

```
[<pre>
Ref. burst_20534_001

A supernova burst candidate has been found by the first level trigger
and has been analysed by the second level trigger.

Burst ZDAB file: burst_20534_001.zdab
                 [in /scratch/lt/satrean/snwatch/zdabs on SURF]
Analysis summary PDF file: burst_20534_001.pdf
                 [in /scratch/lt/satrean/snwatch/level2/pdf on SURF]
Analysis Info Summary:
~~~~~~~~~~~~~~~~~~~~~~
SNOMAN version ........... 4.0186
SNOMAN analysis time .....    3.63 minutes

Run Info Summary:
~~~~~~~~~~~~~~~~~
Run type ................. NEUTRINO
Run flags ................ UC bit OFF, BUBBLERS ON
Run crate flags .......... 0-18, Tub ON
Run N100_med threshold ... 15.983 hits

Supernova Level 2 Analysis Summary:
~~~~~~~~~~~~~~~~~~~~~~~~~~~~~~~~~~~
RUN # ..................... 20534  [starting at GTID =   338912 ]
Date / Time ............... 06/07/2001 at 01h 34m 34s (Sudbury local time)
Time duration .............      1.6125163 s
Burst size ................     72 events
NHIT100 triggers .........  43.1%
ESUM triggers ............  84.7%
OWL triggers .............   1.4%
HYDROPHONE triggers ......   0 events

Data cleaning tags:
                           #Passed
 MUON_TAG .................     0

Data cleaning cuts:
                           %Failed
 AMB_CUT ..................  95.8%
 NECK_CUT .................   0.0%
 RING_OF_FIRE_CUT .........   0.0%
 QvT_CUT ..................  88.9%
 FIT_CUT ..................  50.0%
 QvNHIT_CUT ...............   2.8%
 CRATE-ISOTROPY_CUT .......   0.0%
 QCLUSTER_CUT .............  95.8%
 ITC_CUT ..................  15.3%
 FGC_CUT ..................  95.8%

--> Events remaining after all cuts:  1.4% (     1 events)

--> Event type: FLASHER

</pre>]
```

Figure 3.9: The level 2 summary file is archived in an online log-book and sent by email to the appropriate recipients.

Level 2 Short Summary File This is a one line file, containing much of the same information as the level 2 summary file. This file is intended to be parsed by machine for later analysis. The short summary files from all bursts are concatenated to form a level 2 summary log file.

Level 2 Summary Audio File This is a wav audio file which contains a small part of the information from the level 2 summary file.

Level 2 Summary PDF File This is a file in the Adobe Portable Document Format (PDF). Perhaps the most informative output file, this file contains most of the information in the summary text file, as well as several histograms. There are two pages in the file, the first displaying histograms for all of the burst events, and the second showing the same histograms for the events which passed all of the data cleaning cuts. An example of a level 2 summary PDF file is shown in Figure 3.10.

Clean zdab File This file is much like the original burst zdab files, except with the events that failed data cleaning cuts removed. Looking at this file in Xsnoed can be useful when investigating the cause of a burst.

Log Files Many log files are created by the level 2 system in snwatch/level2/log.

3.5 Supernova Monitoring: Level 3

3.5.1 Introduction

The purpose of the level 3 system is to further evaluate bursts identified as significant by level 2, and to initiate an alert to the astronomical community if necessary. The level 3 system processes the clean zdab files generated by level 2. Event reconstruction with the elastic and time fitter are used to extract the energy, position, and direction of the burst events.

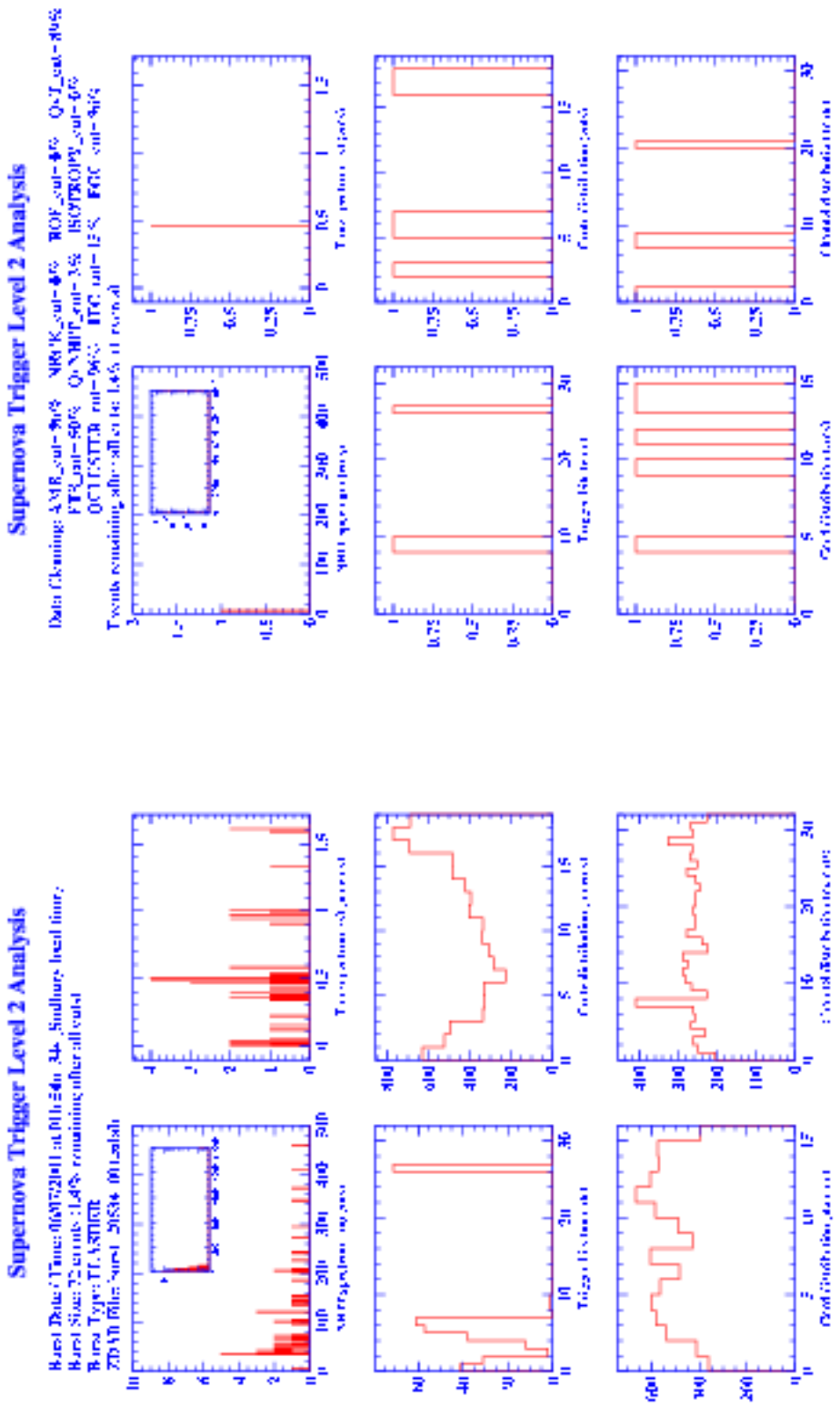

Figure 3.10: The level 2 summary histograms show informative distributions for all burst events (left), and for events which passed the data cleaning cuts (right).

A program attempts to fit the global supernova direction from the angular distribution of events.[29] This is done mainly by identifying the elastic scattering peak. The supernova direction is of interest to the astronomical community, but is not likely to be of direct use to the detector operator or supernova experts.

A text summary (Figure 3.11) and three pages of histograms (Figure 3.12) are sent to the supernova experts and the detector operator. The first page contains histograms for all events in the clean zdab file, the second for events which reconstructed in the D_20 region, and the third for events which reconstructed in the H_20 region. Events from a supernova will be distributed roughly equally between the H_2O and D_2O regions, with the D_2O region being favoured during the salt phase. Within each of the two regions events will be distributed uniformly.

The histograms include NHIT, event time, radial position, directions in theta and phi (detector coordinates), and cosine of theta relative to the calculated supernova direction. By studying the output of the level 3 analysis, and through discussion, the supernova experts and the detector operator evaluate the probable source of the burst.

3.6 SNEWS

The Supernova Early Warning System (SNEWS) is a collaboration of scientists representing experiments around the world capable of detecting galactic supernovae. The experiments currently participating in SNEWS include Super-Kamiokande, SNO, and LVD, with several existing and proposed experiments to hopefully join later. The primary goal of SNEWS is to provide an automated alert to the astronomical community in the event of a galactic supernova. Other offerings of the SNEWS group include: 1) increased sensitivity and confidence for supernova detection, by blind coincidence study of signals from multiple detectors 2) coordinated effort to establish and test timing synchronization between experiments, ensuring that future analysis of com-

```
[<pre>
Ref. clean_20413_001

A supernova burst candidate has passed the level 2 analysis threshold
and is now being analysed by the third level trigger.

Cleaned ZDAB file: clean_20413_001.zdab
                          [in /scratch/lt/sstream/snwatch/clean_zdab on SURF)
Analysis Info Summary:
~~~~~~~~~~~~~~~~~~~~~~
SNOMAN version ............ 4.0186
SNOMAN analysis time .....    0.73 minutes

Supernova Level 3 Analysis Summary:
~~~~~~~~~~~~~~~~~~~~~~~~~~~~~~~~~~~
RUN # ............................. 20413  (starting at GTID =  34266T2 )
Date / Time ....................... 16/06/2001 at 23h 32m 51s (Sudbury time)
Time duration of clean events ...       0.0232496 s    (50 MHz)
Total number of clean events ....      93 events

Fitted Data Results (elastic fitter, vertex within PSUP)
~~~~~~~~~~~~~~~~~~~~
Date / Time ........ 17/06/2001 at 03h 32m 50.7170342 s (Universal time)
Time duration ......       0.023249619 s    (50 MHz + fit)
Number of events ...      91
NHIT100 triggers ... 100.0%
  NHIT  < 75 .......  98.9%
  NHIT >= 75 .......   1.1%
ESUM triggers ......   0.0%
OWL triggers .......   0.0%
Summed dircos ...... -0.121343 -0.964237 -0.235448  (toward SN)

                                    D2O region           H2O region
                                    ----------           ----------
Fraction of events .............       92.3%                7.7%
Fraction of NHIT100 triggers ..       92.3%                7.7%
  Fraction of NHIT  < 75 ......       91.2%                7.7%
  Fraction of NHIT >= 75 ......        1.1%                0.0%
Fraction of ESUM triggers .....        0.0%                0.0%
Summed dircos (toward SN) ..... -0.46  0.67  0.58   -0.06 -0.96 -0.28

Supernova Direction Analysis Results
~~~~~~~~~~~~~~~~~~~~~~~~~~~~~~~~~~~~
Direction cosines (toward SN) ... -0.57735 -0.57735  0.57735
Zenith, azimuth .................  54.73563 degrees  135.00000 degrees W of N
Declination, right ascension ....  -8.02095 degrees   16.21352 hours

</pre>]
```

Figure 3.11: The level 3 summary file is archived in the online log-book and sent by email to the appropriate recipients.The fraction of events in D_2O vs. H_2O can indicate how isotropically the events are distributed, and aid in determining the source.

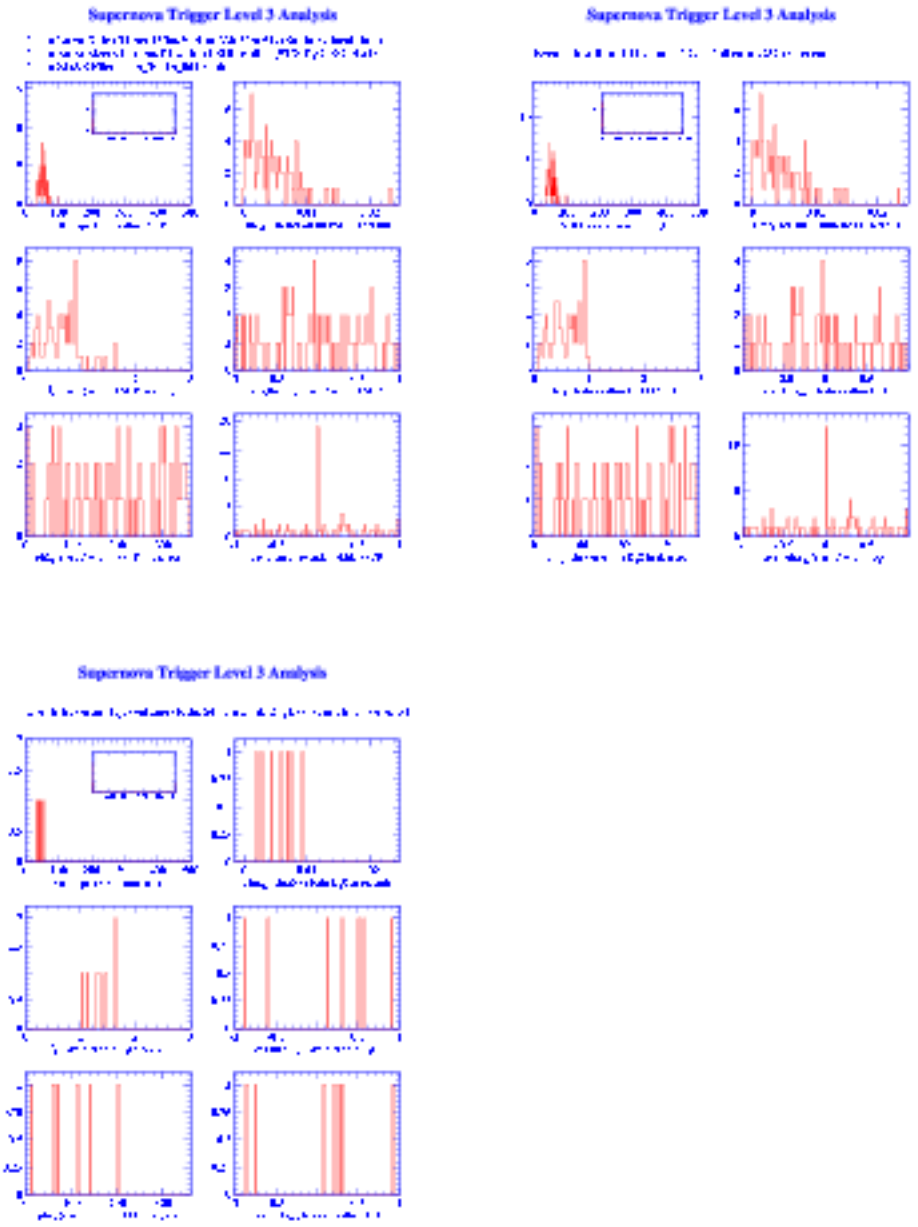

Figure 3.12: The level 3 summary histograms show event distributions for all clean events (upper left), for clean events in the D_20 (upper right), and clean events in the H_20.

bined data is not limited by uncertainties in timing 3) provide a trigger signal to experiments not capable of independently detecting a supernova, allowing them to archive data that might otherwise be discarded.

Several features of the automated alert have been identified as important by the astronomical community and the SNEWS experiments. Astronomers require that the alert be as prompt as possible, providing the greatest time to locate and observe the event. It should also provide any pointing information possible, to help astronomers locate the supernova in the sky. A third feature important to astronomers is that the alert be positive, with a false alarm rate of less than one per century, avoiding costly interruptions to observing schedules. An issue important to the participating experimental collaborations is that information sent to SNEWS be kept private, providing sovereignty over the experiment data, and ensuring the blindness of the coincidence measure.

The coincidence measure is implemented using a central coincidence server with multiple identical servers present for redundancy. The server application accepts alert datagrams from individual experiment clients over TCP/IP protocols. Datagrams are encrypted with OpenSSL to provide security. The datagrams contain the start time of the burst (specified in UT), and a number identifying the sending experiment. Other information such as the magnitude of the burst or the confidence of the burst source can also be included. Alerts are stored in a buffer sorted by time, and searched for coincident alerts. Nominally a coincidence consists of at least two different experiments reporting a burst within ten seconds.

When a coincidence is found, an alert is sent to the astronomical community through a mailing list. This alert is signed with the SNEWS PGP key for security. The alert contains the supernova event time, and pointing information if available.

Chapter 4

Supernova Monitor Performance

The performance of the supernova monitoring system is difficult to measure without actually detecting a supernova or two (waiting would greatly delay this writing!). In this chapter, performance is evaluated in terms of the main goals of the system, which are to provide prompt and positive alert. The first section of this chapter studies the online response time using muon induced spallation bursts and the second section studies burst identification using data from an offline search.

4.1 Response Time

The response time goal is motivated by the SNEWS target of issuing an automated alert to the astronomical community within 20 minutes. Before contacting SNEWS, SNO must detect the events, record the burst, perform the level 2 analysis, and likely acquire confirmation from a supernova expert. If no human confirmation is required, or the detector operator confirmation is sufficient, then an alert could be sent shortly after the level 2 analysis is completed.

The most realistic test of the response time is provided when spallation bursts trigger the supernova monitor. These bursts consist of real physics events as described in chapter 3, and offer the advantage of exercising the entire system from particle detection to expert notification. These bursts occur randomly in time which

provides a periodic measure of the performance of the system, much like a completely spontaneous fire drill.

A drawback to using these bursts as a measure of performance is the fact that the bursts are not actually very supernova-like. The ability to inject Monte Carlo supernova data into the datastream would provide a more realistic test, but would incur other costs. This idea has been discussed, but has not yet been implemented.

During the period from Oct 16 2001 to Feb 05 2002, a total of 18 bursts were identified online by the level 2 spallation ID. Of these bursts, 3 were excluded from further study; one was a misidentified calibration burst, one occurred while the Dialout computer was offline [1], and one had no entry in the Dialout log file [2].

The response times to the remaining 15 bursts are listed in Table 4.1. For each burst, the time of the first event and the time of the first supernova expert acknowledgment is listed. The level 2 analysis and dialout notification durations are also listed, and can be compared to the time elapsed from first event to first acknowledgment.

The level 2 analysis duration and the dialout notification duration are known to account for the majority of the total response time. The level 2 analysis duration is less than 3 minutes for all instances, but will increase with larger burst size. The dialout notification time is generally under 7 minutes, and varies depending on the number of phone calls required to contact a supernova expert. The total response time is less than ten minutes for most instances, which is consistent with the level 2 analysis and dialout durations, and is well within the 20 minute window identified by SNEWS.

In performing this study, it was necessary to compare time stamps from more than one clock, namely the MTC clock which records the time of the first event, and the Dialout clock which records the expert acknowledgment time. In doing so, an offset

[1] Notification and remedy of the situation was effected in less than 1 hr.

[2] Detector shift report mentions file corruption in logbook and/or email records.

Burst	Date	First Event	First Ack.	Total	L2 Dur.	Dial Dur.	Total
21706_005	Sat Oct 6	17:40:21	17:44:25	**4:04**	1:58	1:11	**3:10**
21707_001	Sun Oct 7	23:23:09	23:36:30	**13:21**	2:53	10:27	**13:20**
21852_001	Sat Oct 20	22:55:11	23:02:34	**7:23**	2:18	4:26	**6:34**
21864_001	Sun Oct 21	12:22:30	12:29:41	**7:11**	2:11	4:16	**6:27**
21911_001	Fri Oct 26	13:02:32	13:11:31	**8:59**	1:57	6:16	**8:13**
22031_001	Sun Nov 4	16:41:49	16:45:51	**4:02**	1:57	1:07	**3:04**
22033_001	Mon Nov 5	18:03:29	18:34:43	**31:14**†	2:35	1:06	**3:41**
22090_001	Sat Nov 10	11:08:59	11:13:08	**4:09**	2:08	1:09	**3:17**
22736_005	Sun Dec 23	12:16:31	17:57:40	**>1hr**‡	0:57	4:12	**5:10**
22809_001	Wed Jan 2	22:22:23	22:32:02	**9:38**	0:53	7:50	**8:44**
23040_001	Sun Jan 20	16:23:55	16:26:59	**3:04**	0:59	1:08	**2:07**
23137_001	Fri Jan 25	06:54:01	06:56:52	**2:51**	1:00	1:10	**2:11**
23180_001	Thu Jan 31	03:12:01	03:15:30	**3:29**	1:03	1:23	**2:26**
23208_001	Mon Feb 4	12:21:39	12:29:46	**8:07**	1:03	6:02	**7:05**
23221_001	Tue Feb 5	17:13:41	17:16:35	**2:54**	1:01	1:07	**2:08**

Table 4.1: Response and analysis times for spallation bursts are obtained from event time stamps, level 2 logfiles, and the Dialout logfile.
†'builder off' noted in shift report
‡10 MHz problems noted in shift report

of several minutes as well as a 30 ppm (18 seconds per week) drift was found between the two clocks. This was determined using a third clock on Sanduleak, which was periodically in contact with the other two clocks.

Figure 4.1 shows the relative offsets of the two clocks as a function of time. The variation in the Dialout clock clearly exhibits a drift, while the variation of the MTC clock is consistant with random jitter. The drift and the periodic correction of the Dialout clock is most likely an artifact of poor time keeping in the operating system (MS Windows 95). This exercise points out the importance, and relative complexity, of proper clock maintenance.

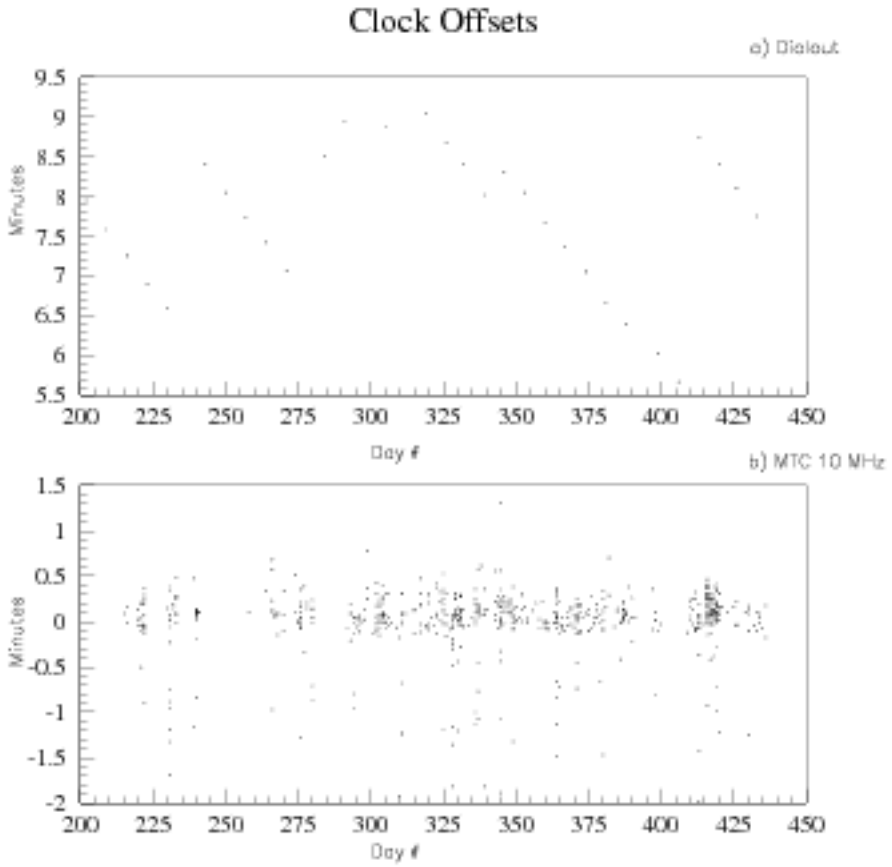

Figure 4.1: a) Time offset for Dialout clock vs. Sanduleak clock from weekly dialout test data. b) Time offset for MTC clock vs. Sanduleak clock from all burst data.

4.2 Burst Identification

A positive and automated supernova burst ID cannot be implemented without making assumptions based on model-specific predictions of the supernova signal. To ensure that all supernova signals are recognized, the philosophy adopted instead is one of automated background identification and rejection. Supernova detection thus hinges on the ability to identify background bursts and to direct sufficient attention to unidentified bursts.

Although the full attention of the detector operator and the supernova experts is reserved for significant bursts, non-significant bursts of unknown identity still require some attention, primarily from the detector operator. Minimizing the number of unknown bursts helps to focus the attention of the detector operator. In this section the efficiency of the level 2 burst identification is studied using bursts found in an offline reprocessing analysis.

4.2.1 Level 2 Burst ID Summary

In 439 days of data collected between 1999/11/03 and 2001/01/15, a total of 14670 bursts were found. This dataset is not directly comparable to bursts detected online, as the online system concatenates level 1 bursts which occur in rapid succession. Table 4.2 shows the number of bursts identified by the various level 2 IDs during several different run conditions.

The burst rate is highly dependent on run type. During neutrino running the burst rate is low, averaging only 12 bursts per day. The rate for other types of runs is higher, averaging more than 90 bursts per day.

The fraction of unidentified bursts is also highly dependent on run type. During neutrino running only 12% of bursts are identified as unknown, while during other run types this is approximately 95%. This may be due to several reasons such as changes in detector thresholds which affect the efficiency of data cleaning cuts, increased activity on and around the electronics systems, and a generally noisier detector.

4.2.2 Alternative Method of Burst Classification

The existing level 2 IDs (described in section 3.4.2) allow no easy method to evaluate the efficiency or accuracy of identification. An alternative method of burst classification may be helpful to 1) independently confirm the existing level 2 burst IDs, 2) Refine the level 2 ID parameters, and 3) discover previously unknown burst classes.

	Neutrino	Calibration	Maintenance	Other	Total
Livetime Fraction	**73%**	**10%**	**7%**	**2%**	**93%**
D_2O Circulation	1136	94	2	1	**1233**
Electrical Pickup	852	73	4	18	**947**
Flasher	519	37	23	11	**590**
Flat TAC	467	12	16	10	**505**
Dry End Breakdown	223	1	48	0	**272**
Neck	164	12	1	0	**177**
Manipulight	0	199	0	0	**199**
Wet End Breakdown	38	1	4	0	**43**
Spallation	20	3	2	0	**25**
Broken Clock	1	12	1	4	**18**
Unknown	486	4717	3674	1784	**10661**
Total	**3906**	**5161**	**3775**	**1828**	**14670**
% Unknown	(12%)	(91%)	(97%)	(98%)	73%

Table 4.2: A total of 14670 bursts were found in an offline analysis of 439.5 days of data. The burst rate is far lower during neutrino running than all other run types. During neutrino running a large fraction of bursts are identified by the level 2 IDs, but for other run conditions this fraction is quite small.

In this section the method of principal component analysis is used to search for burst classes in the offline reprocessed dataset. The classes found are compared to the existing level 2 IDs.

Principal Component Analysis (PCA) is a common tool in multidimensional data analysis and is often used for dimensional reduction and pattern recognition. PCA applies a linear transformation to the original variables of a dataset, which hopefully allows easier identification of features in the data. The transformation is described by an orthogonal matrix, and is equivalent to a rotation of the original space to a new set of coordinate vectors.

It can be shown[30] that of all complete orthonormal bases of the dataset, that

formed by the eigenvectors of the covariance matrix and associated with the largest eigenvalues correspond to the most significant features for describing the original dataset. The eigenvector associated with the highest eigenvalue is called the first principal component and corresponds to the most significant parameter for describing the original data. The most prominent features of a high dimensional dataset can thus be viewed by plotting the projection of the dataset onto the first few principal components.

For this analysis, the original variables used are results of the ten data cleaning cuts described in Section 3.2.3. These variables were selected because they are believed to adequately describe the bursts, and they are easy to work with (real valued and bounded[3]). Each burst is described by a ten dimensional vector defined by the percentage of events failing each cut. The principal components of the 14670 bursts described in the previous section were computed using the LINTRA package from CERN.[30]

Table 4.3 shows the eigenvectors and eigenvalues of the first two principal components. The first principal component is most strongly influenced by the NECK and QCL variables, and the second by NECK and FTS. The eigenvalues indicate that about 59% of the variance in the original dataset is accounted for by these two principal components.

Figure 4.2 shows the distribution of bursts projected onto the first two principal components. Many features can be seen, including several distinct groups of bursts. Fourteen regions of interest are identified by eye and defined as shown in Figure 4.3. The regions serve as the basis for the discussion to follow, but are purely empirical and not statistical in nature.

[3]Further gains could most certainly be made by including other variables such as the run bitmask and the source bitmask, which are discrete variables.

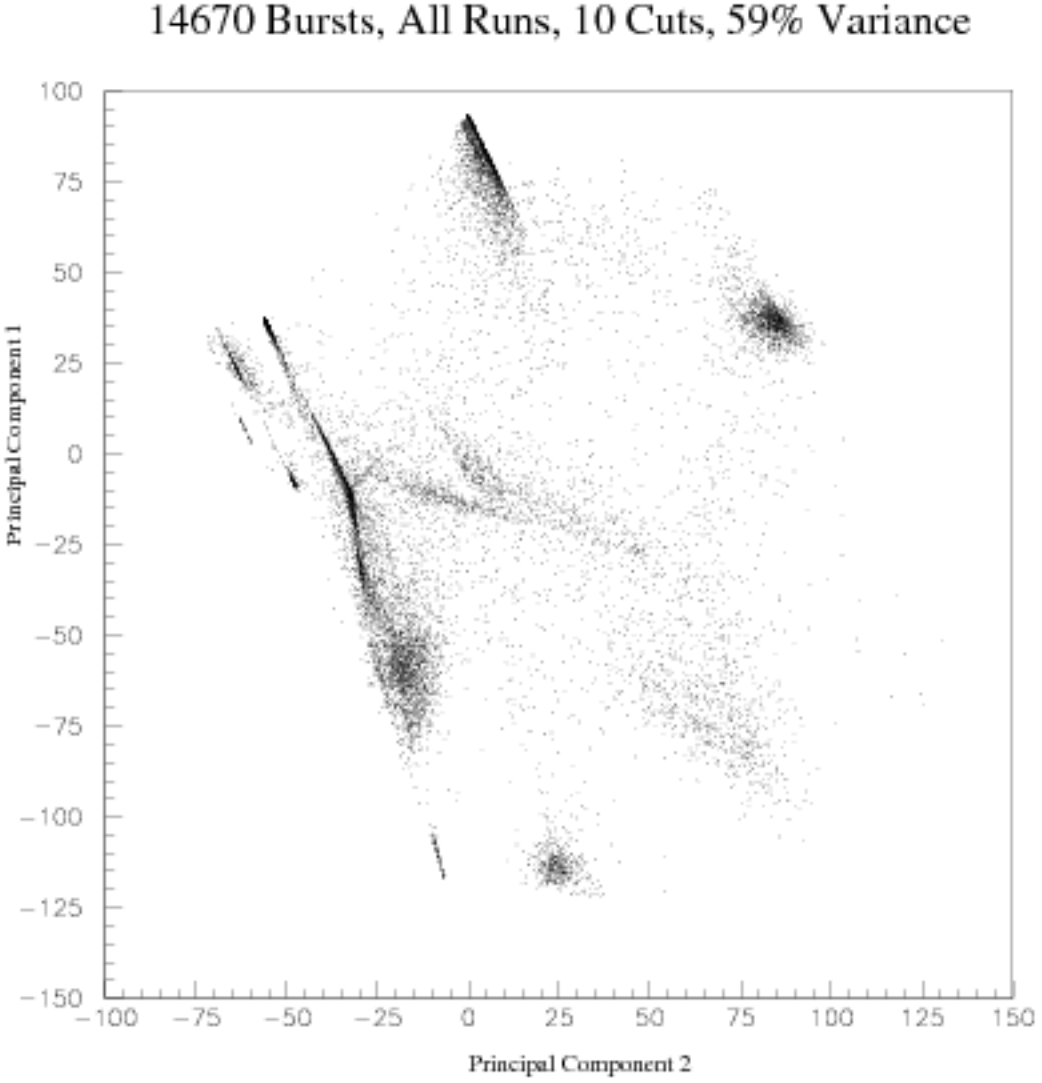

Figure 4.2: The distribution of the 14670 bursts projected onto the first two principal components. This projection describes 59% of the total variance present in the ten data cleaning cuts. Several features inherent in the burst data set can be readily distinguished.

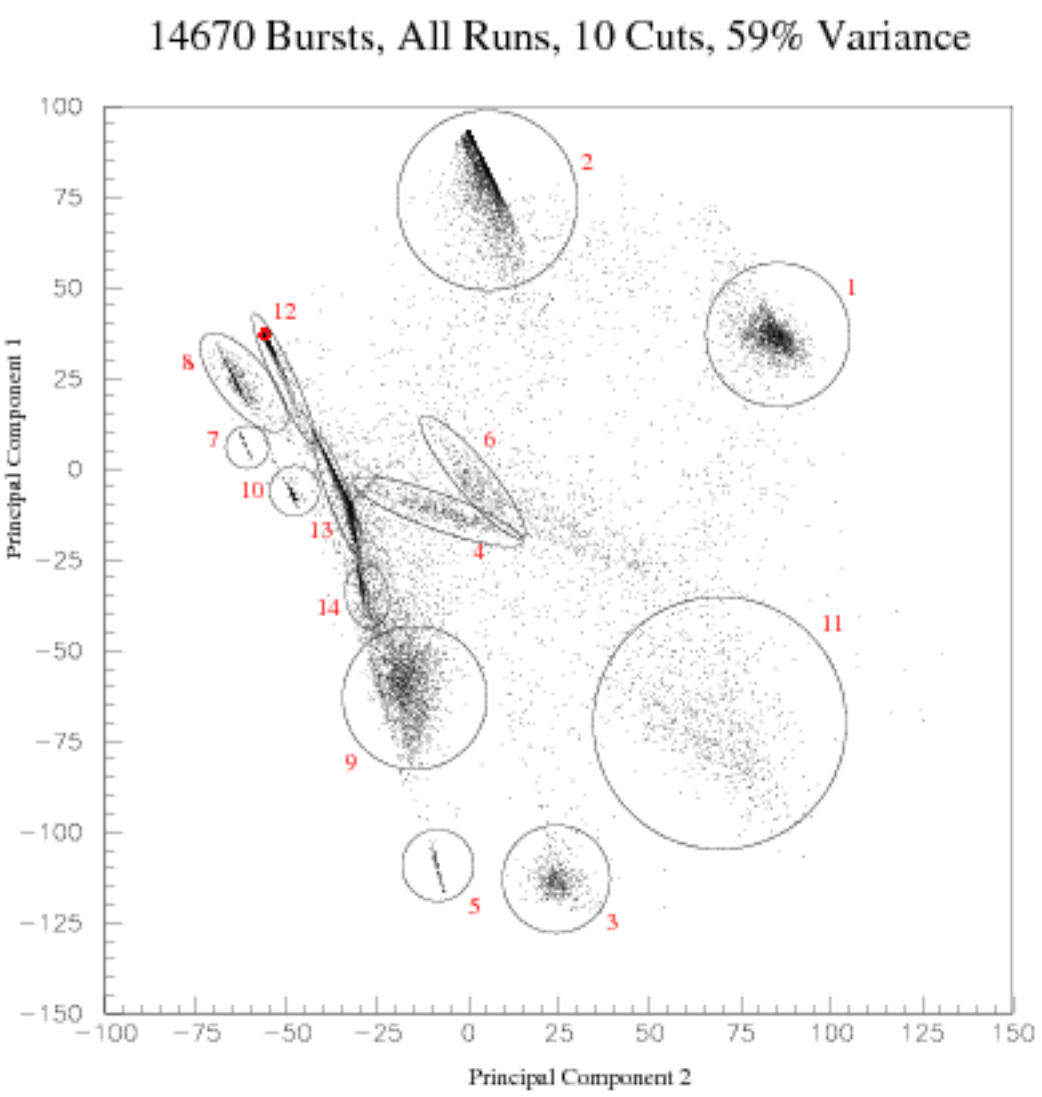

Figure 4.3: Fourteen regions of interest are defined by elliptical cuts as shown. These are not statistical measures but aid in this exploratory analysis. The red circle indicates the location of a burst for which 100% of the events pass all of the data cleaning cuts (a supernova perhaps?).

Original Variable	Eigenvector PC 1	Eigenvector PC 2
AMB	-0.46	0.23
NECK	0.56	0.56
ROF	0.01	-0.15
QVT	-0.33	0.04
FTS	-0.10	0.63
QVN	-0.03	0.18
ISO	0.01	-0.07
QCL	-0.55	0.12
ITC	-0.10	0.38
FGC	-0.19	0.10
Eigenvalue	0.36	0.23

Table 4.3: Summary of first two principal components.

Confirmation of Existing Level 2 IDs

Many of the existing level 2 IDs are associated with the regions defined above. The associations between regions and IDs are quite obvious for the most frequent level 2 IDs, as shown in Figures 4.4, 4.9, 4.12, 4.14, and 4.5. (The exception to this is Electrical Pickup bursts, which are very common but are spread out across several regions.) The associations are not all one to one mappings however; for example both D_2O Circulation and Neck bursts map to region 1 (Figures 4.4 and 4.5), while Flasher bursts map to both region 3 and 5 (Figure 4.9). These strong associations between the defined regions and the existing level 2 IDs amount to a confirmation of several existing IDs and is a reassurance that the analysis method is sound.

Proposed Adjustments to Level 2 ID Parameters

Region 1: D_2O Circulation and Neck Bursts

D_2O Circulation and Neck bursts cannot be distinguished by this analysis without information from the run header as they are indistinguishable in PCA space (Figures

4.4 and 4.5). Most of these bursts fall in region 1, with some D_2O bursts outlying into region 11. These outliers all come from an existing definition of D_2O circulation which requires that the FTS be the highest cut. A full 94% of the 1410 bursts identified as D_2O Circulation and Neck fall in region 1 (1325 bursts).

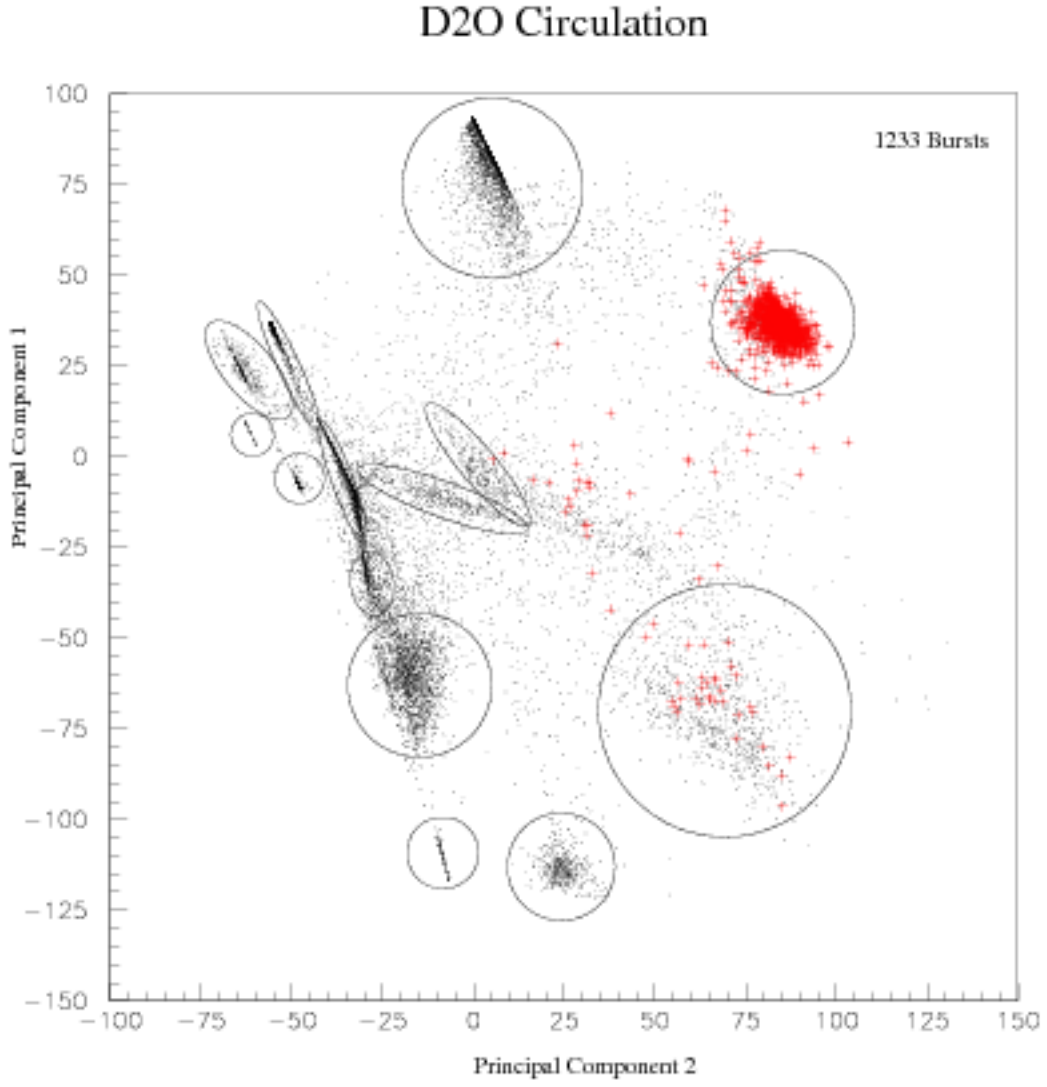

Figure 4.4: The distribution of D_2O Circulation bursts is mainly confined to region 1 (along with Neck bursts), with 93% of the 1233 bursts falling within the defined region.

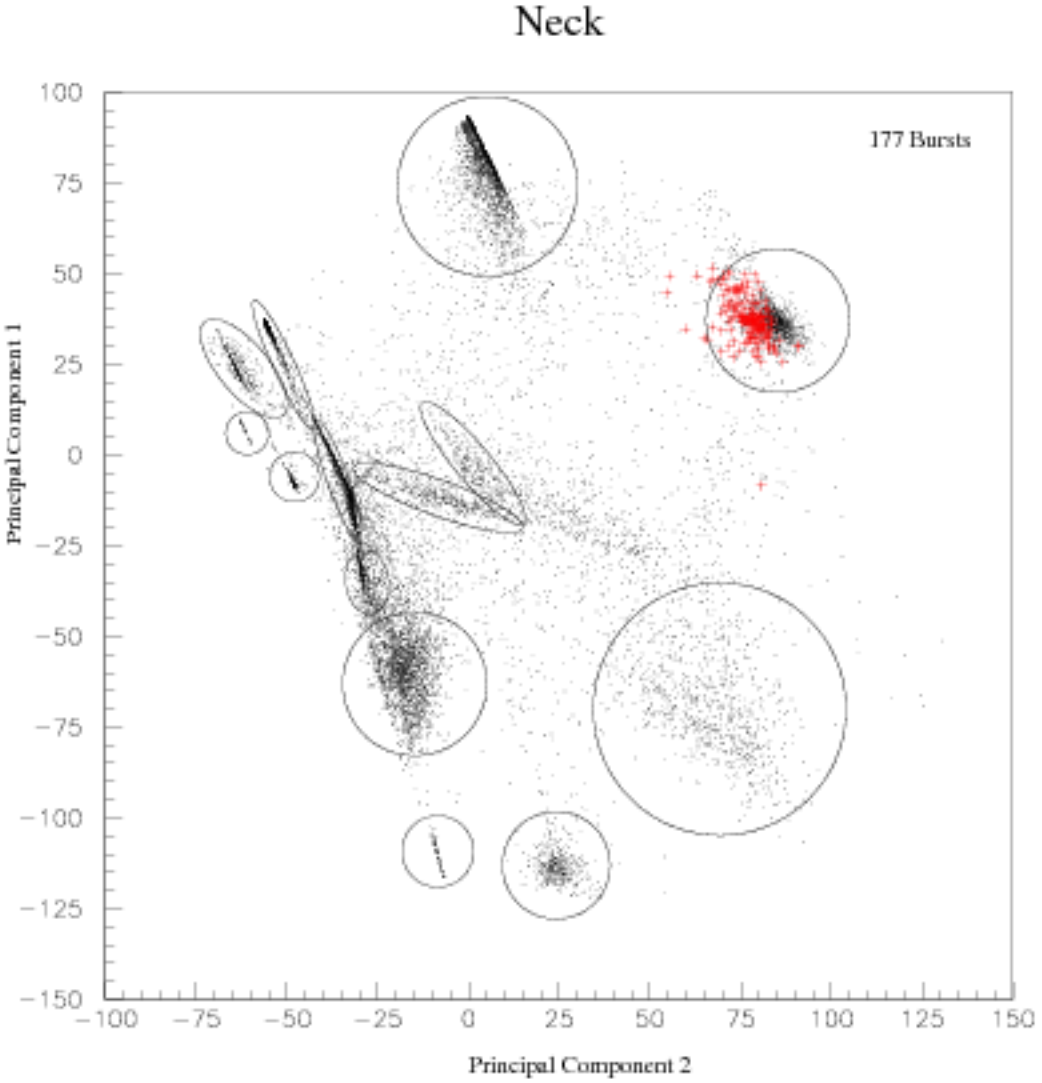

Figure 4.5: The distribution of Neck bursts is mainly confined to region 1 (along with D_2O Circulation bursts), with 95% of the 177 bursts falling within the defined region.

Assuming that this sample (Region 1) is descriptive of the class (D_2O and Neck), Figure 4.6 suggests some adjustments to the existing burst IDs. The proposed adjustment offers a single set of parameters which identify effectively the same set of bursts in a more standard form. Under the proposed adjustments, 97% of the 1397 bursts now identified fall in region 1 (1355 bursts). This is at most a modest improvement on the existing IDs, and the ability to discern D_2O Circulation from Neck bursts has been lost. This adjustment is not highly recommended, but serves as a good example of the power of the analysis.

The proposed change to the D_2O and Neck ID is:

Current	(D_2O)(Neck)	**Proposed**
AMB	(−−) (>65)	AMB>55
Neck	(>75) (>90)	Neck>80
FTS	(>50) (>50)	FTS>50
QVN	(−−) (<33)	QVN<50

Region 4: Electrical Pickup Bursts

Figure 4.7 shows that bursts identified as electrical pickup are not very tightly clustered except for a distinctive grouping in region 4. Only 37% of the 947 bursts identified fall in region 4 (351 bursts). The broad distribution is not a surprise as electrical pickup is the most loosely defined level 2 ID.

Figure 4.8 suggests several adjustments to the electrical pickup ID. The proposed changes both tighten the existing requirement, and add two new requirements to remove outliers which fall in regions 1 and 11. Under the proposed adjustments, 70% of the 469 bursts now identified fall in region 4 (328 bursts). These changes drastically change the nature of this ID, and closer inspection of the new sample should be performed. This might require the name of the ID to be refined.

The proposed change to the Electrical Pickup ID is:

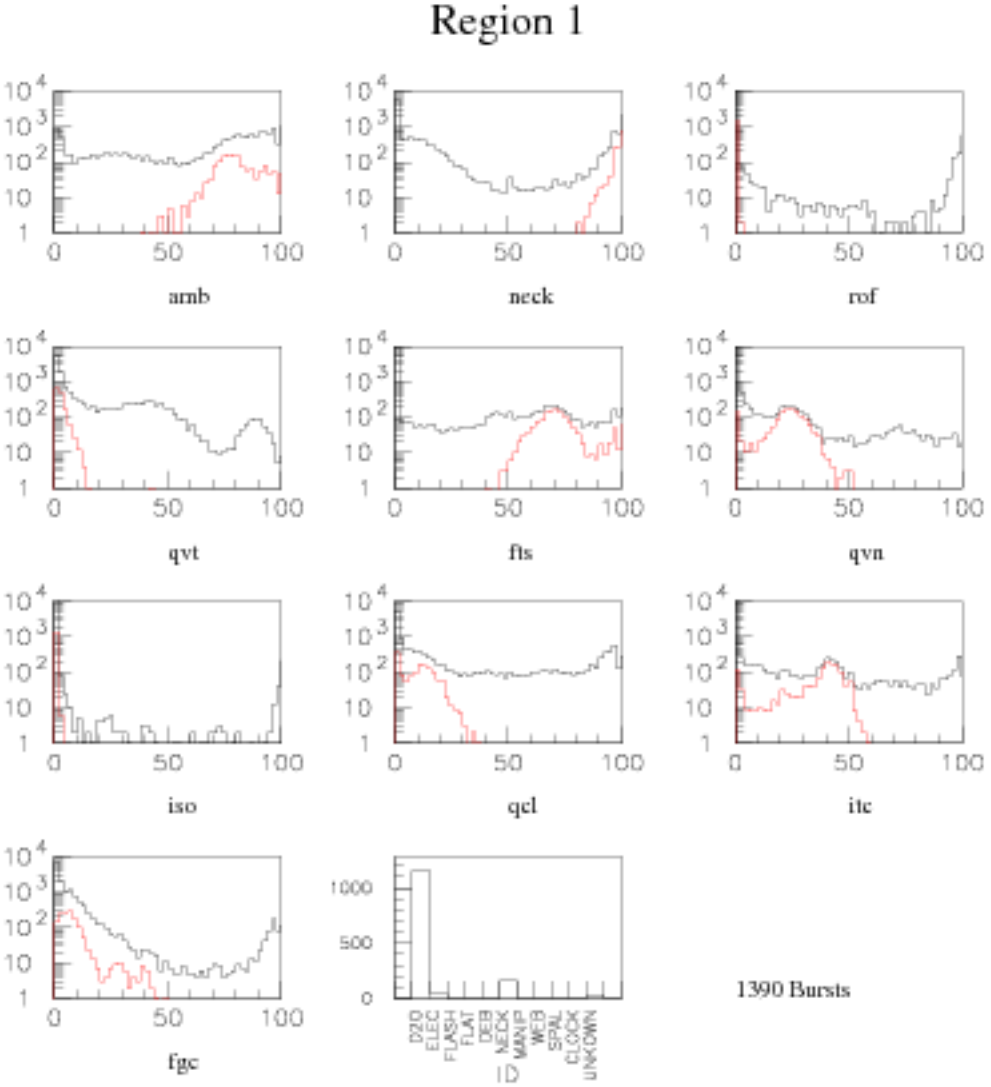

Figure 4.6: Data cleaning cut distributions of bursts found in region 1 compared to all bursts. The number of bursts of each ID type found in the region are also shown.

Current	Proposed
QVN>33	QVN>50
	FGC<12
	ITC<50

Regions 3 and 5: Flasher Bursts

Figure 4.9 shows that bursts identified as flasher bursts are tightly clustered in two regions, namely 3 and 5. A full 91% of the 590 bursts identified as flashers fall in regions 3 and 5 (536 bursts).

Figures 4.10 and 4.11 suggest some changes to the flasher burst ID. First, an additional parameter of FTS greater than or less than 5% will distinguish between Flasher IDs of region 3 and those of region 5. Secondly, the existing parameters can be tightened considerably without significant loss. Under the proposed adjustments, 97% of the 560 bursts now identified fall in regions 3 (93 bursts) and 5 (451 bursts).

The proposed change to the Flasher ID is:

Current	Proposed	(Reg. 3)	(Reg. 5)
QCL>50	QCL	(>80)	(>80)
FGC>45	FGC	(>80)	(>80)
FTS>45	FTS	(<5)	(>5)

Region 6: Flat TAC Bursts

Figure 4.12 shows that these bursts are somewhat concentrated in region 6, with some outliers extending into region 11. Only 59% of the 505 bursts identified as Flat TAC bursts fall in region 6 (298 bursts).

This ID is currently defined as those bursts for which the ITC cut removes the highest fraction of events. This type of definition is difficult to adjust, so a redefinition of the cut based on Figure 4.13 is proposed. Under the proposed changes, 87% of the 342 bursts now identified fall in region 6 (298 bursts).

The proposed change to the Flat TAC ID is:

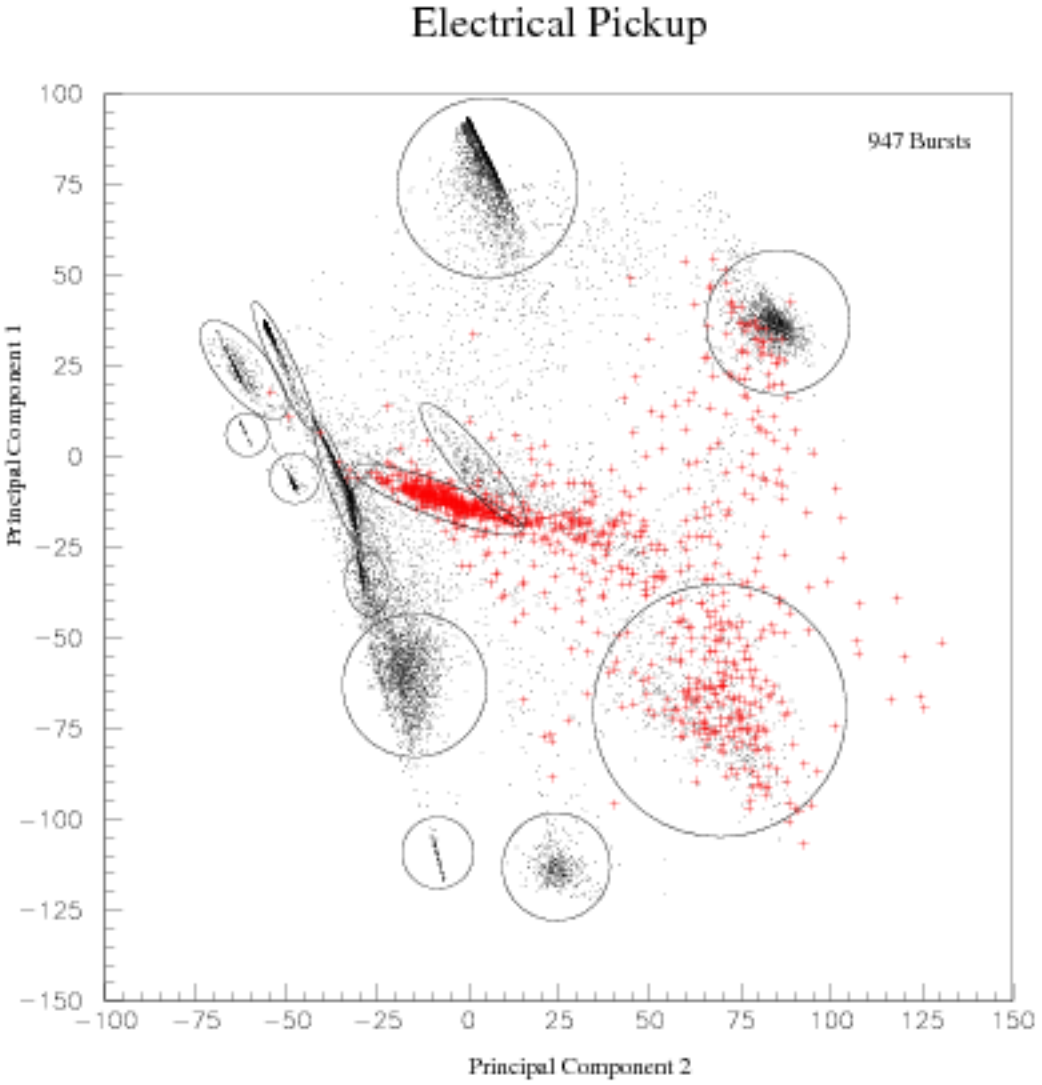

Figure 4.7: The distribution of Electrical Pickup bursts is not tightly confined to any one region, however a distinct group of electrical pickup events (37%) seem to be associated with region 4.

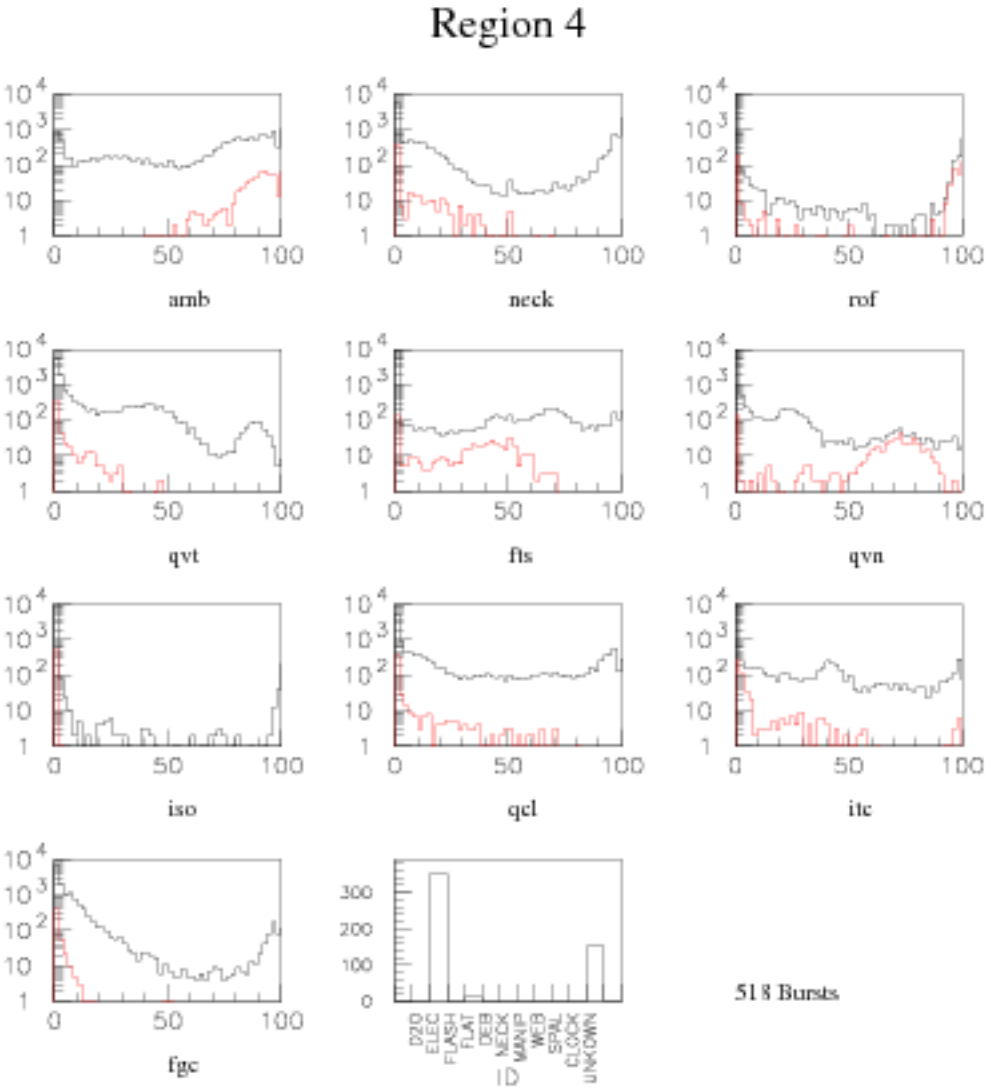

Figure 4.8: Data cleaning cut distributions of bursts found in region 4 compared to all bursts. The number of bursts of each ID type found in the region are also shown.

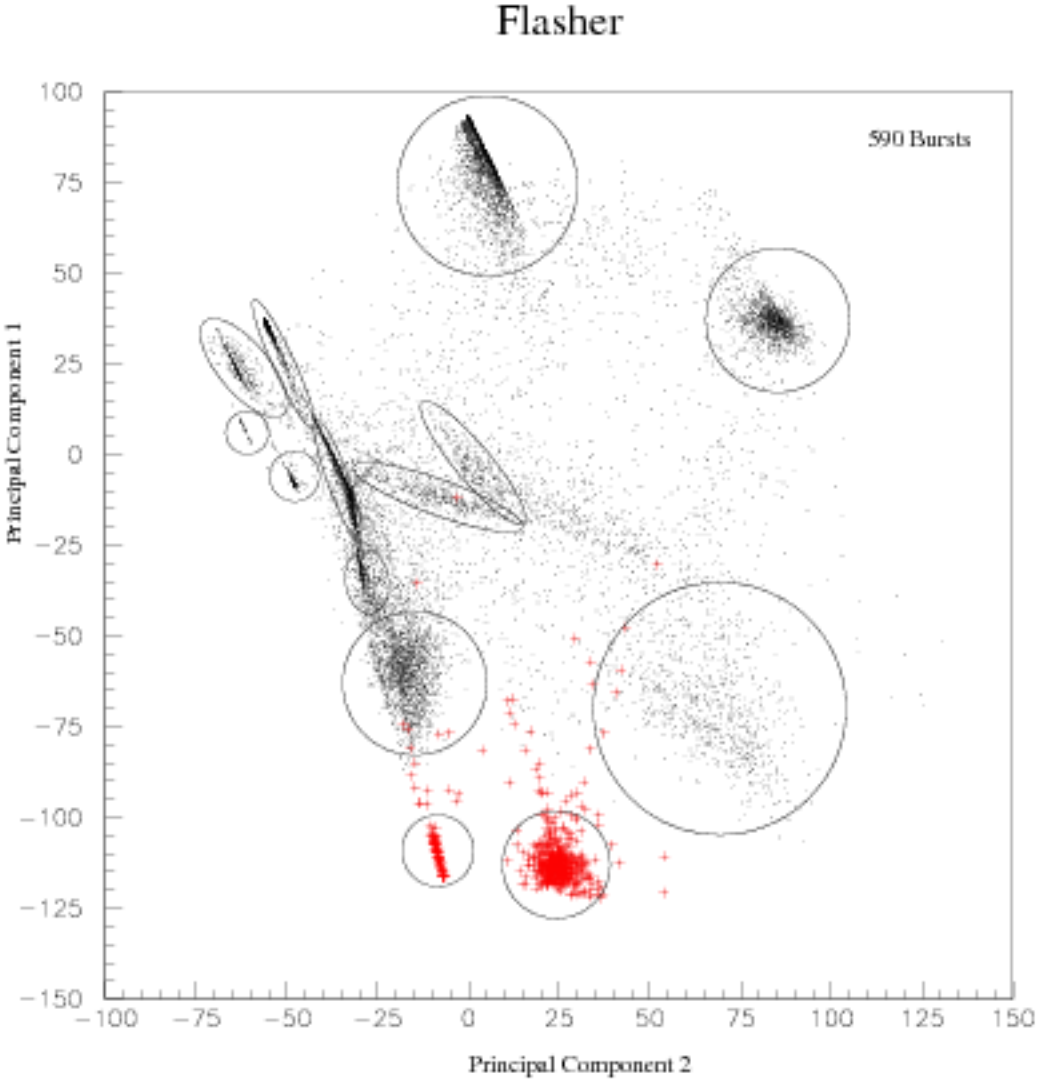

Figure 4.9: The distribution of Flasher bursts is mainly confined to regions 3 and 5, with 91% of the 590 bursts falling within the defined regions. The difference between the two regions is the FTS cut, with bursts in region 5 having FTS<5.

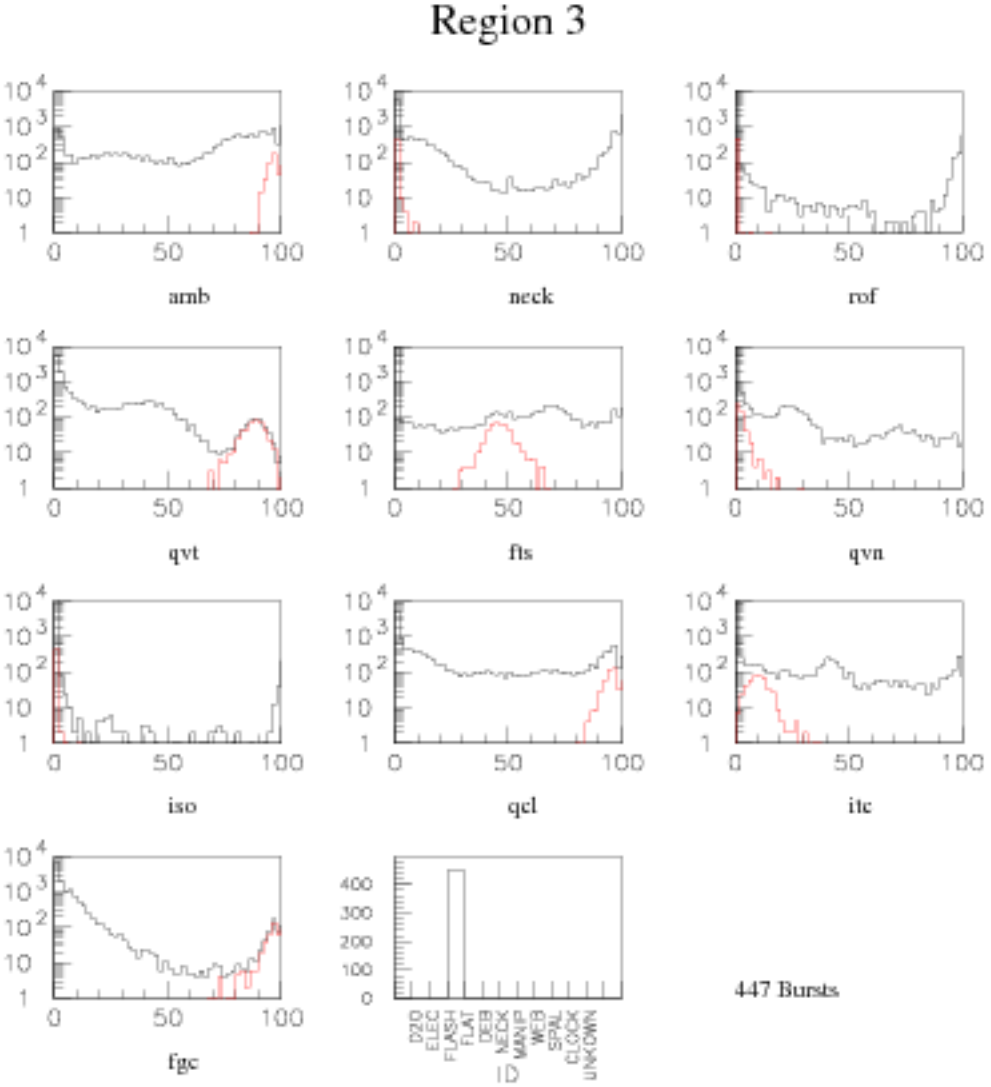

Figure 4.10: Data cleaning cut distributions of bursts found in region 3 compared to all bursts. The number of bursts of each ID type found in the region are also shown.

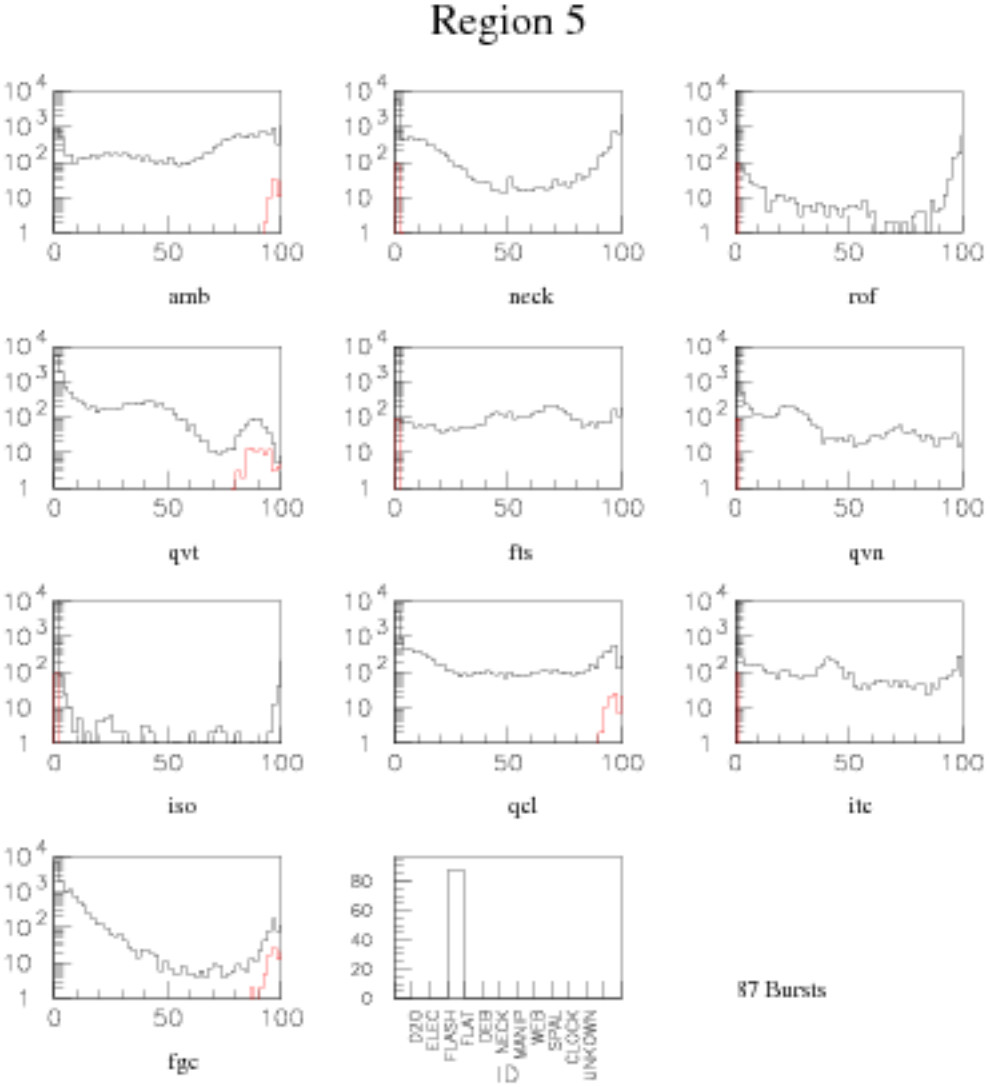

Figure 4.11: Data cleaning cut distributions of bursts found in region 5 compared to all bursts. The number of bursts of each ID type found in the region are also shown.

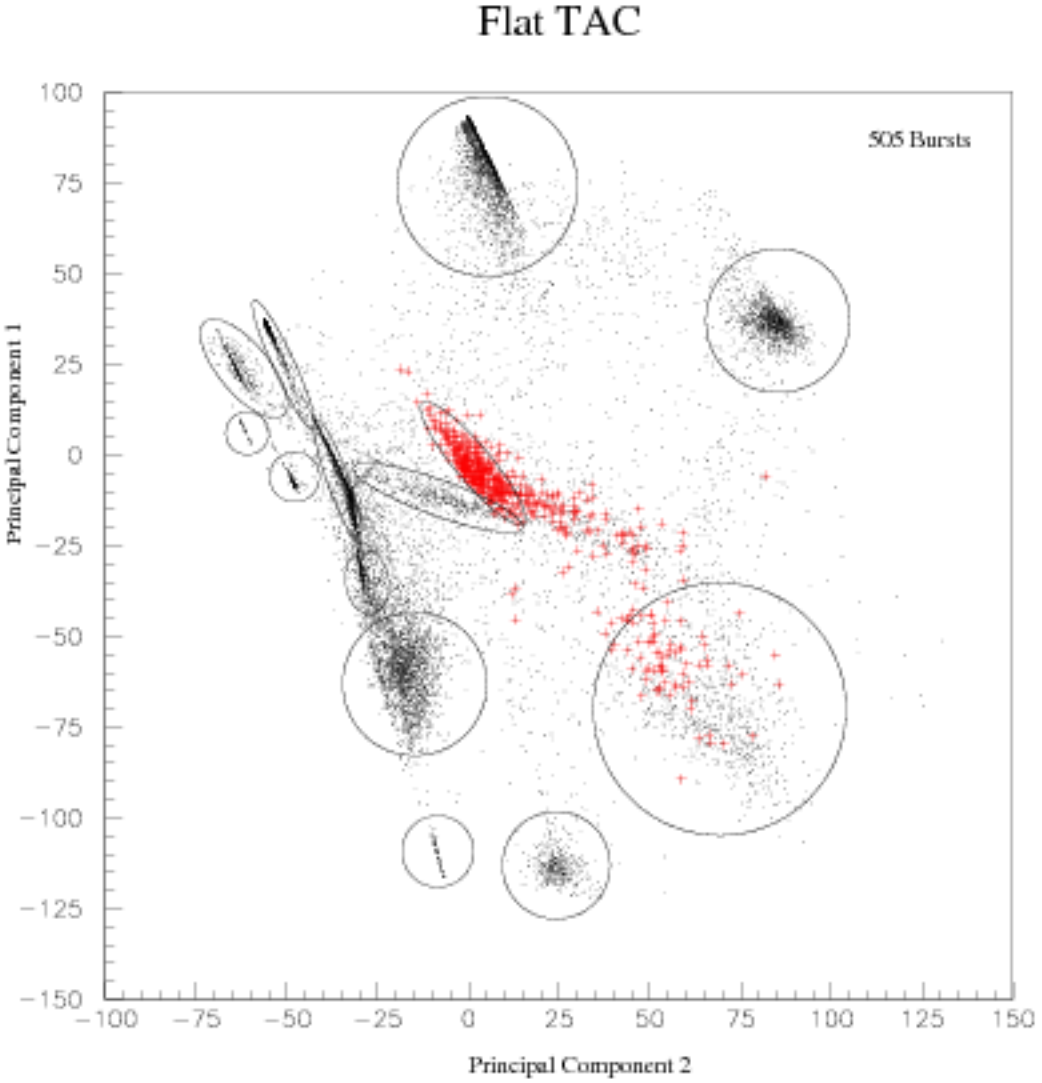

Figure 4.12: The distribution of Flat TAC bursts is partially confined to region 6, with 59% of the 505 bursts falling within the defined region.

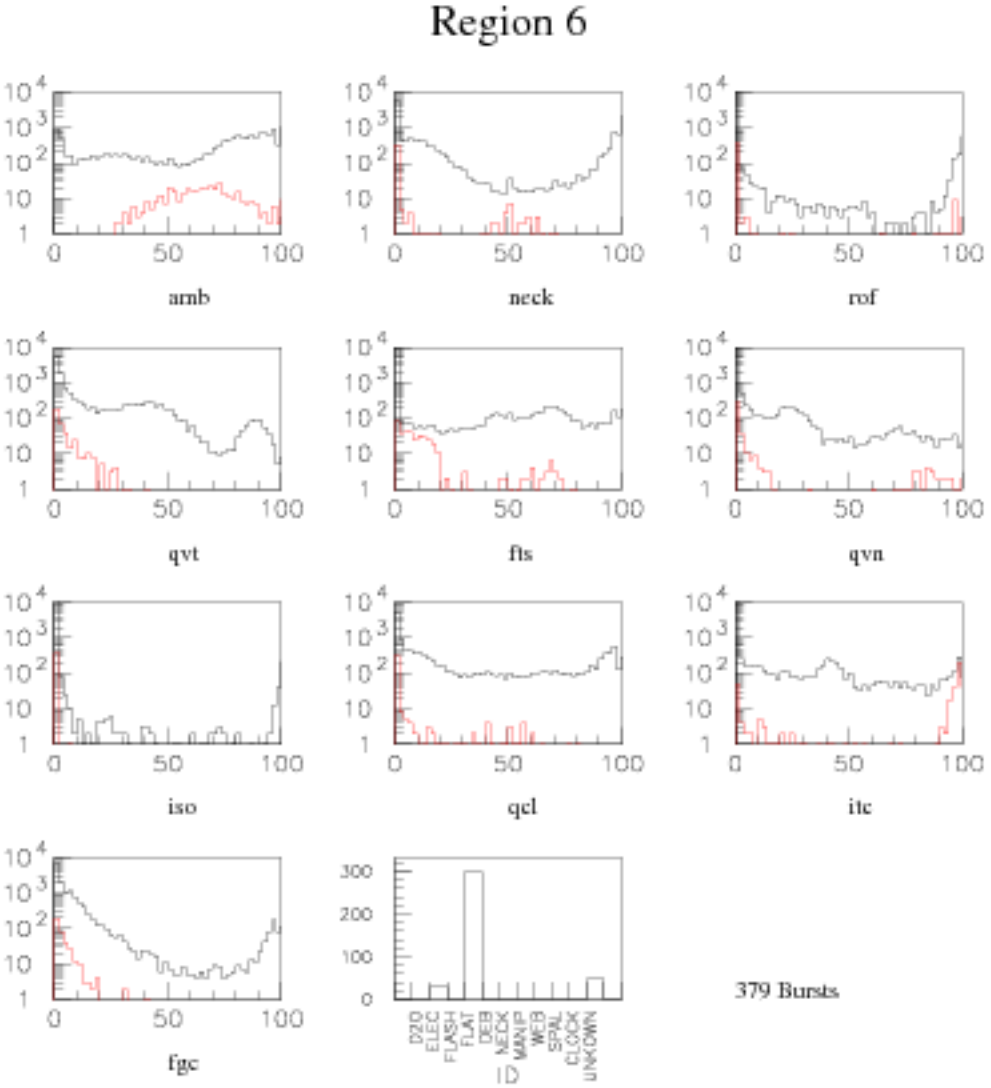

Figure 4.13: Data cleaning cut distributions of bursts found in region 6 compared to all bursts. The number of bursts of each ID type found in the region are also shown.

Current	Proposed
ITC>all other cuts	ITC>75 FTS<25

Regions 7 and 8: Dry End Breakdown Bursts

Figure 4.14 shows that bursts identified as dry end breakdown are tightly clustered in two regions, namely 7 and 8. A full 90% of the 272 bursts identified as dry end breakdown land in regions 7 and 8 (245 bursts).

Looking at Figure 4.15 and 4.16, no recommendation to adjust the existing cut is proposed. Note however that an additional parameter of ITC greater than or less than 5 will distinguish between dry end breakdown in region 7 from that in region 8. Also of note is that there are several Unknown bursts in region 8, all with ISO << 80. The difference between the two types of Dry End Breakdown, as well as the similarity between Dry End Breakdown and the population of Unknown bursts in Region 8 bears further investigation.

Region 11: Manipulight

Figure 4.17 shows that bursts identified as manipulight are restricted to a portion of region 11. In all, 88% of the 199 bursts identified as manipulight fall in region 11 (175 bursts).

Figure 4.18 shows that the cut parameters can be loosened substantially. Although the bursts in this region are not as tightly grouped as in others, the source moving bit is included in the cut definition, and provides confidence in loosening the cut parameters. The additional parameter of QVT>10 is also suggested to exclude some outlying bursts. Under the proposed adjustments, 88% of the 555 bursts now identified fall in region 11 (488 bursts).

The proposed change to the manipulight ID is:

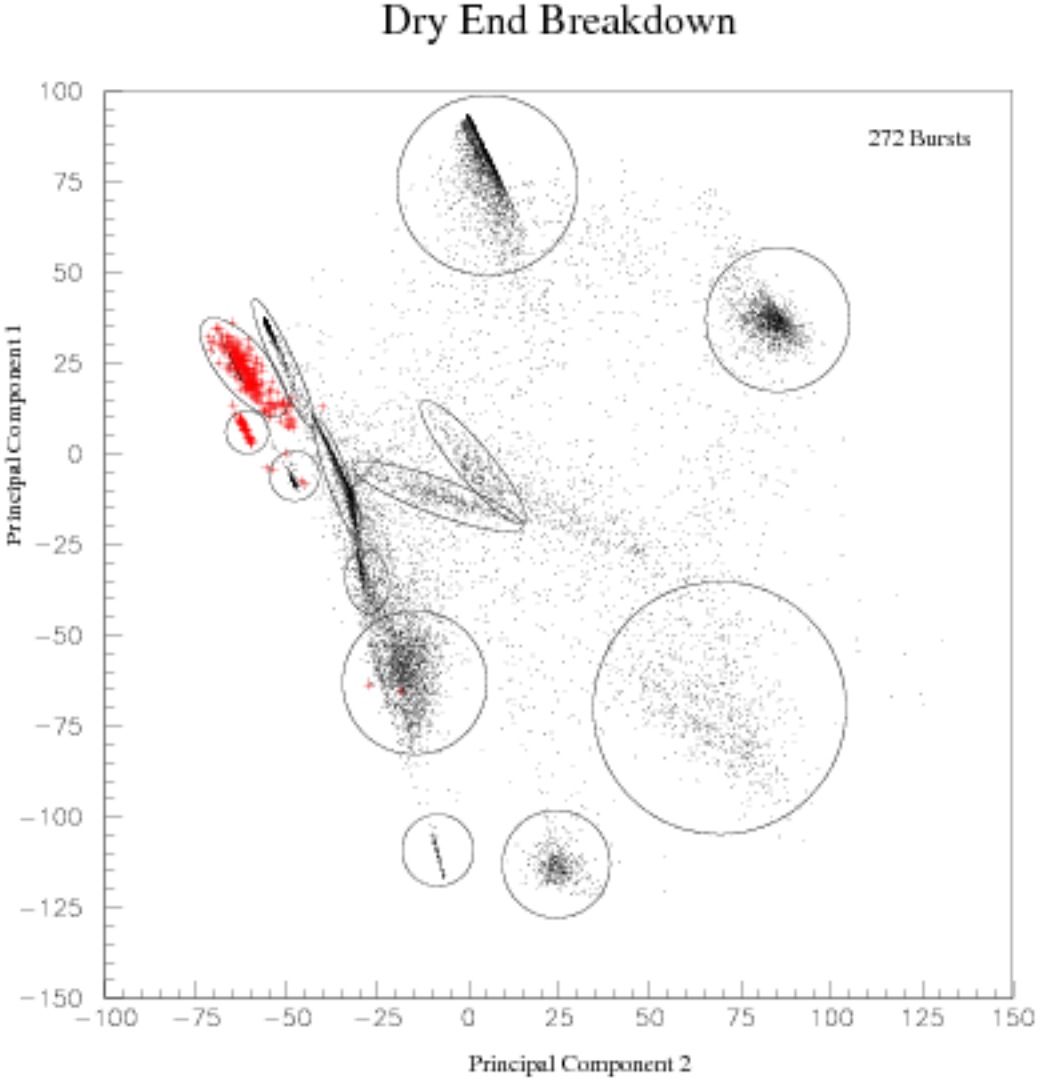

Figure 4.14: The distribution of Dry End Breakdown bursts is mainly confined to regions 7 and 8, with 90% of the 272 bursts falling within the defined regions. The difference between the two regions is the ITC cut, with bursts in region 7 having ITC<5.

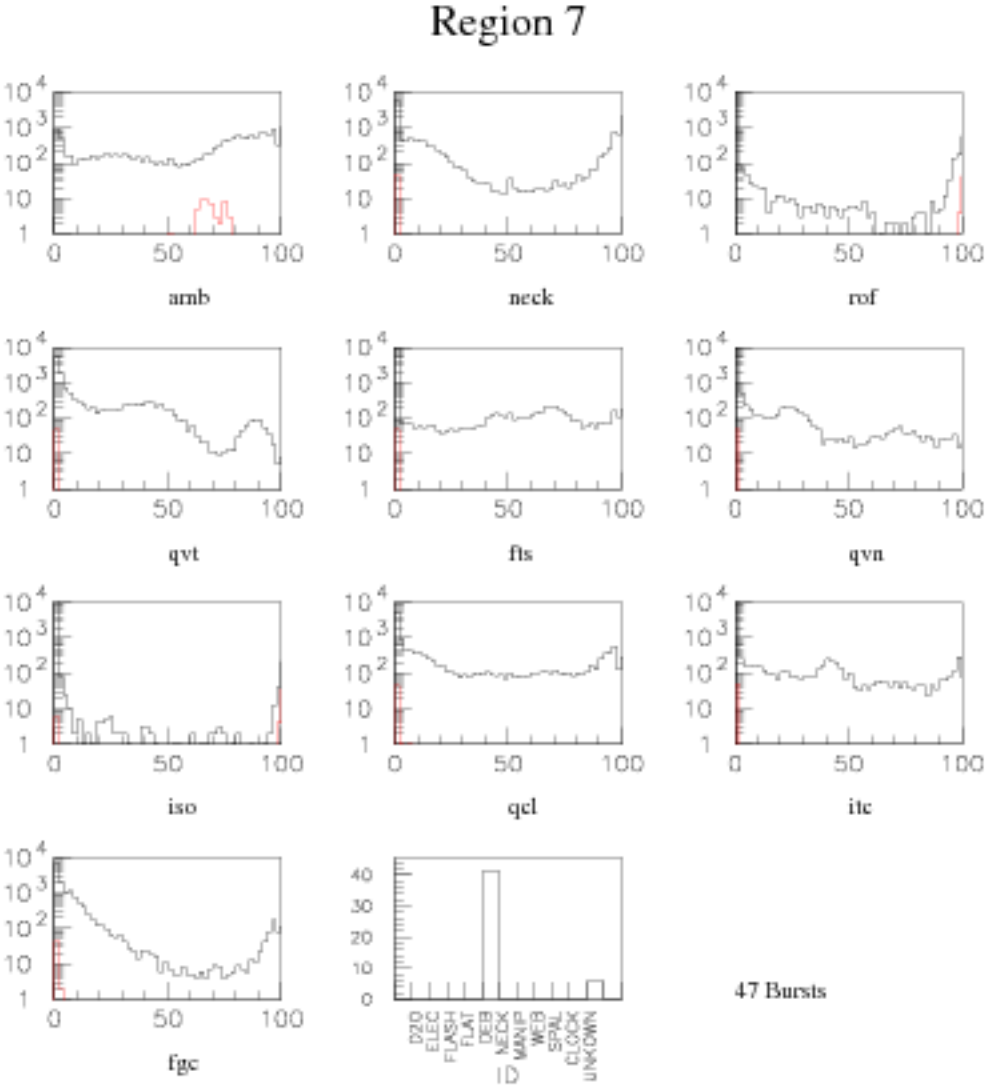

Figure 4.15: Data cleaning cut distributions of bursts found in region 7 compared to all bursts. The number of bursts of each ID type found in the region are also shown.

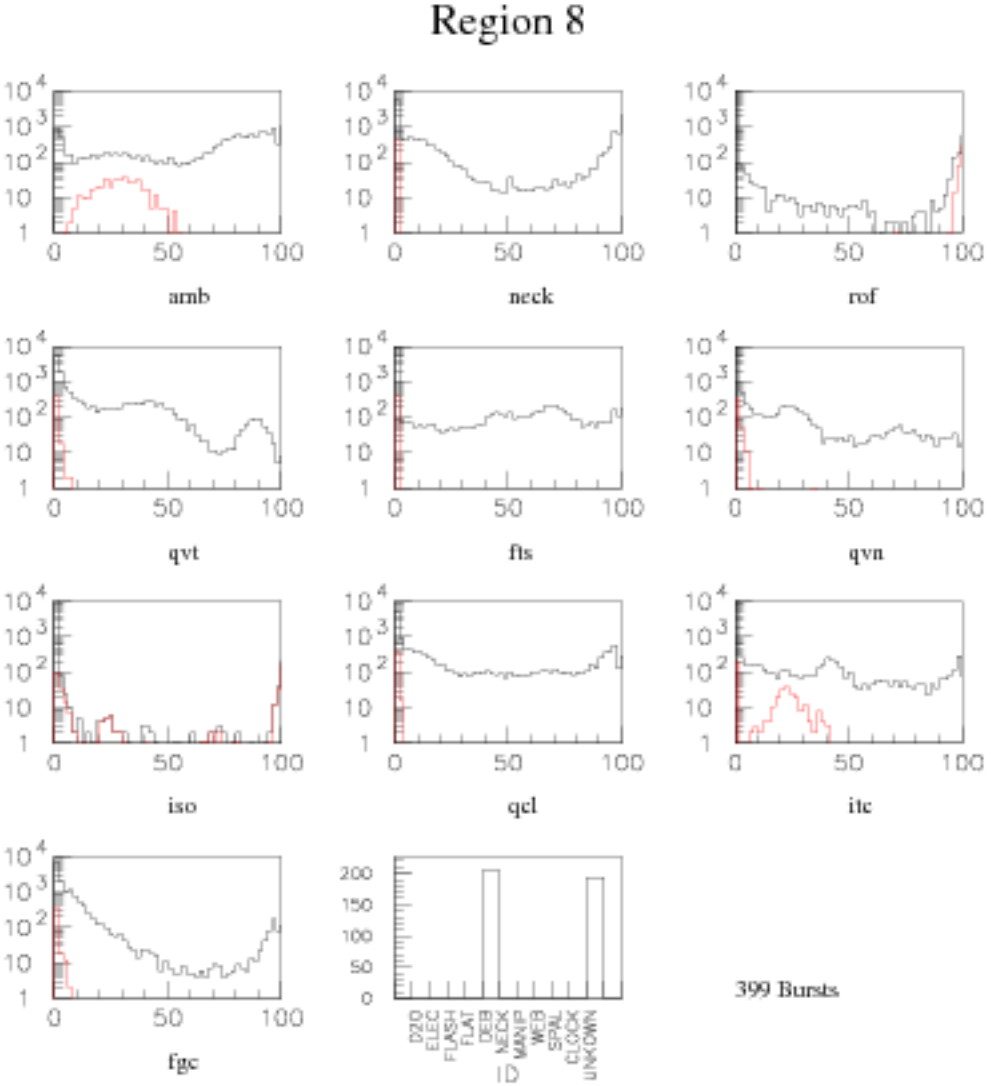

Figure 4.16: Data cleaning cut distributions of bursts found in region 8 compared to all bursts. The number of bursts of each ID type found in the region are also shown.

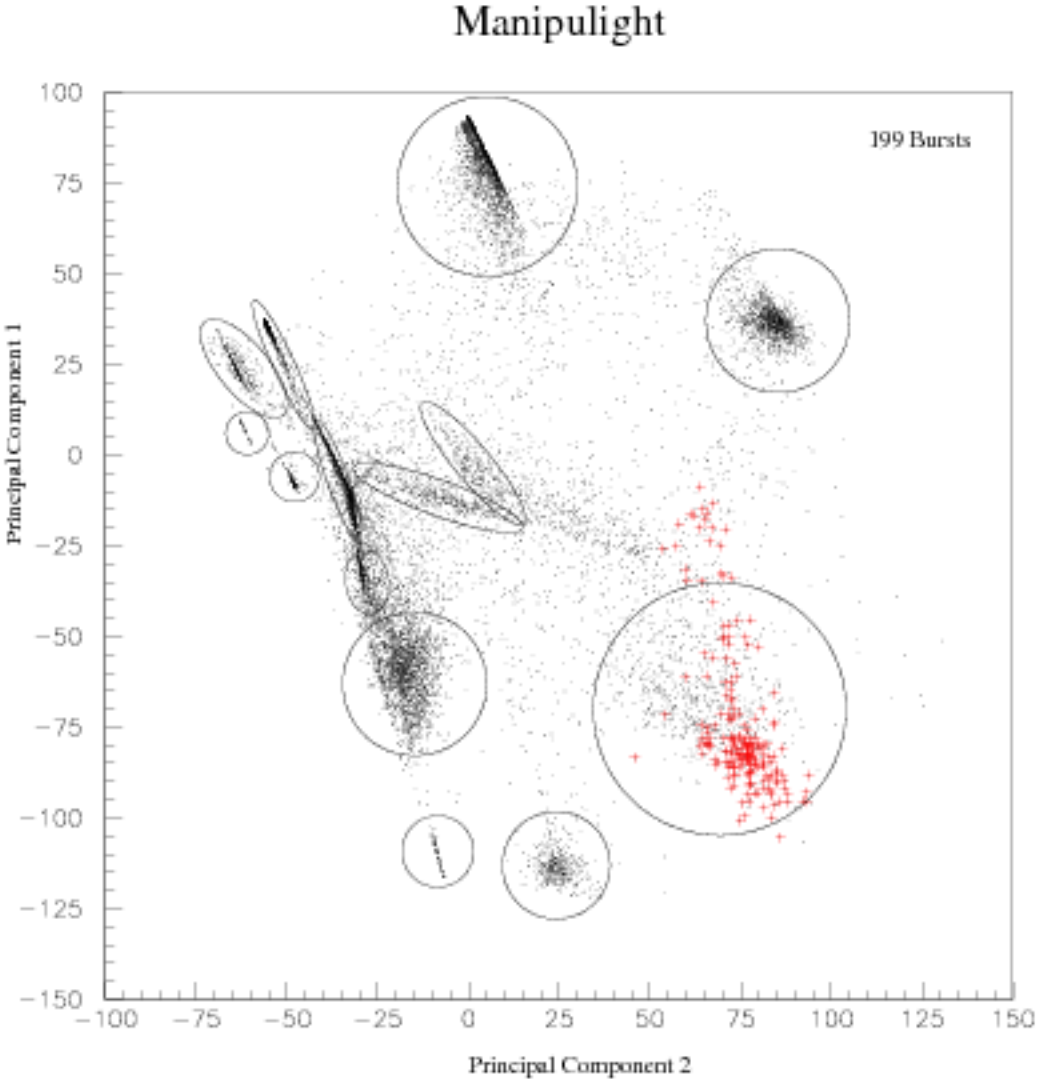

Figure 4.17: The distribution of Manipulight bursts is mainly confined to a portion of region 11, with 88% of the 199 bursts falling within the defined region.

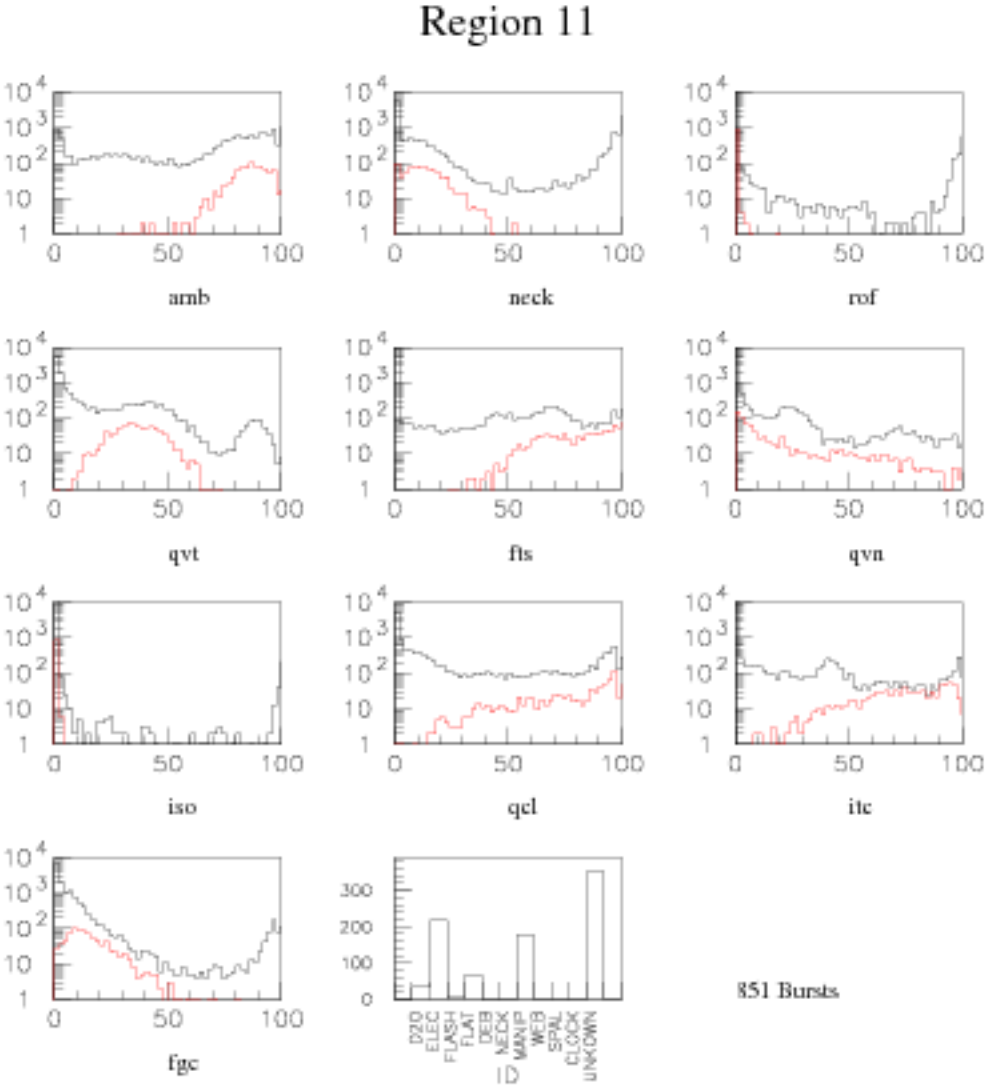

Figure 4.18: Data cleaning cut distributions of bursts found in region 11 compared to all bursts. The number of bursts of each ID type found in the region are also shown.

Current	Proposed
AMB>75	AMB>50
ITC>65	ITC>25
Neck<20	Neck<45
	QVT>10

New Burst Categories

Figure 4.19 shows that the bursts identified as Unknown can be categorized into several distinct groups. The most clearly defined groups are those in regions 2, 9, and 10. These regions are assumed to be distinct burst types, and are described below. Although many bursts are also tightly grouped in regions 12, 13, and to a lesser degree 14, they are not studied further because they are not well separated from other groups.

Region 2: Unknown

All bursts in this region are identified as Unknown. They have a high fraction of events cut by the Neck cut, and a low fraction by all other cuts. A set of parameters based on Figure 4.20 to identify these bursts is proposed below. Under this new definition, 93% of the 2639 bursts identified fall in region 2 (2454 bursts).

Proposed ID
Neck>60
FTS<40
AMB<70

Several of the above bursts were randomly selected for manual inspection. These bursts show light at the bottom of the detector as well as outside of the PSUP (OWL and BUTTS[4] tubes). The bursts are distributed across run types, favouring

[4]BUTTS is a small array of test PMTs suspended outside of the PSUP and connected to the DAQ.

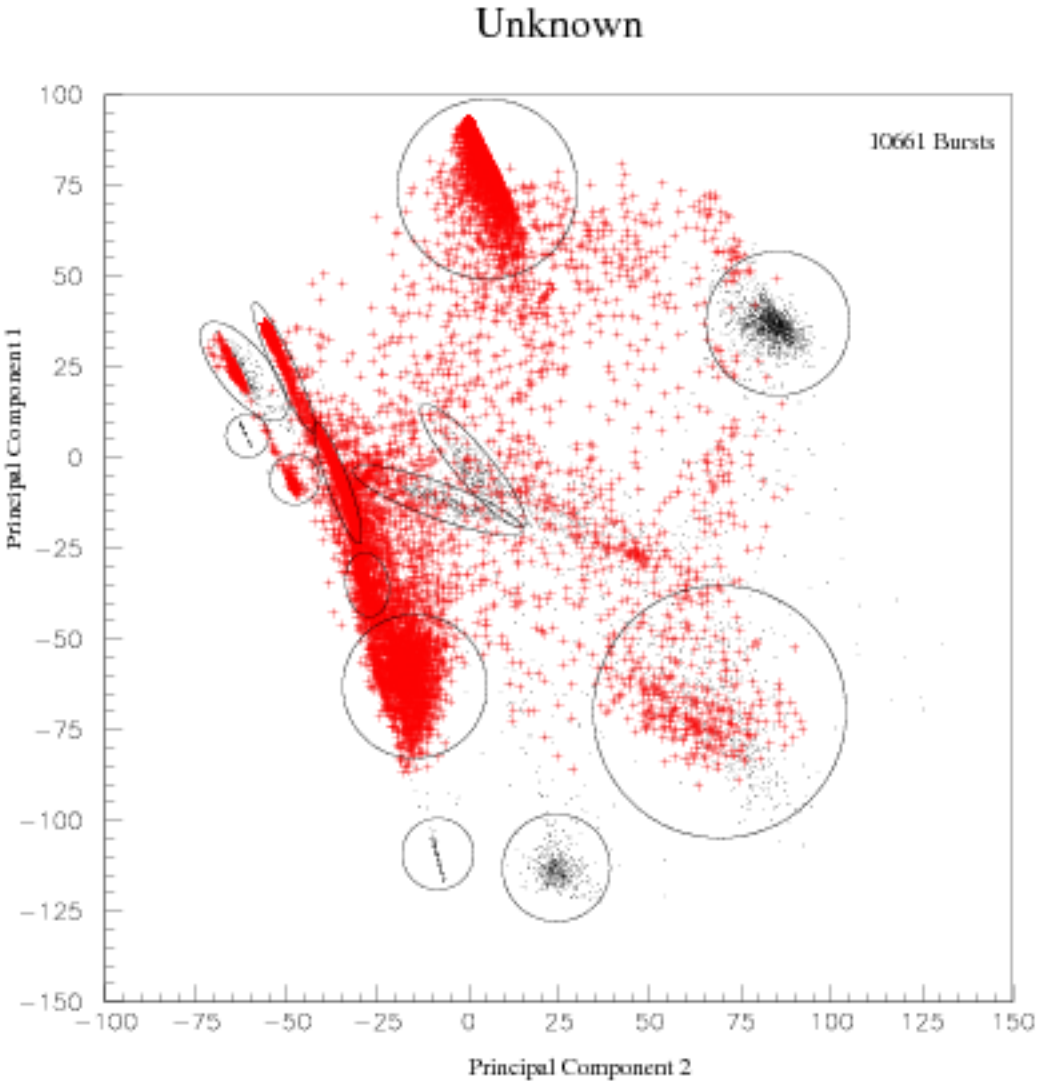

Figure 4.19: The distribution of Unknown bursts is not confined to one but several defined regions. The most easily discernable groups of Unknown bursts are those in regions 2, 9, and 10.

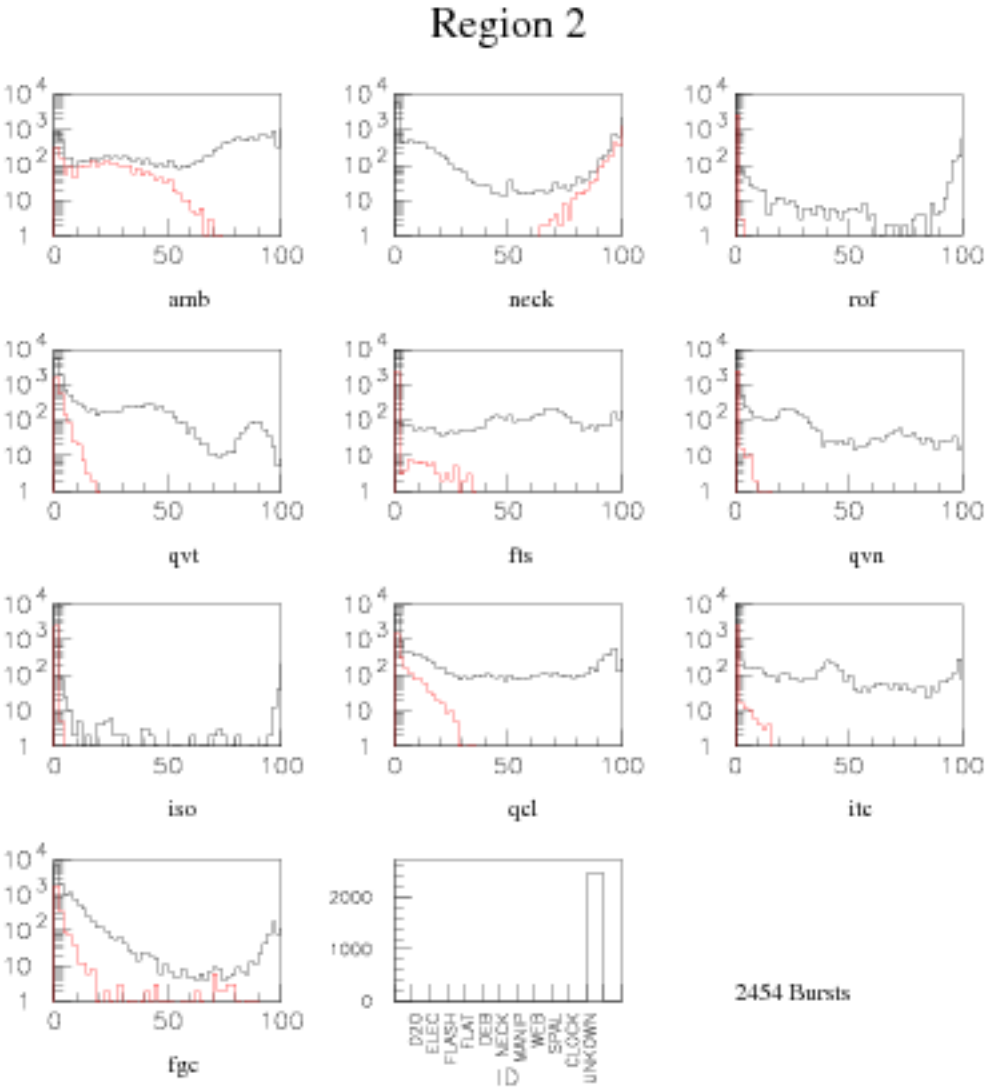

Figure 4.20: Data cleaning cut distributions of bursts found in region 2 compared to all bursts. The number of bursts of each ID type found in the region are also shown.

mainly Maintenance and 'Other' run types. Several of the bursts inspected manually occurred during Supernova Watch runs with D_2O circulation on. It is possible that these bursts are caused by D_2O Circulation (or Neck) events, but that they respond differently to the data cleaning cuts due to the run condition (detector thresholds are raised considerably for supernova watch runs). It is likely safe to attribute these bursts to an instrumental background. To truly identify this or any other Unknown burst class however, a significant fraction of the sample must be closely examined.

Region 9: Unknown

All bursts in the region are identified as Unknown. All bursts contain a high fraction of events with high AMB and QCL fractions. A set of parameters based on Figure 4.21 to identify these bursts is proposed below. Under this new definition, 97% of the 2037 bursts identified fall in region 9 (1976 bursts).

Proposed ID

QCL>65
QVT<70
ITC<10
Neck<35

Again, several of the above bursts were selected for manual inspection. These bursts contain events with high charge deposited at the bottom of the detector rapidly followed by several events with broad time spectra. These bursts occur mainly during calibration activity, specifically during Source Transitional runs with the Laserball source deployed. These bursts are almost certainly attributed to the Laserball source.

Region 10: Unknown

All bursts in this region are identified as Unknown. These bursts have a high fraction of events cut by the ROF and AMB cuts, and a very low fraction by all other cuts. A set of parameters to identify these bursts based on Figure 4.22 is proposed below.

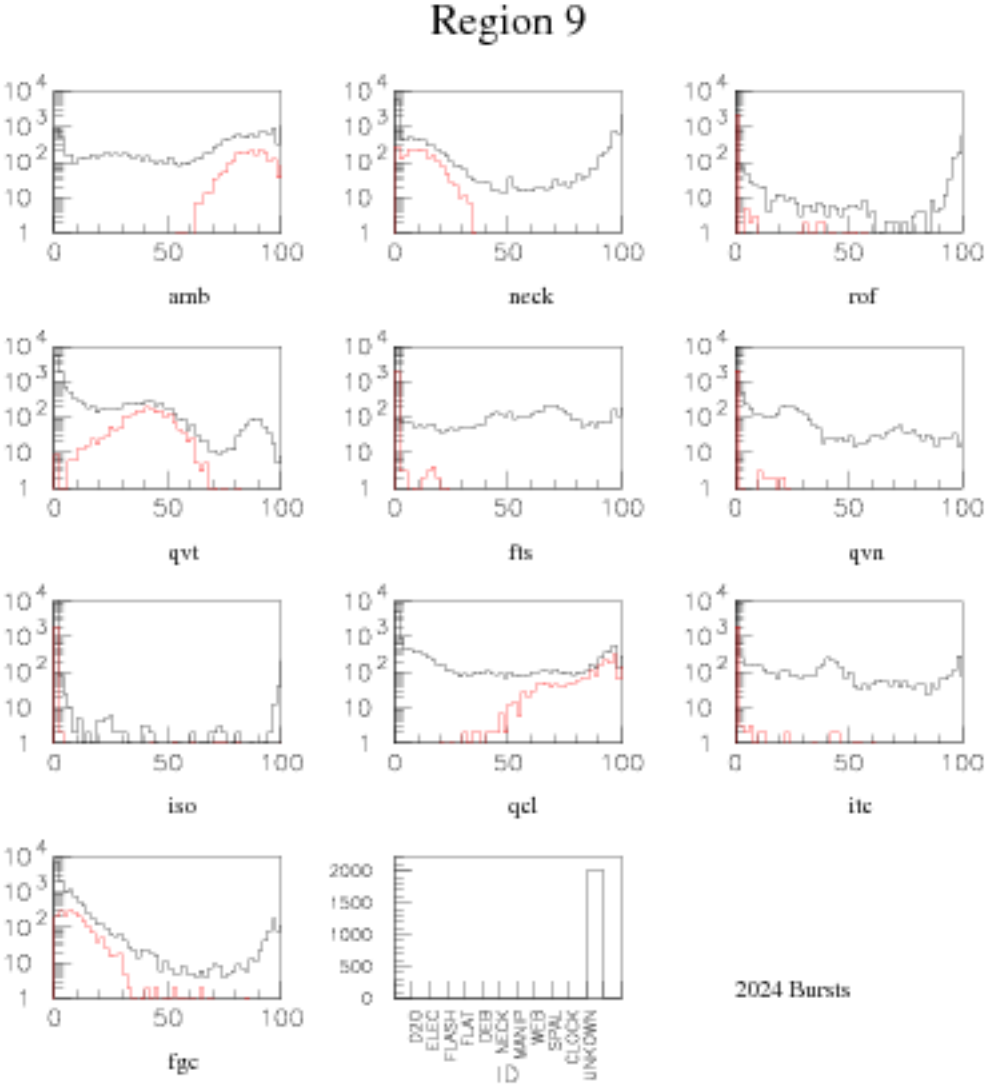

Figure 4.21: Data cleaning cut distributions of bursts found in region 9 compared to all bursts. The number of bursts of each ID type found in the region are also shown.

Under this new definition, 93% of the 159 bursts identified fall in region 10 (148 bursts).

Proposed ID

ROF>75
AMB>75
QVN<5

All of the bursts selected for manual inspection from this group contained events for which all hits were isolated to a single crate. These bursts occur mainly during maintenance runs. These are almost certainly attributed to electronics problems.

Revised Burst ID Summary

Table 4.4 shows the number of identified bursts for the modified IDs. The recommended adjustments decrease the number of Unknown bursts considerably. The most significant gain can be made by confirming the identity of the burst types associated with regions 2, 9, and 10. This would allow close to 50% of the previously Unknown bursts to be positively identified.

Broadening the Manipulight definition increases the number of bursts identified during non-neutrino running, while tightening the Electrical Pickup, D_2O circulation, and Flat TAC definitions reduce the number of bursts identified during neutrino running. Together these adjustments counteract each other, and increase the total number of Unknown bursts by less than 5%.

Adding the sub-categories of Flasher and Dry End Breakdown does not change the number of bursts identified, but does increase the resolution of identification.

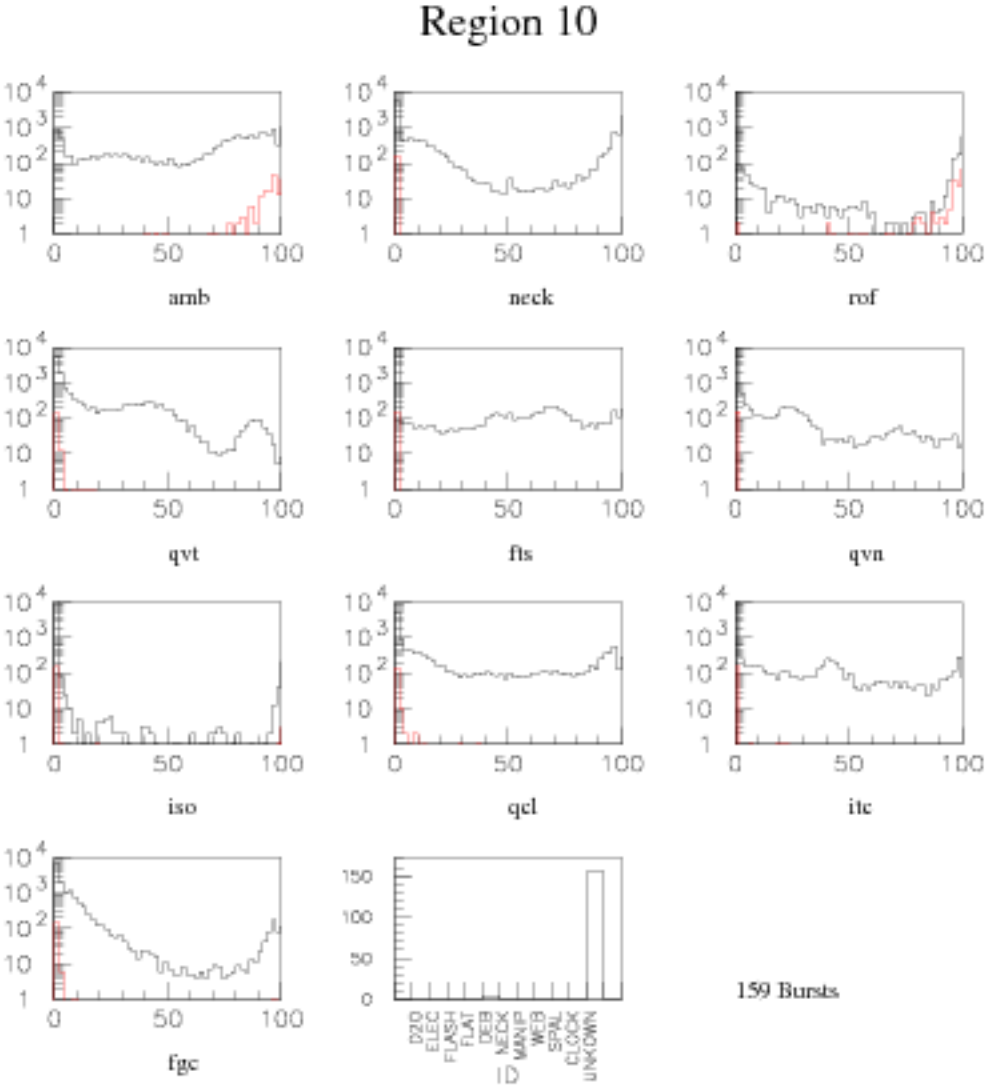

Figure 4.22: Data cleaning cut distributions of bursts found in region 10 compared to all bursts. The number of bursts of each ID type found in the region are also shown.

	Neutrino	Calib.	Maint.	Other	Total	(Old)
Livetime Fraction	**73%**	**10%**	**7%**	**2%**	**93%**	**93%**
D20 and Neck	1356	40	1	0	**1397**	1233
Electrical Pickup	455	12	1	1	**469**	947
Flasher 1(fts<5)	40	24	21	8	**93**	590
Flasher 2	443	7	0	1	**451**	-
Flat TAC	322	4	13	3	**342**	505
D.E.B. 1 (ITC<5)	1	1	44	0	**46**	272
D.E.B. 2	222	0	0	4	**226**	-
Manipulight	0	555	0	0	**555**	199
Region 2	63	495	924	1157	**2639**	-
Region 9	43	1476	366	152	**2037**	-
Region 10	15	1	143	0	**159**	-
Unknown	946	2546	2262	502	**6256**	10661
Total	**3906**	**5161**	**3775**	**1828**	**14670**	14670
% Unknown	24%	49%	60%	27%	**43%**	73%

Table 4.4: Under the modified level 2 IDs the fraction of bursts identified during neutrino running is slightly lower, but overall there are far fewer unknown bursts.

Chapter 5

Conclusion

An online monitoring system providing detection, analysis, and notification of bursts in the SNO datastream has been implemented. A large part of this thesis concerned the design and implementation of the burst detection algorithm, the dialout system, and the audio-visual operator alerts. The system is currently in stable operation, monitoring for neutrino bursts from galactic supernovae and helping to monitor the stability of the SNO detector. To date the supernova detection efficiency is difficult to measure as there have been no supernovas detected, no supernovae undetected, and no unsupernovae detected. Response time and burst identification were studied to gauge the performance of the system in lieu of actually detecting a supernova.

The online response time of the system was studied using muon induced spallation bursts. The response time to these bursts, which are the most supernova-like bursts available, is generally under 10 minutes. This is well within the 20 minute window identified by the SNEWS collaboration.

Burst identification was studied using data from an offline reprocessing analysis. For neutrino running, which accounts for the majority of livetime, the fraction of Unknown bursts was quite low at only 12%. For the remaining fraction of livetime, a much higher rate of unidentified bursts was seen, with more than 95% of being identified as Unknown.

An alternative method of burst classification was developed and used to validate,

refine, and expand the existing burst IDs. Three new IDs, two sub-classes of existing IDs, and several adjustments to other ID parameters were proposed. The net result of the proposed changes was that the fraction of unidentified bursts decreased from 73% to 43%.

Future and ongoing work includes improvements to both the response time and the burst identification. Although quite respectable already, the time and effort required to contact supernova experts and convey the burst analysis information can be improved. New mobile communication technologies such as digital text messaging and mobile networking are currently being investigated to accomplish this. To further improve burst identification, some of the suggested adjustments to the level 2 burst IDs should be implemented. In addition to the suggestions presented, the analysis itself can be expanded in many ways. The most obvious way to do this is to redo the analysis with the inclusion of several other burst variables.

REFERENCES

[1] W. S. C. Williams. *Nuclear and Particle Physics.* Oxford University Press, Oxford, 1997.

[2] H. V. Klapdor-Kleingrothaus and A. Staudt. *Non-accelerator Particle Physics.* Institute of Physics Publishing, Bristol, 1995.

[3] The SNO Collaboration. Measurement of the rate of $\nu_e + d \rightarrow p + p + e^-$ interactions produced by ^8B solar neutrinos at the sudbury neutrino observatory. *Physical Review Letters*, 87:071301, 2001.

[4] Thomas L. Swihart. *Astrophysics and Stellar Astronomy.* Wiley, New York, 1968.

[5] George W. Collins. *The Fundamentals of Stellar Astrophysics.* W. H. Freeman and Company, New York, 1989.

[6] Adam Burrows. Supernova explosions in the universe. *Nature*, 403:727, 2000.

[7] Virginia Trimble. The greatest supernova since Kepler. *Reviews of Modern Physics*, 60:859–871, 1988.

[8] John N. Bahcall. *Neutrino Astrophysics.* Cambridge University Press, Cambridge, 1989.

[9] Adam Burrows, D. Klein, and R. Gandhi. The future of supernova neutrino detection. *Physical Review*, D45:3361–3385, 1992.

[10] Kate Scholberg. Supernova neutrino detection. *Nuclear Physics B*, Proceedings of the XIXth International Conference on Neutrino Physics and Astrophysics:331–337, 2001.

[11] John Beacom, R. N. Boyd, and A. Mezzacappa. Technique for direct eV-scale measurements of the mu and tau neutrino masses using supernova neutrinos. *Physics Review Letters*, 85:3568–3571, 2000. hep-ph/0006015.

[12] J. M. Roney. Review of the tau neutrino mass. *Nuclear Physics B*, Proceedings of the XIXth International Conference on Neutrino Physics and Astrophysics:287–292, 2001.

[13] J.F. Beacom and P. Vogel. Mass signature of supernova ν_μ and ν_τ nuetrinos in the Sudbury Neutrino Observatory. *Physical Review*, D58:093012, 1998.

[14] Jaret Heise. *A Search for Supernova Neutrinos with the Sudbury Neutrino Observatory*. PhD thesis, University of British Columbia, 2001.

[15] J. Boger et al. The Sudbury Neutrino Observatory. *Nuclear Instrumentation and Methods*, **A449**:172–207, 2000. nucl-ex/9910016.

[16] The SNO Collaboration. The SNOman user's manual.

[17] S. W. Bruenn, K. R. De Nisco, and A. Mezzacappa. General relativistic effects in the core collapse supernova mechanism. *Astroparticle physics*, 2001. astro-ph/0101400.

[18] M. Liebendörfer et al. Probing the gravitational well: no supernova explosion in spherical symmetry with general relativistic boltzmann neutrino transport. *Physical Review*, D63:103004, 2001.

[19] The SNEWS Collaboration. Proposal for the supernova early warning system -draft, 2000.

[20] J. Klein. The SNO trigger system. *SNO Technical Report*, 97-035, 1997.

[21] The zebra system, CERN program library long writeups Q100/Q101, 1995.

[22] J. Klein and V. Rusu. Data cleaning: the qcluster cut. *SNO Analysis Report*, 2000.

[23] J. Klein. Data cleaning: the qvt cut. *SNO Analysis Report*, 2000.

[24] N. McCauley. Data cleaning: the neck cut. *SNO Analysis Report*, 2000.

[25] M. S. Neubauer. Data cleaning: the in-time channel cut. *SNO Analysis Report*, 1999.

[26] J. Klein. Data cleaning: an analog measurement board cut. *SNO Analysis Report*, 1999.

[27] R. Van de Water. Data cleaning: the q/nhit cut. *SNO Analysis Report*, 2000.

[28] A.W.P. Poon et al. A compact ^{3}H(p,γ)^{4}He 19.8-MeV gamma-ray source for energy calibration at the Sudbury Neutrino Observatory. *Bulletin of the American Physical Society*, 42:1632, 1997.

[29] P. Emond and C. Pagnutti. *Summer student progress reports*. Laurentian University, 2001

[30] R. Brun et al. *Lintra - principal components analysis program*. CERN , 1980